

BRAIN-be

**Belgian Research Action
through Interdisciplinary
Networks**

2012-2017

MASC

Modelling and Assessing Surface Change impacts on Belgian and Western European climate

Louis FRANCOIS (University of Liège) - Ingrid JACQUEMIN (University of Liège) - Alexandra HENROT (University of Liège) - Alain HAMBUECKERS (University of Liège) - Bernard TYCHON (University of Liège) - Julie BERCKMANS (Royal Meteorological Institute of Belgium) - Rafiq HAMDJ (Royal Meteorological Institute of Belgium) - Véronique BECKERS (University of Namur) - Nicolas DENDONCKER (University of Namur) - Joanna HOREMANS (University of Antwerp) - Reinhart CEULEMANS (University of Antwerp) - Gaby DECKMYN (University of Antwerp) - Bos DEBUSSCHER (Ghent University) - Robert DE WULF (Ghent University) - Frieke VAN COILLIE (Ghent University) - Nabil Laanaia (CNRM-GAME, Toulouse, France) - Jean-Christophe CALVET (CNRM-GAME, Toulouse, France) - Dominique CARRER (CNRM-GAME, Toulouse, France)



NETWORK PROJECT

MASC

Modelling and Assessing Surface Change impacts on Belgian and Western European climate

Contract - BR/121/A2/MASC

FINAL REPORT

PROMOTORS: L. FRANCOIS (University of Liège), A. HAMBUECKERS (University of Liège), B. TYCHON (University of Liège), R. HAMDY (Royal Meteorological Institute of Belgium), N. DENDONCKER (University of Namur), G. DECKMYN (University of Antwerp), R. CEULEMANS (University of Antwerp), R. DE WULF (Ghent University), F. VAN COILLIE (Ghent University), J.-C. CALVET (CNRM-GAME, Toulouse, France), D. CARRER (CNRM-GAME, Toulouse, France)

AUTHORS: L. FRANCOIS (University of Liège), I. JACQUEMIN (University of Liège), A. HENROT (University of Liège), A. HAMBUECKERS (University of Liège), B. TYCHON (University of Liège), J. BERCKMANS (Royal Meteorological Institute of Belgium), R. HAMDY (Royal Meteorological Institute of Belgium), V. BECKERS (University of Namur), N. DENDONCKER (University of Namur), J. HOREMANS (University of Antwerp), R. CEULEMANS (University of Antwerp), G. DECKMYN (University of Antwerp), B. DEBUSSCHER (Ghent University), R. DE WULF (Ghent University), F. VAN COILLIE (Ghent University), Nabil LAANAIA (CNRM-GAME, Toulouse, France), Jean-Christophe CALVET (CNRM-GAME, Toulouse, France), Dominique CARRER (CNRM-GAME, Toulouse, France)





Published in 2019 by the Belgian Science Policy
Avenue Louise 231
Louizalaan 231
B-1050 Brussels
Belgium
Tel: +32 (0)2 238 34 11 - Fax: +32 (0)2 230 59 12
<http://www.belspo.be>
<http://www.belspo.be/brain-be>

Contact person: Martine Vanderstraeten
Tel: +32 (0)2 238 36 10

Neither the Belgian Science Policy nor any person acting on behalf of the Belgian Science Policy is responsible for the use which might be made of the following information. The authors are responsible for the content.

No part of this publication may be reproduced, stored in a retrieval system, or transmitted in any form or by any means, electronic, mechanical, photocopying, recording, or otherwise, without indicating the reference:

Francois, L., I. Jacquemin, A. Henrot, A. Hambuckers, B. Tychon, J. Berckmans, R. Hamdi, V. Beckers, N. Dendoncker, J. Horemans, R. Ceulemans, G. Deckmyn, B. Debusscher, R. De Wulf, F. Van Coillie, N. Laanaia, J.-C. Calvet, D. Carrers. **MASC - Modelling and Assessing Surface Change impacts on Belgian and Western European climate**. Final Report. Brussels : Belgian Science Policy 2019 – 85 p. (BRAIN-be - (Belgian Research Action through Interdisciplinary Networks)

TABLE OF CONTENTS

CONTENTS

ABSTRACT	5
CONTEXT.....	5
OBJECTIVES.....	5
CONCLUSIONS	6
KEYWORDS	6
1. INTRODUCTION	6
2. STATE OF THE ART AND OBJECTIVES	7
3. METHODOLOGY	10
4. SCIENTIFIC RESULTS AND RECOMMENDATIONS	23
5. DISSEMINATION AND VALORISATION	64
6. PUBLICATIONS	65
7. ACKNOWLEDGEMENTS	70
ANNEXES	71

ABSTRACT

Context

The interactions between land surface and climate are complex. Climate change can affect ecosystem structure and functions, by altering photosynthesis or inducing thermal and hydric stresses on plant species. These changes then impact socio-economic systems, through e.g. lower farming or forestry incomes. Ultimately, it can lead to permanent changes in land use structure, especially when associated with other non-climatic factors, such as urbanisation pressure. These interactions and changes impact the climate system, in terms of changing: (1) surface properties (albedo, roughness, evapotranspiration, etc.) and (2) greenhouse gases emissions (mainly CO₂, CH₄, N₂O). The first type of feedbacks alters directly the local/regional atmospheric circulation, whilst the second feedback affects the global system in the long run, through a modification of the atmospheric greenhouse gas budget. This project has addressed the first type of feedbacks.

Current studies remain quite limited in their assessment of the interactions between climate and land surface dynamics, because (1) they do not fully couple the climate, the land surface and the socio-economic sphere, implying that the strength of the feedbacks existing between these three systems cannot really be evaluated, and (2) they usually use low resolution models, so that atmospheric processes like regional winds, thunderstorms or other local convective systems cannot be represented, while these meso-scale circulation features are probably central in governing the land surface-climate feedbacks at the scale of a region or a country.

For those reasons, in this project, we have attempted to build a country-scale assessment tool using high-resolution coupled models of climate, land surface dynamics and socio-economic processes. This tool was specifically designed for Belgium and applied over its whole territory.

Objectives

The overall objective of the MASC project (“Modelling and Assessing Surface Changes impacts on Belgian and Western European climate”) was thus to build such a high resolution assessment tool to **study the feedbacks between climate changes and land surface changes.**

With this tool, the project aimed to:

- (1) produce coherent **projections of climate and land surface changes over Belgium** and Western Europe up to 2035;
- (2) isolate the **climatic impacts of land use/land cover changes** in these projections;
- (3) assess the impacts on the **productivity and the carbon budget** of Belgian ecosystems.

Through these objectives, the ultimate goal is to provide better climate projections and climate change evaluation tools to policy makers, stakeholders and the scientific community.

The tool that has been constructed combines a regional climate model, a dynamic vegetation model and an agent-based model. The first step was the construction/adaptation, the validation and the assembly of the models. A particular attention was given to the dynamic vegetation model, which was compared with two other models at several eddy covariance sites to test its ability to simulate gross primary productivity and net ecosystem fluxes of carbon and water.

The next step was the production of high resolution scenarios for the Belgian territory, in an iterative way. The regional climate model was run first to provide scenarios of climate change for Belgium, which do not account for land use/land cover changes. Then, the dynamic vegetation model and the agent-based model were coupled together, and, forced with the climatic projections, they produced scenarios of land use/land cover, crop yield and forest productivity changes up to 2035. These scenarios respond dynamically to climate change. They take into account the urbanisation pressure, which is very important around the main cities of Belgium. They also assume that the observed recent increase of farm sizes in Belgium can be extrapolated into the near future. Finally,

these scenarios were introduced in the regional climate model to evaluate the impacts of land use/land cover changes on the regional climate at high resolution.

Conclusions

The simulations of the regional climate model performed in this project show which regions will be most vulnerable to climate and land use change in the near future, and where mitigation and adaptation strategies should be applied. The main result of these simulations indicate that the land use/land cover changes expected in Belgium for the next 20 years will tend to reinforce climate change, by producing an additional warming as high as 0.4°C on average for the summer season. This is because these surface changes will be dominated by conversion from crops or pastures to urban areas. The effect is particularly marked around the cities of Charleroi and Liège.

According to the scenarios of the agent-based model, the farm sizes and, hence, the agricultural parcel sizes, can be expected to increase. The enlargement of parcels results in a decrease in linear elements (ditches, edges and hedges) and point elements (tree islands), grasslands and wetlands. These changes could not be included in the climate simulations performed here, since their scale is significantly lower than the scale of the grid cells in the climate model. Anyway, it can be expected that they will also impact local climate.

The simulations of the dynamic vegetation model indicate that, on average, ecosystem productivity will increase over the next 20 years in response to the warming and the rise of atmospheric CO₂. This will induce a slight overall increase of crop yields. However, during extreme years (e.g., droughts), very large decrease of crop yields can be expected and these extreme years will possibly become more frequent. As a result, the inter-annual variability of crop yield can be expected to significantly increase in the future. Phenological changes can also be expected, with for instance a significant advance of leaf onset in the spring.

Many of these results should be useful to landscape planners, urban planners, forest managers, farmer agencies and local governments.

Keywords

Climate change, land surface, feedbacks, regional climate modelling, dynamic vegetation modelling, agent-based modelling

1. INTRODUCTION

Climate change impacts the distribution, structure and functioning of ecosystems. This applies both to natural vegetation and agricultural systems. Climate change also impacts human societies and interferes with economic growth and trade exchanges. On the other hand, man is the main actor of climate change and his activities can amplify or mitigate the changes. This action is, of course, well known for the emission of greenhouse gases, which are responsible for climate warming at the global scale. However, the action of man on climate is also important at the local scale, through processes not directly linked to greenhouse gas emission, but involving changes in some land surface properties, such as the albedo, the roughness length, the fraction of vegetation or the average root depth, which affect the radiation budget and/or the exchange of heat and water between the surface and the atmosphere. For instance, climate tends to be slightly warmer in the cities compared to surrounding countryside, an effect known as “urban heat island”, and this effect intensifies during a heat wave. Similarly, the microclimate of a forest is different from that of nearby agricultural fields, due to differences in evapotranspiration rates, which result in different efficiencies for recycling water towards the atmosphere. Consequently, it can be expected that local climate will be altered by the changes in land use and land cover caused by man, as a result of urbanisation pressure, conversion of forests or pastures to croplands, or even the replacement of cultivated crop species by others, more adapted to the new climate or simply generating more economic profit. These changes in land use and land cover correspond to changes in the distribution

and structure of the ecosystems. However, changes in the functioning of ecosystems are also impacting local climate. For instance, during a drought, the stomatal cavities at the leaf surface tend to close, which reduces the evapotranspiration rate and thus the latent heat transfer to the atmosphere. The surface temperature will then increase, which enhances the sensible heat flux to the atmosphere at the expense of the latent heat flux. The warming results in an increase of the evaporative demand, inducing a further decrease of soil water, which leads to drought intensification. Moreover, the reduction in evapotranspiration also ends up into a decrease of air humidity in the lower layers of the atmosphere, which may prevent cloud formation and further reduce precipitations. Such feedbacks are quite important during a drought. They tend to increase the intensity and the duration of the drought.

The overall objective of the MASC project (“Modelling and Assessing Surface Changes impacts on Belgian and Western European climate”) was to **study the feedbacks between climate changes and land surface changes** in order to improve regional climate model projections at the decennial scale over Belgium and Western Europe and thus provide better climate projections and climate change evaluation tools to policy makers, stakeholders and the scientific community.

The research has been conducted within a multidisciplinary network involving internationally recognized teams with complementary expertise. This network included five Belgian partners and a French one: (1) the Unit for Modelling of Climate and Biogeochemical Cycles of the University of Liège (coordinator), (2) the department of Meteorological and Climatological Research of the Royal Meteorological Institute of Belgium, (3) the Namur Research Group for Sustainable Development of the University of Namur, (4) the Biology Department of the University of Antwerp, (5) the Department of Forest and Water Management of the University of Ghent, and (6) the Research Group of Atmospheric Meteorology of the National Centre for Meteorological Research, CNRS, Toulouse, France.

In this report, after a quick summary of the objectives and the state of knowledge in the field, we present the methodology used and the main results achieved in the MASC project.

2. STATE OF THE ART AND OBJECTIVES

Impacts of climate change on natural and human systems are now being observed globally and regionally. Latest studies show that changes in regional climates force species to change location seeking for more suitable living conditions, or to alter their phenology; otherwise, those unable to react are facing extinction risks (Thuiller et al., 2008; Wright et al., 2009; Lurgi et al. 2012). There is convincing evidence covering more than a decade of such adaptations already occurring in the temperate regions and at higher latitudes (Hughes 2000; Parmesan and Yohe 2003; Root et al. 2003; Gian-Reto et al. 2005; Lenoir et al. 2008, Thomas, 2010). On the contrary, there is relatively limited evidence of climate change impact on agricultural systems (Peltonen-Sainio et al., 2009), since the constant efforts of adaptation to the local conditions and the phytotechnical measures (varietal selection, fertilisation and irrigation, pest control, technology, etc.) mask the effect of climate change. However, as emphasized by Faloon and Betts (2010), it is expected that the combined effect of climate change and increased CO₂ level in the future should result in an overall increase of crop productivity in Europe. In Belgium, overall growing conditions will improve over the next 30 years and yields could rise considerably, from 37 to 101% according to Ewert et al. (2005).

Scenarios of possible futures indicate that these impacts of climate change will increase, especially if anthropogenic emissions of greenhouse gases continue to rise without any control. When considering climate change responses, it is recommended (e.g., IPCC, 2007, 2014) that efforts should focus on reducing the greenhouse gas emissions (mitigation) and on helping societies and the environment to adapt to climate change (adaptation).

To assess the efficiency of technological/societal innovations set up for mitigation of or adaptation to climate change, it is necessary to develop assessment tools that can reliably simulate climate change at the scale of a country or region at high spatial resolutions. Atmospheric General

Circulation Models (GCMs) currently have a spatial resolution in the range of 100 to 400 km. With such a resolution, only general trends of climate variables on a continental scale can be represented. This is unsuitable to be relevant for small nations such as Belgium. Regional Climate Models (RCMs) with slightly higher spatial resolution are also used and simulation experiments over Europe are already available to the scientific community (e.g., ENSEMBLES project; Hewitt and Griggs, 2004; as well as the ongoing CORDEX initiative; Jacob et al., 2014), but these models are still unable to represent small-scale meteorological systems, like thunderstorms, tornadoes or regional winds systems, which may strongly impact human and natural systems with, for instance, heavy precipitations. To design effective adaptation measures, a better knowledge of the future trends in extreme weather events is required, because these extremes have much more impacts on human population and ecosystems than the mean meteorological conditions (Reyer et al., 2013). Hence, the production of country-scale high-resolution (i.e. less than 10 km) climate projections is a prerequisite to evaluate impacts of future climate change on human societies and ecosystems and formulate adaptation measures.

Moreover, to more accurately simulate climate change, these country-scale climate assessment tools must not only be run at increased spatial resolution, they must also integrate the changes of the land surface, i.e. the changes in ecosystems, land use (LU) and land cover (LC), which can significantly impact local and regional climates through modification of albedo, roughness length and evapotranspiration rates. For instance, Raddatz (2007) has reviewed published evidence of the impacts on regional climate of various land conversions (grassland to dry-land crop, forest to cropland, urban to forest, forest to desert, etc.) or agricultural practices (irrigation, overgrazing, etc.). These land surface changes are mostly the results of the socio-economic evolution of the studied area (demography, new land surface needed for housing, price evolution in agriculture and forestry, development of tourism, etc.) and the existing land management policies (e.g. agricultural/environmental policy, building construction policy, etc.). Conversely, human societies and their economies will be impacted by climate change, because it is bound to affect crop yields or induce damages on human infrastructures if, for instance, the frequency of extreme weather events increases. More generally, climate change will alter the services provided by ecosystems to the society. Human communities will have to face these changes and react by adapting the way they manage the ecosystems and the land surface to optimise ecosystem service production. Obviously, climate, land surface dynamics and socio-economics are closely interacting systems, connected by many feedback loops. Climate projections themselves can alter the evolution of this complex system, since attenuation/adaptation measures, which anticipate climate change, are based on these climate projections. For instance, optimistic climate projections may reduce the need for attenuation or adaptation, and hence climate change may be amplified. In this respect, it is of paramount importance to quantify uncertainties on climate projections.

This link between climate (or any natural systems) and socio-economic systems is known for a long time. However, according to Hibbard et al. (2010), existing studies have not integrated both systems, because the researches are conducted by separate scientific communities. For that reason, the feedbacks between climate and socio-economic systems have largely remained unexplored. As an example, at the global scale, integrated assessment models (IAM) have been widely used to study interactions between socio-economy, energy needs and energy production with the purpose of providing greenhouse gas emission scenarios. Examples of such emission scenarios are the SRES scenarios of IPCC (Nakicenovic et al., 2000). These scenarios were the basis of the GCM global climate simulations performed for the fourth assessment report (AR4) of IPCC (Meehl et al., 2007). In a similar way, scenarios of greenhouse gases concentrations, named representative concentration pathways (RCP scenarios, Moss et al., 2010) have been established for the CMIP5 (Coupled Model Intercomparison Project Phase 5; Taylor et al., 2012) experiments that have been used in the fifth assessment report of IPCC (AR5). Besides greenhouse gas emissions or concentrations, IAMs also provide other climate forcings in the form of scenarios, such as land use/land cover (LULC), to the climatic community. These are also used in the climate projections. However, the focus on how the

results of the climate models can impact IAM projections has not been very much studied (Hibbard et al., 2010), so that the feedbacks between socio-economic systems and climate remain largely unknown. This remains true at the continental/regional scales, where previous studies were also largely based on scenarios, such as for studying the climatic impacts of deforestation/afforestation (e.g., Bala et al., 2007; Bonan, 2008) or land degradation/desertification (Sivakumar, 2007, and references therein). Over Europe, land use scenarios for the future have been constructed within the ALARM project (Spangenberg, 2007).

The interactions between land surface and climate are complex (Figure 1). Climate (as well as CO₂ and O₃) changes can affect ecosystem structure and functions, by altering photosynthesis and productivity or inducing thermal and hydric stresses on plant species. These ecosystem changes then impact socio-economic systems, through for instance a reduction of incomes in agriculture or forestry and ultimately can lead to changes in land use. These climate-induced changes in land use add to those associated with other (non-climatic) factors, such as urbanisation pressure. These overall changes in land use and ecosystems feedback on the climate system by (1) modifying the surface properties (albedo, roughness, evapotranspiration, etc.) which alter the local/regional atmospheric circulation and by (2) changing the ecosystem emission (or sink) of greenhouse gases (mainly CO₂, CH₄, N₂O) in the atmosphere. The first factor has a direct effect on climate at regional scale, while the second affects climate through the atmospheric budget of greenhouse gases, which means that it impacts climate via the global system, since the residence time of major greenhouse gases in the atmosphere is longer than the mixing time of the atmosphere. Regional climate/land surface models can thus only address the first type of feedbacks. For the second type, these models can only evaluate the contribution of the local/regional land use change to the global greenhouse gas budget. A third (less understood) type of feedback can also occur through the emission from the land surface or vegetation of aerosols (e.g., soot from forest fires or dust from dry areas) or of (non methane) biogenic volatile organic compounds (BVOCs). Aerosols impact the absorption of radiation in the atmosphere and can also serve as condensation nuclei in the formation of cloud droplets (Forster et al., 2007). BVOCs can impact the budget of atmospheric methane and increase the formation of some aerosols (Peñuelas and Staudt, 2010). Both emissions can significantly influence regional climate, although the processes are still poorly quantified.

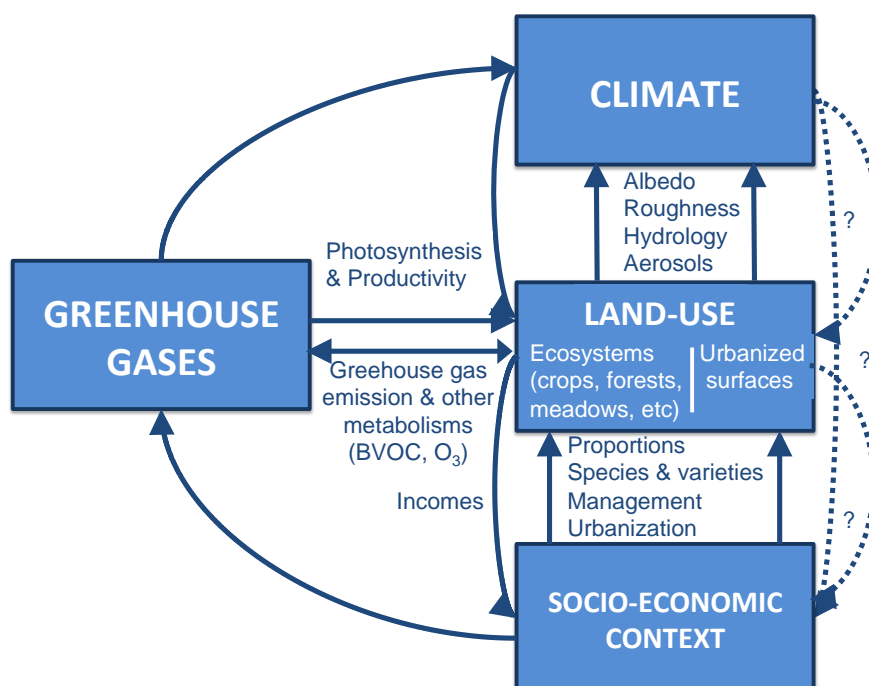


Figure 1: Schematic illustration of the complex interactions between climate and land surface

Other poorly quantified aspects are the interactions (dotted arrows in Figure 1) between socio-economic systems and land use, as well as the socio-economic response to climate change and associated land use change. Modelling these interactions is a challenge, but it is also a necessity for the quantification of climate feedbacks and the achievement of more realistic climate change projections. Fontaine et al. (2014) have presented a new method to quantify these interactions (named hereafter "land surface dynamics"): the VOTES methodology combining a dynamic vegetation model (DVM), describing ecosystems, with an agent-based model (ABM), describing ecosystem management and land use changes as the response of a set of pre-defined agents to the socio-economic context and climate change. The approach has been developed within the VOTES project funded by BELSPO and applied to an area covering four municipalities in central Belgium.

The objectives of the current project were to study the feedbacks between land surface changes and climate over Belgium and Western Europe, by combining high-resolution models of the climate and of the land surface. More specifically, the objectives were:

- (1) to produce **high resolution projections of climate and land use/land cover changes at the decennial scale (2013-2030) over Belgium and Western Europe**, taking the **feedbacks** between all these changes into account,
- (2) to assess the **impacts of expected land surface changes** related to ecosystem cover (including structure, functioning and management) and socio-economic use **on the future climate** of Belgium and Western Europe,
- (3) to evaluate **the impacts** of the resulting climate and land surface dynamics **on the carbon budget of land ecosystems** (crops, meadows, forests, wetlands, etc.).

To reach these objectives, we combine a high-resolution version of the regional climate model ALARO (Gerard et al., 2009) and its externalized surface scheme SURFEX (Masson et al., 2013) with a land surface dynamics (LSD) module. This module is based on the CARAIB DVM (Dury et al., 2011) coupled to an ABM (ADAM, Beckers et al., 2018), specifically developed for this project and addressing spatial scales ranging from the agricultural parcel to the whole territory of Belgium. The transfer of information between the regional climate model (ALARO/SURFEX) and the LSD module will be made through a coupler developed within the framework of the ECOCLIMAP II database (Faroux et al., 2013) used by SURFEX.

3. METHODOLOGY

In this section, we first present the data that have been gathered by the project partners and that were necessary to feed or test the various models that are run and assembled in MASC. Then, we shortly describe these models themselves, their upgrade and the methodology used for their validation during the project. The models include three vegetation or forest ecosystem models (CARAIB, ISBAcc, and 4C), the agent-based model (ADAM) and the regional climate model (ALARO).

3.1. DATA

3.1.1. DATA FOR VEGETATION MODELLING

The use of the CARAIB model, at the Belgian scale and for the MASC objectives (e.g., for crop yield simulations), requires the gathering of many data, for model inputs as well as for model validation.

Input data

During the design of the agent-based model, we need a first reliable LU dataset to adapt and test our dynamic vegetation model. We prepare a “working” LU dataset, based on the combination of the LU data from the Flemish (from the ECOPLAN project funded by the Flemish agency for Innovation by Science and Technology, 2013-2016) and Walloon (COS-W - <http://geoportail.wallonie.be/catalogue-cartes>) regions of the country. This dataset meets the DVM and project requirements: based on the 1 km grid of the project and simplified, to stick to the 6 land use (forests/natural vegetation, crops, pastures, urban, water, rocks) and to the 6 crop cover (winter wheat, fodder maize, potatoes, sugar beets, winter barley, rapeseed) classes. The crop cover classes (Figure 2) were defined for each municipality thanks to the statistical data from FPS Economy (<https://statbel>) between 2000 and 2007. The simulations performed at this scale require also more detailed inputs for soil texture data (the original data were from the Harmonized World Soil Database) and, in consequence, the map (Figure 3) was improved on the basis of Flemish Soil Associations Map (AGIV – GDI Vlaanderen) and the Digital Soils Map for the south of the country (“Carte Numérique des Sols de Wallonie, Belgique - <http://geoportail.wallonie.be/catalogue-cartes>).

The scale and the project objectives lead to the addition or the improvement of the different vegetation input parameters, both for crops, pastures and forests/natural vegetation. Regarding forests, CARAIB is run with tree species instead of plant functional types. Thus, in addition to input parameters, these simulations require the selection of (1) the most representative Belgian trees species and (2) the use of data giving the relative abundance of each species. These data should cover the whole area and be spatially explicit at the adopted resolution, i.e. at 1 km². This is important not only for running CARAIB, but also to model the Meta-Agents and their behaviour rules for forests in Belgium. Such data exist for Flanders, coming from the Flemish Forest Inventory, but it does not exist for the Walloon region. Forest attribute data covering the Walloon region largely pertain to owner’s status, pedological region and species distribution. This data, while reasonably up to date, is not spatially explicit. Interpolation or random spreading of the statistics is not an appropriate method for the nature of the data (forest-stands). This renders the presently available data unsuitable to underpin a strategy for an active forest agent, as planned initially in the project. Consequently, it was decided to leave the active forest-agents out of the ABM. The influence of this decision will be minimal because the projected period is considered short in terms of forest management.

The best available homogeneous forest data can be provided directly to the DVM, i.e. forest area (per species/stand type) by natural region, coming from the Walloon and Flemish Forest Inventory. As this is especially important for the main forested regions in the south of the country, we supplement these data with data from the “Walloon Forest Inventory”. Based on that, we fixed a list of 14 species and we roughly adjusted the species relative abundances by agricultural region in order to stick to the data from the forest inventory (Figure 4).

Validation data

For this step, we mainly need data for the validation of the crop module. In consequence, we collected data for the site level validation from sites with eddy-covariance measurements (FLUXNET network, sites of Lonzée in Belgium and Grignon in France). These data were supplemented with yield data from the Belgian statistics at the Belgian and Agricultural Regions scales (Figure 5) available between 1980 and 2016. Note that eddy covariance data from several forest sites were also acquired to validate forest tree productivity and growth in the models.

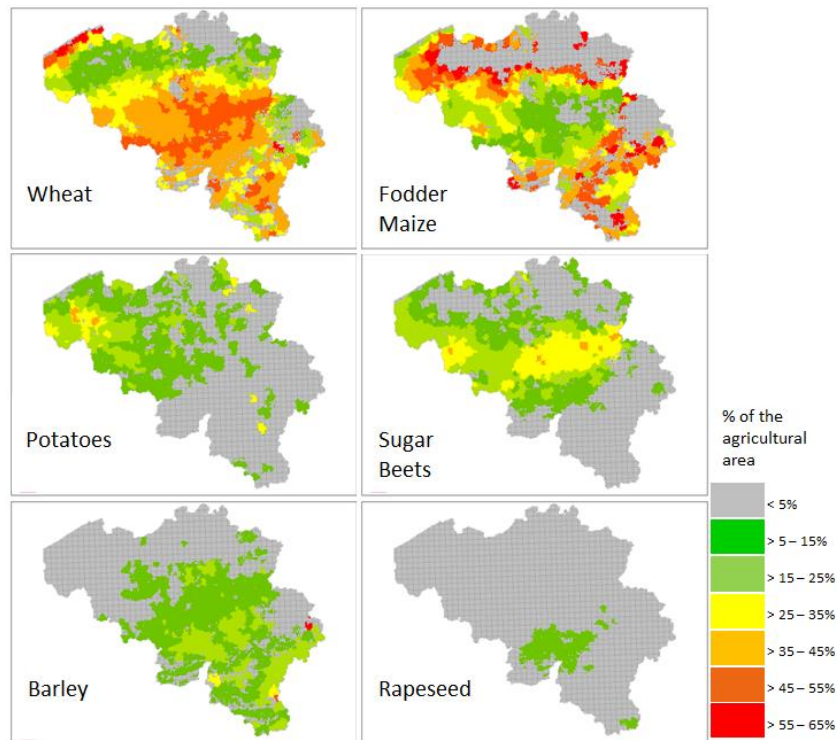


Figure 2: Percentage of a given crop area in the agricultural area (based on the simplification of the agricultural statistics) by pixel (1km²)

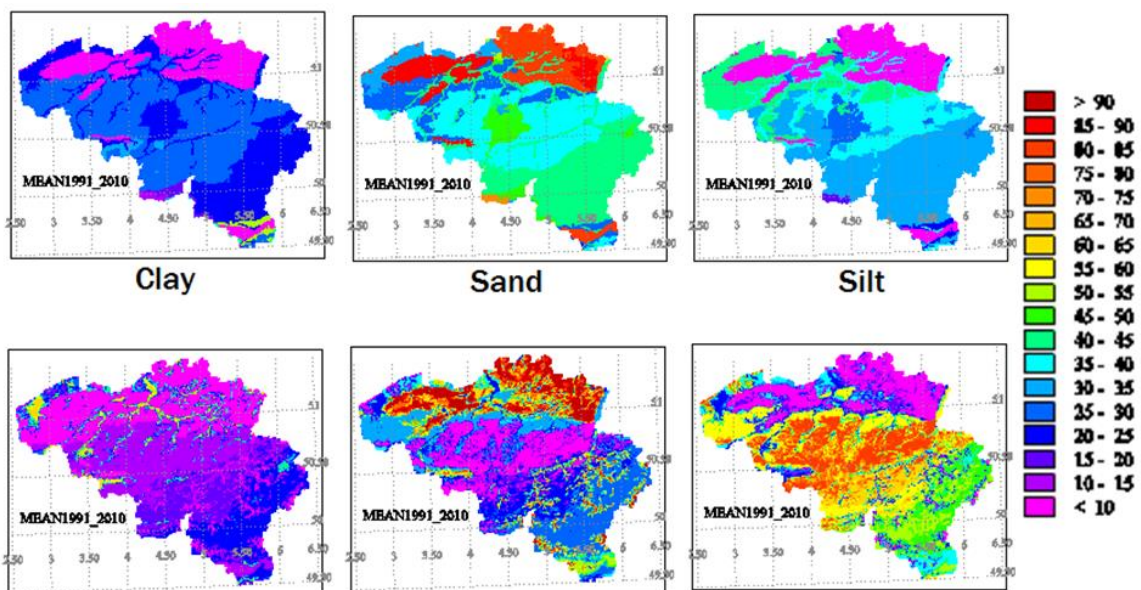


Figure 3: Top, the former soil texture map from the Harmonized World Soil Database and, bottom, the new soil texture map drawn up for the MASC project.

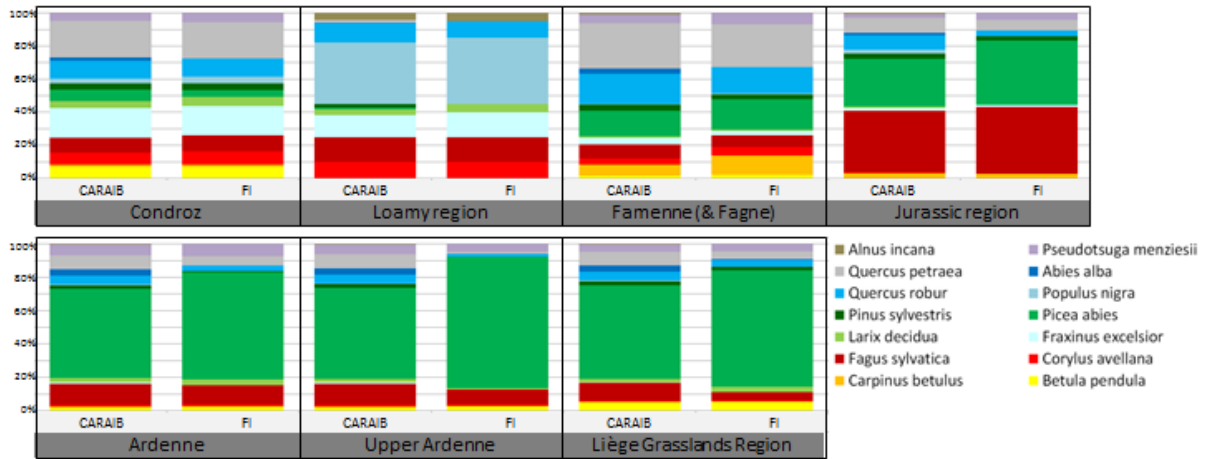


Figure 4: Comparison of the tree species relative abundance (per agricultural regions) between the CARAIB inputs and the Walloon forest inventory (FI).

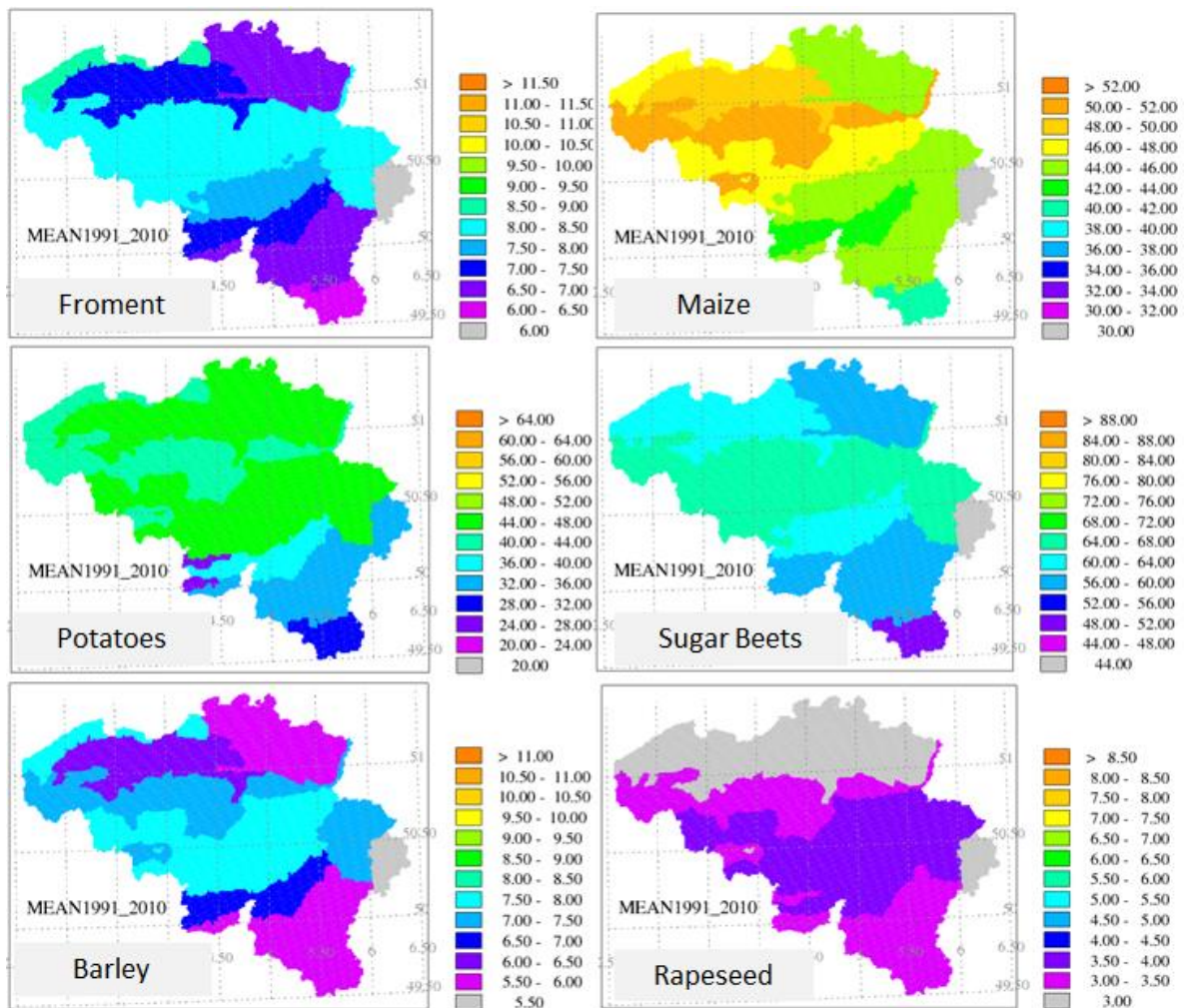


Figure 5: Average yield between 1991 and 2010 (based on the agricultural statistics - <https://statbel>)

3.1.2. DATA FOR LAND USE CHANGE MODELLING (AGENT-BASED MODELLING)

Agricultural population data

Data providing information on the agricultural population was obtained from the agricultural surveys, which were organized for a long time on a yearly basis by the National Institute of Statistics of Belgium (NIS) (Statistics Belgium, 2015). The data of the survey of 2000 were used to create a realistic farmer population in the initialization phase of the model. Later surveys were used to calibrate and validate the modelled results.

Agricultural land use data

The agricultural LU data are derived from the “Système intégré de gestion et de contrôles” (SIGEC) and “Landbouwgebruikspcelen” datasets, which contain data at the agricultural parcel level for respectively Wallonia and Flanders-Brussels. The combined data for 2000 of Flanders, Brussels and Wallonia are used to initialize the model.

Crop yield data

The crop yield data are obtained from CARAIB and are further discussed in the sections on the dynamic vegetation model and on the coupling.

Urbanisation and forest data

Data on urbanisation are obtained from the LU change data created during the BELSPO GroWaDRISK project. Projections were made with yearly outputs until 2040 under different scenarios: a business-as-usual scenario, a global economy scenario, a strong Europe scenario and a regional communities scenario.

Other data

Apart from these datasets, the model uses data on the mortality rates for the male Belgian population in 2000 for each age, from 18 until 105, where the chance of decease is put on 100%. This dataset was chosen since in Belgium, farmers are still mostly male (85% in 2000, Statistics Belgium, 2015) and mortality rates differ between sexes at all ages. For the economic data on the prices per ton for each crop, the yearly producer prices in local currency unit per ton from the database of the Food and Agricultural Organization of the United Nations (FAO) for Belgium-Luxembourg from 2000 to 2015, are used.

3.1.3. UPGRADE OF THE ECOCLIMAP DATABASE

The ECOCLIMAP database was updated using the ESA-CCI Land Cover map. This new release of ECOCLIMAP was called ECOCLIMAP-SG (Second Generation). A first version of ECOCLIMAP-SG is now freely available (<https://opensource.umr-cnrm.fr/projects/ecoclimap-sg>). It was shown that issues in the old version of ECOCLIMAP (1km x 1km) over Belgium (e.g., underestimation of the forest, grassland, and crop fractions in the regions where they are dominant) are mitigated to a large extent by ECOCLIMAP-SG (300m x 300m). This is illustrated in Figure 6 for the fraction of forests.

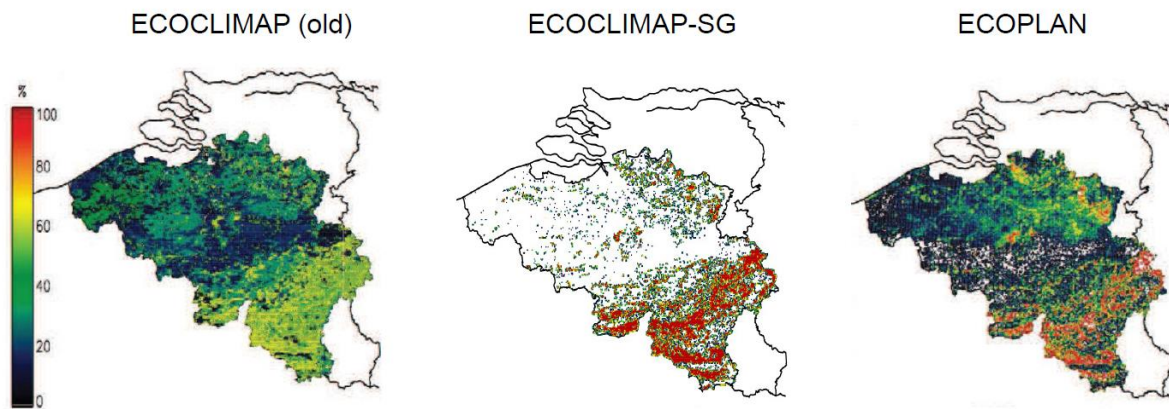


Figure 6: Fraction of forests over Belgium at a spatial resolution of 1km x 1km: comparison of old ECOCLIMAP (Faroux et al., 2013) and ECOCLIMAP-SG (Second Generation) with the ECOPLAN reference dataset.

Finally, the ability of LDAS-Monde to retrieve key model parameters (in addition to the analysis of model state variables) was evaluated. The calibration of key model parameters using LDAS-Monde was evaluated by Dewaele et al. (2017). It is shown that the sequential assimilation of the Copernicus Global Land GEOV1 LAI product can be used to estimate the maximum available water content of the soil (MaxAWC) for straw cereals over France. This parameter is key for drought modelling and impacts LAI increments resulting from the assimilation. Minimizing these increments is a way to retrieve this soil parameter. This shows that LAI products can be used to better constrain model parameters relevant for hydrological applications. Dewaele et al. (2017) also showed that observed LAI characteristics can be directly used to estimate MaxAWC for straw cereals. Using MaxAWC values derived from LDAS-Monde as a reference, a correlation is found between the median annual maximum LAI and MaxAWC. Using this simple linear regression model, MaxAWC can be estimated with a RMSD score of 28.7 mm.

3.2. THE MODELS, THEIR UPGRADE AND THE METHODOLOGY FOR VALIDATION

3.2.1. VEGETATION MODELLING

Several process-based vegetation models were used to address the questions raised in the project. They are briefly described below.

CARAIB (CARbon Assimilation In the Biosphere) is a physically-based DVM developed to study the role of the vegetation in the global carbon cycle (Warnant et al. 1994; Gérard et al. 1999) and to study the vegetation distributions in the past (François et al. 1998, 2011; Henrot et al. 2017), in the present and in the future (Laurent et al. 2008, Dury et al. 2011). In this model, the plant units can be plant functional types (PFT) or species. The possibility of simulating species makes this model well designed for conducting studies at small spatial scales, such as over a region or a small country like Belgium. CARAIB includes several modules dealing with (i) soil hydrology, (ii) photosynthesis and stomatal regulation, (iii) carbon allocation and biomass growth, (iv) litter and soil carbon dynamics, (v) vegetation cover dynamics, (vi) seed dispersal, and (vii) vegetation fires. Climate and other environmental parameters (e.g., atmospheric CO₂) are the primary inputs to the DVM. The model calculates all major water and CO₂/carbon fluxes and pools. Many upgrades of the model were performed in the framework of the MASC project (see below).

The interactions between soil, biosphere and atmosphere (ISBA; Noilhan and Mahfouf 1996; Gibelin et al. 2008; Masson et al. 2013) land surface model simulates the soil-plant system in the “surface externalisée” (SURFEX) open-source modelling platform. SURFEX (<https://www.umr-cnrm.fr/surfex/>) is mainly developed by CNRM but is shared with many meteorological services in

Europe (e.g. Belgium) and in North Africa. The ISBA model includes a CO₂-responsive option (called here ISBAcc for ISBA – Carbon Cycle) able to simulate photosynthesis, plant growth, autotrophic and heterotrophic respiration, and net primary production. ISBAcc is able to represent the inter-annual variability of vegetation variables such as LAI, as well as the impact of climate change and CO₂ concentration rise on LAI, and on sub-daily water, CO₂ and energy fluxes (Laanaia et al. 2016, <https://doi.org/10.1016/j.crm.2016.06.001>). A range of PFTs is simulated by ISBA-cc and the water and carbon budget is simulated for each PFT within a model grid-cell. A relatively parsimonious approach is used in ISBA and the number of key plant and soil parameters is limited. Model parameters are geographically distributed using the ECOCLIMAP database within SURFEX. ECOCLIMAP is based to a large extent on satellite-derived observations and on look-up-tables. An open-source land data assimilation system called LDAS-Monde (<https://www.umr-cnrm.fr/spip.php?article1022>) was developed in the SURFEX environment. It is now the only LDAS able to sequentially assimilate satellite-derived vegetation data such as LAI together with surface soil moisture observations.

4C (FORESEE – FORESt Ecosystems in a changing Environment) is a stand-scale, process-based model developed to study the effects of environmental change on forest ecosystems (Bugmann et al. 1997; Suckow et al. 2001; Lasch et al. 2005). It is used here with the aim of comparing the performances of the two large-scale vegetation models used in the project with those of a more detailed stand-scale forest model.

The main features of the models are summarized in Table 1; a more extensive overview of the model processes, model input variables and model specifications for the set-up is presented in Tables A1 (CARAIB), A2 (ISBA_{cc}) and A3 (4C).

Table 1: Short description of the main features of the models used in the project

Model characteristics	CARAIB	ISBAcc	4C
Spatial scale	grid or point scale	grid or point scale	stand-scale
Smallest temporal Scale	2-hourly	hourly	daily
Spin up	Yes	yes	no
Plant functional type options	Multiple	multiple	only tree species
Number of PFT dependent parameters	55	40	99
Number of calibrated tree (PFT) species	15 (26)	8	14
Forest structure	one layer of trees and one layer containing herbs and shrubs	one layer of trees	cohorts with different tree characteristics
Driving variables	CO ₂ , air temperature, amplitude of air temperature (T _{day_{max}} -T _{day_{min}}), precipitation, air relative humidity, short-wave incoming radiation, wind velocity	CO ₂ , air temperature, precipitation, air relative humidity, short-wave incoming radiation, long-wave incoming radiation, wind velocity	CO ₂ , air temperature, precipitation, air relative humidity, net radiation, wind velocity
Developed in	University of Liège, Belgium	Météo France/CNRS, Toulouse, France	Potsdam Institute for Climate Impact Research, Germany

CARAIB is the vegetation model that was selected in this project with the aim of (1) producing high resolution (1 km²) spatial simulations over the Belgian territory (i.e., over a mosaic of different LC units, including forests, crops, pastures and urban areas), and (2) coupling the model with an ABM to produce LU change maps designed to force the ALARO regional climate model (see below).

Within the MASC project, the model was adapted and improved. Initially, the standard spatial resolution of the model was 10'x10' in longitude and latitude, and the model could be run with either plant functional types (PFT) or species (up to 100 different modelled species for European-scale simulations). For the simulations over Belgium, the model has been (1) downscaled and used to perform high-resolution (at 1x1km) simulations and (2) it was performed for a selection of species only (trees and crops). This selection of crop species led to another major development involving the improvement of the crop module for simulations at the Belgian scale. Compared to the initial version of the crop module (developed in the framework of the VOTES project, funded between 2010 and 2012 under SSD programme from BELSPO), several parameters were adapted (growing degree-day sums, base temperature, C:N ratio, specific leaf area,...). We can also emphasize that:

- the module now allows the simulation of crop growing over 2 civil years (which is especially important for winter cereals in Belgium) ;
- we integrate the yield calculation in the model, based on several parameters, gathered and sometimes calibrated for Belgium, as the water content, the carbon ratio (dry matter vs. carbon matter) and the harvest index ;
- the module can now stop the crop growing period when the required growing degree-day sum is not reached within a fixed number of days (defined for each crop) ;
- with the aim of introducing more contrasted results between the north and the south of the country, we have adapted the crop mortality (of the “green” reservoir) based on a new critical threshold for water stress and we have added a critical threshold when the soil is saturated.

Other important changes were also performed in order to prepare the coupling with the agent-based model and the joint use of CARAIB with the regional climate model. For instance, several routines were added in the code to allow explicitly in the model the possibility of changing land use from one year to the next, including the quantification of related impacts on the ecosystem carbon budget. Also, some parametrizations of the acclimation of photosynthesis and respiration to higher CO₂ and warmer temperatures were implemented. Finally, some refinements of the surface albedo parameterization were performed and trait data for the species to be simulated were retrieved from the TRY database (<https://www.try-db.org/TryWeb/Home.php>).

Regarding the validation of the crop module, it consists of 2 steps:

- a comparison with eddy covariance data on several FLUXNET sites in Belgium and Western Europe (France, Germany,...), in terms of carbon and water fluxes (GPP, NEE, ET), for the main crops (winter wheat, sugar beets, maize,...),
- spatial simulations of the CARAIB DVM (with actual LU and LC) at 1 km² have been run over the Belgian territory for crops with ALARO daily climate forcing (1 km climate derived from 4km-ALARO simulation) and compared with the yearly average yields for Belgium and agricultural regions.

This validation is presented in section 4.

3.2.2. AGENT-BASED MODELLING

Agricultural land use change is modelled by using the ABM 'ADAM' (Agricultural dynamics through agent-based modelling) (Figure 7). ADAM simulates the number of farmers, the size of farms and the corresponding land use at the parcel level, trying to capture the main current processes of farms' abandonment or growth. The model starts from a set of different types of farmers that are combined with agricultural parcels to create farms. The farmers and their farms have different characteristics, listed in Table 2: a farm is of a certain farm type and is managed by a farmer of a certain age. The farm consists out of a number of parcels that, combined, form the entire of the farm and determine the total acreage or size of the farm. A combination of internal (farm size, farm type) and external (market, policies and physical environment) properties together form the profitability of a farm. The model is driven by the decisions yearly made by the individual farmers. Every year, farmers can make the following decisions: (1) continue or stop farming, (2) take over an entire farm or an individual parcel, (3) keep or change the agricultural land cover of a parcel. These decisions are steered by the (1) characteristics of the farmer (age), (2) the characteristics of his farm (size and type of the farm, parcels' location) and (3) the environment (type and location of parcels that have become available).

In the first phase, each farmer decides whether he continues or stops farming. A farmer will stop farming if he retires or dies. Since many farmers continue farming, even after they reach the legal retirement age, a farmer will retire immediately if he has a successor. If there is none, farmers continue and might decide to retire when they are older.

In the next phase, new farmers enter the system by taking over the farms of farmers that stopped farming and are considered profitable. Profitability is determined through the proxy of farm size and dependent on farm type. The age of the newcomer taking over the farm is set to an age normally distributed around 30 with a standard deviation of 5 and a lower limit of 18 year. Farms that have not been taking over are being split up: the parcel with the home of the farmer is no longer considered to be agricultural land but becomes a residential parcel and leaves the system. The remaining parcels are then taken over by farmers with nearby parcels, with priority given to farmers from the same farming type as the previous owner or who can easily convert the parcel to a desired agricultural land use (crop land, permanent crops and grassland are easily converted, while greenhouses and agricultural buildings are more difficult and costly to convert).

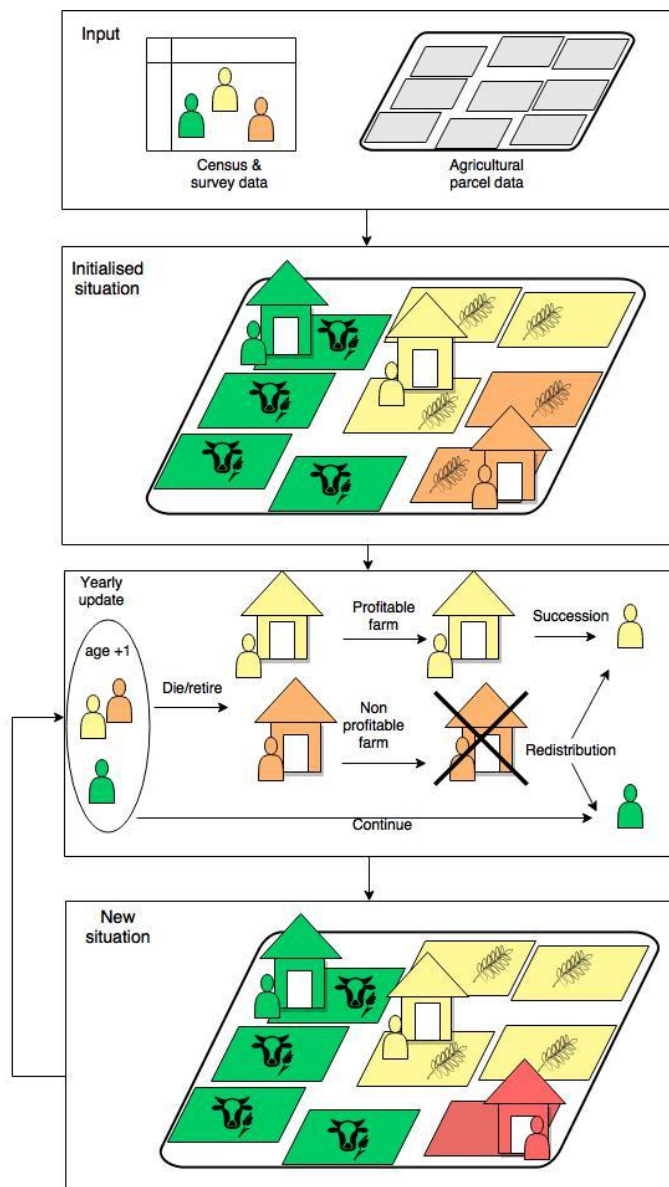


Figure 7: Overview of the ADAM model

Table 2: Overview of the different variables representing the characteristics of farms and farmers in the model

Variable	Variable type	Update
Farm type	Categorical: arable farming, land based animal farming, barn animal farming, greenhouse farming, permanent crop farming	Farm keeps type but individual parcels can be taken over by farms from different type
Age of farmer	Continuous	Yearly update, changes when farmer is succeeded
Parcel	Geographical variable	Owner and agricultural land use can change if parcels are taken over
Farm size	Continuous: sum of size of parcels cultivated by the farm	Increases when farm takes over other parcels
Profitability	Continuous	Depends on a combination of internal and external properties of the farm

In the last phase of the model, the agricultural land use is updated. Agricultural land use change happens due to take over by neighbouring farmers after retirement and by yearly crop farmers changing the crop they grow on the parcel. The new crop is chosen based on the market price per ton for each crop and the expected yield in ton for each crop (which is obtained from the DVM). Farmers can choose between the 6 most prominent crops in Belgium: wheat, barley, maize, sugar beet, rapeseed or potatoes.

Application for Belgium

To initialize the model, the available statistical data from agricultural surveys are used in order to create a situation as close as possible to reality. The first step is the creation of the different individual farmers of different types with a certain age, located in a municipality and who will manage a certain farm type with characteristics according to Table 3. Once the farmer population is created, each farmer receives a first parcel as their home parcel. This parcel contains agricultural buildings according to the parcel dataset (or a random other parcel if there are not enough parcels with agricultural buildings). From this initial parcel, the farm starts growing by adding neighbouring parcels that suit the farmer's type (barns, grassland, greenhouses, permanent crops, arable land). Any remaining parcels are randomly added to a neighbouring farm. The profitability threshold was set to twice the average farm size of each farm type. Below the threshold, profitability or succession probability is directly proportional to the size of the farm (Figure 8).

Forest cover change and urbanisation

Both forest cover change and trends in urbanisation are derived from the results obtained from the GroWaDRISK Belspo project. The agricultural data from the ABM at parcel level is combined with the land use maps of GroWaDRISK to produce area covering land use maps for the entire country.

Interfacing with the dynamic vegetation model

The land use maps, obtained from the land use change model, are generalised to land use percentages per 1kmx1km raster cell, usable as input for the dynamic vegetation model.

The results on yield expectations from the DVM are used to provide the farmers in the ABM information on choosing the crop they will cultivate the coming year.

Table 3: Characteristics of different farm types

Farm type	Main parcel type	Common agricultural product	Take-over preference	Profitability threshold
Yearly rotating crop farmers	Arable land with temporary crops	Wheat, barley, maize, beets, potatoes, rapeseed	Arable land with temporary or permanent crops	80 ha
Greenhouse farmers	Greenhouses	Tomatoes, bell peppers, cucumbers, zucchinis	Greenhouses	7 ha
Barn based animal farmer	Barns	Meat (pork & poultry) & eggs	Barns	30 ha
Land based animal farmer	Barns and grassland	Meat (beef)	Barns and grassland	60 ha
Permanent crop farmers	Arable land with permanent crops	Apples, pears, cherries	Arable land with temporary or permanent crops	40 ha

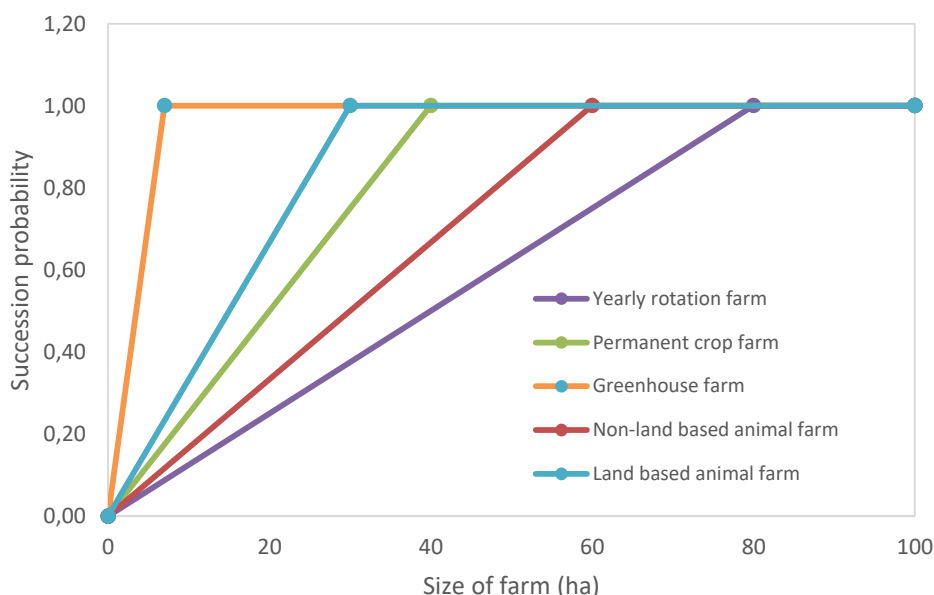


Figure 8: Chance of succession of every type of farm in function of the size

3.2.3. REGIONAL CLIMATE MODELLING

The regional climate model used within this project is the ALARO-0 model, a configuration of the Aire Limitée Adaptation Dynamique Développement International (ALADIN) model with improved physical parameterisations (Gerard et al., 2009), and its first baseline version released in 1998.

The ALADIN model is the limited area model (LAM) version of the global scale Action de Recherche Petite Echelle Grande Echelle Integrated Forecast system (ARPEGE-IFS) (Bubnovà et al., 1995; ALADIN International Team, 1997). An extensive collaboration, established in 1992, currently exists of 16 national services to maintain and develop the shared high-resolution Numerical Weather Prediction (NWP) System of ALADIN. Meanwhile, ALADIN has been further developed with updated parameterisations for the physics part, and this model configuration called ALARO has been operating at the Royal Meteorological Institute of Belgium (RMI) for its operational numerical

weather forecasts since 2010. The ALARO-0 model has proven its potential for regional climate modelling (Hamdi et al., 2012; De Troch et al., 2013; Giot et al., 2016).

A key parameterisation within regional climate modelling is the land surface parameterisation. It describes the exchanges of energy and water between the low-level atmosphere, vegetation and the soil surface (Prein et al., 2015). Initially, the ALARO-0 model used the land surface scheme Interaction Soil-Biosphere-Atmosphere (ISBA, Noilhan and Planton, 1989; Noilhan and Mahfouf, 1996). Meanwhile the more recent Météo-France SURFace Externalisée land surface model (SURFEX, Masson et al., 2013) has been implemented in the ALARO-0 model (Hamdi et al., 2014). This motivated the use of SURFEX as the land surface component for ALARO-0 in a regional climate modelling setup and replace the prevailing setup at the RMI of ALARO-ISBA (De Troch et al., 2013).

The continuous optimisation of the ISBA scheme for natural surfaces, together with the development of an urban scheme, led to the construction of the externalised surface scheme SURFEX (Masson et al., 2013). To account for subgrid heterogeneities, it uses a tiling approach with each tile providing information on the surface fluxes according to the type of surface: nature, town, inland water and sea. The surface fluxes are then spatially averaged over the whole grid box, while the atmospheric forcing is assumed to be homogeneous. The initial parameterisation ISBA for the nature tile was conserved, and the Town Energy Balance (TEB, Masson, 2000) was added as a parameterisation for the town tile. TEB uses a canopy approach with three urban energy budgets for the layers roof, wall and road. Besides, parameterisation schemes were added for inland water and seas.

The nature tile is divided into subtiles, referred to as patches to account for the variety in soil and vegetation behaviour. In SURFEX version 5, twelve patches correspond to the plant functional types described in ECOCLIMAP (Masson et al., 2003). ECOCLIMAP is a global land cover database at 1 km horizontal resolution and the original version ECOCLIMAP-I consists of 215 cover types. Each cover type is an ensemble of pixels with similar surface characteristics. The classification was established using land cover maps and satellite observations. Beside this classification, ECOCLIMAP provides a dataset with surface parameters depending on the land covers and plant functional types, such as leaf area index, albedo, etc. These physiographic data, together with topography data (GTOPO30, Gesch et al., 1999) and soil properties (FAO, 2006), fully interact with SURFEX.

The externalisation of SURFEX has led to the possibility of running SURFEX in a stand alone/offline mode, where only the meteorological forcing is provided, or a fully coupled mode with several atmospheric models (Masson et al., 2013). SURFEX allows for exchanges between the surface and the atmosphere through a standardised interface (Best et al., 2004). At each model time step, the atmospheric model provides the atmospheric forcing to SURFEX for the upper-air temperature, specific humidity, zonal and meridional wind components, atmospheric pressure computed at the lowest atmospheric model level and incoming global radiation, incoming longwave radiation and total precipitation. In return, SURFEX simulates momentum, heat and water fluxes. The standard meteorological variables such as 2 m temperature, relative humidity and 10 m wind are computed prognostically from the surface boundary layer. This can be done using an extrapolation downward from the atmospheric variables at the forcing level by the classical approach of Paulson (1970) or by adding multiple prognostic layers from the ground up to the lowest model level (Hamdi and Masson, 2008; Masson and Seity, 2009) or by the interpolation method of Geleyn (1988). When fully coupled to an atmospheric model, SURFEX sends the computed quantities back to the atmosphere, where it is used as the surface boundary condition (Masson et al., 2013).

The implementation of SURFEXv5 within ALARO-0 has shown its potential for NWP (Hamdi et al., 2014). The results over Belgium have shown neutral effects on the winter 2 m temperature and on the vertical profile of the wind speed, as compared to the original ISBA scheme. However, it has shown positive effects on the summer 2 m temperature, 2 m relative humidity, and resulted in improved precipitation scores. This validation is a prerequisite to the implementation of SURFEX within ALARO in the context of long-term climate simulations.

The coupled model ALARO-0 and SURFEXv5 is validated and used for regional climate modelling, considering the previously mentioned model configurations in a long-term modelling context. ERA-Interim and CNRM-CM5.1 have been downscaled using ALARO-SURFEX. The intermediate domain is centred around Western Europe, and the high-resolution domain is centred around Belgium. The intermediate domain used in this project has a spacing of 20 km, the equivalent of 149x149 grid boxes. Likewise, the high-resolution domain has a spacing of 4 km, the equivalent of 181x181 grid boxes.

Within this project, the ERA-Interim reanalysis product is used for the validation of ALARO-0 coupled to SURFEXv5. Beside validating the models performance, the RCM is used for studying the impact of increasing greenhouse gases on the climate. It is better suited to provide climate projections at the spatial detail required compared to GCMs (Rummukainen, 2010). The dynamical core of ALADIN/ALARO is shared with its parent GCM ARPEGE. In the context of the Fifth Phase of the CMIP (CMIP5), a new version of ARPEGE called CNRM-CM5.1 has been developed by Voltaire et al. (2013). Its spatial resolution is about 1.4° (about 150 km) in both longitude and latitude, with 31 vertical levels. The climate change signals are determined by taking the difference between the climate in a future scenario period (RCP4.5 and RCP8.5) and the recent past climate (hereafter called historical).

Dynamical downscaling approaches

To evaluate the sensitivity of the model to the update frequency of the initial conditions, three types of downscaling approaches were conducted with ALARO-0 coupled to SURFEXv5 and are: (i) a continuous mode for both the atmosphere and the land surface (hereafter called CON ("CONTinuous")), (ii) an approach with daily reinitialisation for both the atmosphere and the land surface (hereafter called DRI ("Daily Reinitialisation")), and (iii) an approach that tries to find the best compromise between previous two approaches with daily reinitialisation of the atmosphere and a continuous mode for the land surface (hereafter called FS ("Free Surface")).

3.3. COUPLING OF THE MODELS

The coupling of the 3 different models involved in the project (ALARO, ADAM and CARAIB, respectively the RCM, the DVM and the ABM) is managed by a new module written in Fortran. This module can be summarized by 5 steps:

- The yearly loop starts with a CARAIB simulation (for the reference year 1999);
- The CARAIB outputs are processed, in order to stick to the requirements of ADAM and be readable by the model ;
- An ADAM simulation is launched (for 2000), using the average yields of the previous year (1999) ;
- The ADAM outputs are processed, aiming at simplify the LU classes to stick to the CARAIB surface scheme (one LU file with 6 classes and one LC file with 6 crops species) ;
- Finally, the ADAM outputs are once again used to produce the LU files for ALARO (following the requirements of the ECOCLIMAP classification).

This procedure implies the need of 2 land use conversions, a first one between ADAM and CARAIB and the second one between the coupled system ADAM-CARAIB and ALARO-ECOCLIMAP (Table 4). Regarding this second conversion, the different rules were fixed in order to stick as much as possible to the initial land use map (from ECOCLIMAP) used by ALARO.

Coupling of the ALARO-SURFEX model with the CARAIB model

The results of ALARO-SURFEX for the present and future climate have been provided as input for the CARAIB model. Next, the land use scenario for Belgium as output from the CARAIB model coupled to the ABM serves as input for ALARO-SURFEX. The first step was to link the species that

come out from CARAIB with the land cover types in ECOCLIMAP. For Belgium, a total of 40 different land cover types were present from ECOCLIMAP.

Table 4: On the left, LU classes equivalence table between ADAM and CARAIB and on the right, LU classes equivalence table between the coupled system outputs ADAM-CARAIB and ALARO (ECOCLIMAP).

ADAM		CARAIB	1 st criteria	2 nd criteria	3 rd criteria	ECOCLIMAP classes	
Class #	Name		CARAIB Dominant Class	ADAM Dominant	CARAIB classes	Class #	Name
101	Winter wheat	Crop	Water	Harbour	Urban > 40%	2	Inland waters
102	Barley	Crop				157	Port facilities
103	Maize	Crop				157	Port facilities
104	Sugar beet	Crop		Mining	Urban > 96%	159	Mineral extraction, construction sites
105	Rapeseed	Crop				4	Bare land
106	Potatoes	Crop				157	Port facilities
107	(permanent) Grassland	Pasture	Rock	Harbour	Urban > 96%	151	Dense urban
112	Permanent crops	Pasture				153	Temperate sub-urban
114	Greenhouses	Urban	Urban	Industry Infrastructure	Urban > 35%	155	Industries and commercial areas
115	Agricultural buildings	Urban				156	Road and rail networks
6	Other (agricultural) activities	Pasture				Urban > 35%	161
7	Deciduous forest	Natural Vegetation	Pasture	Water > 25%	Crops > 35%	240	Peat bogs
8	Coniferous forest	Natural Vegetation				166	Temperate crops
9	Mixed forest	Natural Vegetation				193	Crops and woodland
10	Heathland	Natural Veg. Pasture	Crops	Natural Veg. > 35%	else	182	Temperate pastures
11	Dunes	Others				193	Crops and woodland
12	Wetland	Natural Veg. Pasture				189	Temperate complex cultivation pat.
13	Water	Water	Natural Vegetation	Urban > 45%	Water > 20%	166	Temperate crops
14	Recreation	Urban				160	Urban parks
15	Park	Natural Vegetation				238	Temperate wetlands
16	Residential	Urban	Urban	Pasture > 45%	Deciduous > 50%	180	Temperate fruit trees
17	Military	Urban Natural Veg.				203	Temperate broad-leaved forest
18	Commerce and services	Urban				203	Temperate broad-leaved forest
19	Industry	Urban	Others	Coniferous > 50%	else	211	Temperate coniferous forest
20	Mining	Others				218	Mountain mixed forest
21	Infrastructure	Others				166	Temperate crops
22	Harbour	Urban Water	Urban	Crops > 40%	Crops > 40%	166	Temperate crops
23	Other	Urban				166	Temperate crops

Next, land covers were provided by CARAIB per year for the 30-yr near future period with one value indicated for each grid point. These data served as input for ALARO-SURFEX. A subroutine in Matlab replaced the original ECOCLIMAP values with the reclassified new CARAIB values inside the boundaries of Belgium. For the grid points where CARAIB did not provide data, due to different coordinate systems or binary conversion of ECOCLIMAP data, the nearest neighbour was selected. The values outside Belgium are the original ECOCLIMAP values.

A simulation for the near future climate was performed at 4 km horizontal resolution with each year in parallel by the free surface dynamical downscaling approach. Because of limited time and computing resources, only summer months (June, July, August) were modelled and stored. The summers of 2006 to 2035 were assembled to cover the near future climate and compared to the near future climate without any land use changes.

4. SCIENTIFIC RESULTS AND RECOMMENDATIONS

In this section, we present the main results obtained during the project. First, calibration and validation tests are performed with the CARAIB DVM and ADAM ABM. For the DVM, these tests involve simulations at sites equipped with eddy covariance systems and measuring heat, water and carbon dioxide fluxes. This is done both for forest and crop sites. For forests, the DVM simulations are compared with those of the other two vegetation models presented in section 3.2.1 (ISBacc and 4C). For crops, in addition to this site-level validation with eddy covariance, a larger-scale comparison with the yield statistics is also performed per agricultural regions. In a next step, spatial simulations over Belgium of the DVM, the ABM and the RCM are presented, first for recent years and then for the near future (until 2035).

4.1. TESTS AND VALIDATION OF THE MODELS

4.1.1. VALIDATION OF VEGETATION MODELS OVER FOREST SITES

Set up of the vegetation model evaluation study

We evaluated the three vegetation models used in the project, i.e. the two DVMs CARAIB and ISBA_{cc} and the forest stand-scale model 4C, by comparing the model results for net ecosystem Exchange (NEE) with observed NEE data over a period of at least 16 years. The evaluation was performed for three European beech forest sites, one in Soroe (Denmark), one in Vielsalm (Belgium) and one in Collelongo (Italy). At all sites the dominating vegetation type consisted of mature beech (*Fagus sylvatica* L.) forest (between 76 and 106 years old), with different soil and environmental characteristics. NEE data from eddy covariance measurement towers were available for a 16-year period (1997-2012) for Soroe and for an 18-year period (1997-2014) for Vielsalm and Collelongo. A detailed description of the sites, including stand and soil characteristics, is provided in Table 5.

For the evaluation period the three models were forced by the meteorological data measured at the sites. At the point of initialisation, models were fed with the site specific soil properties that remained constant over the simulations. For CARAIB and 4C, eddy covariance and meteorological data were obtained from the daily aggregated FLUXNET2015 data (FULLSET, <http://fluxnet.fluxdata.org/data/fluxnet2015-dataset/fullset-data-product/>). For ISBA_{cc} the hourly FLUXNET2015 data were used for meteorological forcing. In order to set the model's carbon pools to steady state and to obtain a mature forest at the beginning of the evaluation period, model spin-ups were run for both DVMs, CARAIB (using ERA-Interim reanalysis; Uppala et al. 2005) and ISBA_{cc} (by cycling through the available meteorological data). The model parameters were not calibrated for the specific sites, since that could have concealed the actual problems in the model structure.

The variables NEE, gross primary production (GPP) and ecosystem respiration (R_{eco}) were extracted from model outputs and aggregated to daily values if the time steps were smaller, i.e. for CARAIB and ISBA_{cc}. The objectives of this evaluation were to define environmental conditions under which the models performed poorly and to identify the related model processes that should be revised for the adequate reproduction of NEE dynamics of forest sites. Further, we aimed to highlight the importance of applying multiple statistical evaluation methods (SEMs) for multiple sites in order to perform a useful evaluation of the performance of process-based vegetation models.

Eddy covariance measurements

During the last two decades NEE has been intensively monitored by use of eddy covariance techniques across multiple ecosystems in Europe (Aubinet et al. 2000). The NEE measurements, i.e. the time series of the carbon exchange between ecosystems and the atmosphere, were monitored at a 10 Hz sampling frequency and aggregated to 30-min averages. NEE measurements were processed using a constant friction velocity threshold across years with the reference selected based on model efficiency. Time series of GPP and R_{eco} were calculated by the partitioning of NEE based on nighttime NEE values (Reichstein et al. 2005). Based on the dataset of observations the random uncertainty and the joint uncertainty in NEE were calculated according to the FLUXNET2015 protocols (<http://fluxnet.fluxdata.org/data/fluxnet2015-dataset/data-processing/>). An extensive description of the partitioning of the NEE flux and measurement errors, as well as of the eddy covariance flux calculation and processing protocols has been previously published (Aubinet et al. 2012).

*Table 5: Description of the three beech (*Fagus sylvatica* L.) dominated sites including location, climate, soil and stand characteristics. C: carbon; N: nitrogen.*

	Soroe	Vielsalm	Collelongo
Location			
Country (region)	Denmark	Belgium (Ardennes)	Italy (Abruzzo)
Lat [deg N]	55.5	50.2	41.9
Long [deg E]	11.7	6	13.6
Elevation [m]	40	450	1550
Climate			
Average daily temperature [°C]	8.4	8.3	7.43
Average yearly sum precipitation [mm]	872	964	1159
Average daily relative humidity [%]	82.6	80.6	72.6
Average daily irradiation [J cm ⁻²]	988	991	1489
Soil			
Soil type	Alfisol or mollisol	Dystric cambisol	Humic alisol-calcarous
Clay in top soil [%]	14.2	15.7	14.2
Sand in top soil [%]	59.2	25	55.3
Average C content of root zone [g m ⁻²]	1963	2457	2605
Average N content of root zone [g m ⁻²]	125.2	113	213.1
Average field capacity [vol%]	19.2	30.8	50.1
Average wilting point [vol%]	9.2	12	26.9
Soil density mineral [g cm ⁻²]	1.6	2.65	0.8
Rooting depth [cm]	75	60	86.5
Stand characteristics			
Year of plantation	1921	1908	1891
Age at the beginning of the study period [yrs]	76	88	106
Age at the end of the study period [yrs]	89	103	122
Initial forest density [trees ha ⁻¹]	354	243	900
Initial average diameter at breast height [cm]	38	31.79	20.2
Initial average height [m]	25	26.79	17.3
Initial average basal area [cm ²]	48.77	19.76	28.86

Statistical evaluation methods for model evaluation

A range of SEMs were used to validate and to compare the performance of process-based models. Scalar statistical measures (SSMs) of error and fit provided an indication of the overall match of model output and data, but they offered only limited insight into the potential of the model to capture the variability in the data and they neglected the temporal dimension. Since a residual analysis (RA) examines model errors as a function of simulated or observed data and of

environmental drivers, it may reveal potential model shortcomings (Medlyn et al. 2005). More complex time series analysis techniques including wavelet analysis (WA; Stoy et al. 2005; Dietze et al. 2011) and singular spectrum analysis (SSA; Mahecha et al. 2007; Mahecha et al. 2010; Wang et al. 2012) effectively provided insight into the model fit at different temporal scales. The performance of the three models was evaluated by four SEMs, i.e. SSM, RA, WA and SSA.

Scalar statistical measures

Three fit statistics were used. Firstly, the coefficient of determination (R^2), secondly, R^2 multiplied by the slope of the regression line between simulations and observations (bR^2), allowing to account for the systematic discrepancy in the magnitude of two signals as well as for the proportion of variance in the observations predicted by the simulation results (Krause *et al.* 2005) and thirdly, the Nash-Sutcliffe efficiency (NSE), providing the relative magnitude of the residual variance compared to the measured data variance (Nash and Sutcliffe 1970). Two scalar error estimates were calculated, the normalized root mean squared error (RMSE) and the more robust normalized euclidean error (NMEE; Li and Zhao, 2006, Mahecha et al., 2010).

Residual analysis

The residuals were calculated as the daily-simulated values minus the observed values. The following moments of their distribution were calculated: the mean, here called the mean error (ME), the standard deviation (sdR), expressing the variability in the model errors, the skewness (skR; when skR is between -0.5 and 0.5 the distribution is approximately symmetric) and the excess kurtosis (kurR; positive kurR means fat-tailed and negative kurR means thin-tailed distribution). We analyzed the time course of the residuals and their relation with respect to the observed values. The correlation coefficients between the residuals and the observed values (CorrO) as well as between the residuals of the different models (CorrE) were also calculated.

The relation between the residuals and a number of meteorological variables, i.e. air temperature (T), incoming solar radiation (RAD), vapour pressure deficit (VPD) and the modelled drought index (DRI) were studied. A third order polynomial function was fitted through the daily residuals as a function of each of the meteorological variables to analyze the model performance over the range of those variables. DRI was not an observed variable, but calculated by 4C as the daily ratio of water uptake and demand as follows. The potential canopy transpiration demand (D_{tr}) was calculated from the potential evapotranspiration reduced by the interception evaporation (E_{int}), the unstressed stomatal conductance (g_{tot}) and the maximum stomatal conductance (g_{max}) of the forest canopy (Eq. 1). The transpiration demand of each cohort was derived by considering its relative conductance. The water uptake per cohort was calculated from the soil water availability, itself depending of the daily precipitation and the relative share of fine roots, and was limited by the transpiration demand of the cohort (D_{tr}^c). The DRI of a cohort is defined as the average of the ratios of uptake and demand over the time period of interest (number of days).

$$D_{tr} = E_{int} * \alpha_m * \left(1 - e^{-\left(\frac{g_{tot}}{g_{max}}\right)} \right) \quad (1)$$

In addition, the residuals of the centered and normalized observed and simulated time series (Res_{cn}) were calculated. The centering and the normalization eliminated the effect of consistent model biases and differences in variance amplitude, respectively (Dietze et al. 2011). The day of the year (DOY) averages of Res_{cn} over the whole study period were calculated to check for systematic asynchronies between simulations and observations, and were compared with the intra-annual NEE evolution represented in the same way.

Wavelet analysis

A discrete as well as a continuous wavelet transformation (based on the non-orthogonal Morlet mother wavelet function), were performed on the observed meteorological data (T, RAD, wind velocity (u), VPD, DRI) and on the observed and simulated time series of the ecosystem fluxes (package WaveletComp in R version 3.1.2). With this analysis the model's performance to reproduce the spectral properties of the observed fluxes was quantified. The minimum period in the analysis was two days and the maximum was 6475 days (5844 for Soroe). In order to check the significance of the average power on each frequency of the series, a low resolution (1/20) was used. In addition, a WA was performed on Res_{cn} . More details about the wavelet method can be found in Lau and Wang (1995) and Torrence and Compo (1998). The scaling exponent, which is the slope of the regression of the log-log relation between the time period and the wavelet power calculated for the normalized residuals ((simulated-observed)/observed), was calculated to check if errors at one scale were correlated with errors at larger scales (cfr. Richardson et al. 2008).

Singular spectral analysis

We conducted an SSA that quantified the relative amount of variance in the time series explained by specifically defined frequency bins (package Rssa in R version 3.1.2). The following frequency (period) bins were defined: 0-0.002 (infinity-500 days, multi-annual trend, bin 1), 0.002-0.004 (500-250 days, yearly variability, bin 2), 0.004-0.006 (250-166 days, half-yearly variability, bin 3), 0.006-0.009 (166-111 days, seasonal variability, bin 4) and 0.009-0.015 (111-66 days, inter-weekly variability, bin 5) and 0.015-0.05 (66 to two days, day to day variability, bin 6). Some of these bins were linked to the evolution of meteorological variables and consequently to physiological processes; others appeared as powerful spectrum peaks for one or more of the environmental variables during the wavelet analysis. A full description with implementation guidance of the SSA method is available (Golyandina and Zhigljavsky 2013). NMEE was used to quantify the goodness of fit between observed and simulated time series for each of the bins (cfr. Mahecha et al. 2010). To include the uncertainty on the eddy covariance data, the SSA was also performed for the observed value plus and minus its joint uncertainty. Additionally, the significance of the extracted subsignals (bins) was tested by a red noise test (package dplR in R version 3.1.2). Based on the Lomb-Scargle Fourier Transform 1000 surrogate time series were generated within the borders of a first order autoregressive (AR(1)) spectrum. Assuming that the background noise could be approximated by an AR(1) model, the hypothesis of a spectrum being purely appointed to noise could be rejected at the chosen confidence levels (95% and 99%). For a detailed description of the method see Schultz and Mudelsee (2002).

Model evaluation results

Observed NEE values and scalar statistical measures

NEE values diverged largely between the three FLUXNET sites. In Soroe, the annual NEE averages were close to zero, and even positive in the first three years of the study, with an average net carbon storage rate of $-0.42 \mu\text{mol m}^{-2} \text{s}^{-1}$. The other forests were more productive with an average storage rate of $1.26 \mu\text{mol m}^{-2} \text{s}^{-1}$ in Vielsalm and of $1.97 \mu\text{mol m}^{-2} \text{s}^{-1}$ in Collelongo (see Table 6). The evolution of NEE over the year clearly differed among sites, with less extreme values in summer and a longer growing season in Vielsalm compared to the other two sites. In Collelongo and Soroe, the maximum carbon uptake rate occurred at the same time of the year (absolute maximum on DOY 165 in Soroe and on DOY 173 in Collelongo), but overall, Collelongo was a more active carbon sink than Soroe with a higher maximum and a less rapid activity decline. Although GPP was highest in Soroe (avg. of $234.8 \text{ gC m}^{-2} \text{y}^{-1}$), the extremely high R_{eco}/GPP ratio (0.92 for the mean yearly values) undermined the

net storage of carbon. For Vielsalm this R_{eco}/GPP ratio was 0.74 and for Collelongo 0.48. Under similar meteorological conditions (see Table 5) GPP at Vielsalm was approximately 10% lower and R_{eco} 30% lower as compared to Soroe, resulting in a higher carbon storage rate in Vielsalm. The three models underestimated yearly averages of R_{eco} for Soroe consistently over the whole study period. For Collelongo (a forest at high altitude with a high tree density) CARAIB and 4C constantly overestimated R_{eco} . For Vielsalm, 4C and ISBA_{CC} strongly and systematically underestimated R_{eco} , while CARAIB overestimated it for the first 11 years, and turned it into an underestimation later on when the observed R_{eco} values strongly increased (yearly values not shown).

The model-site dependent errors in the simulations for either GPP or R_{eco} or both, resulted in diverged biases and random errors in the NEE simulations (Figure 9). Overall, ISBA_{CC} and CARAIB underestimated the net storage of carbon for Vielsalm and Collelongo (positive ME and skR, Table 7), but not for Soroe. Even though the DVMs exhibited higher R^2 values for those two sites as compared to 4C, larger biases were observed (lower bR^2 and higher ME). For Soroe all models overestimated the carbon storage over time leading to large values for ME, NRMSE and NMEE and low NSE for the NEE simulations of 4C. For the two other models, however, the combined effect of underestimating both R_{eco} and GPP resulted in an apparently adequate fit with NEE. Although the NEE simulations by ISBA_{CC} and CARAIB were similar, the simulations of its underlying components (GPP and R_{eco}) diverged.

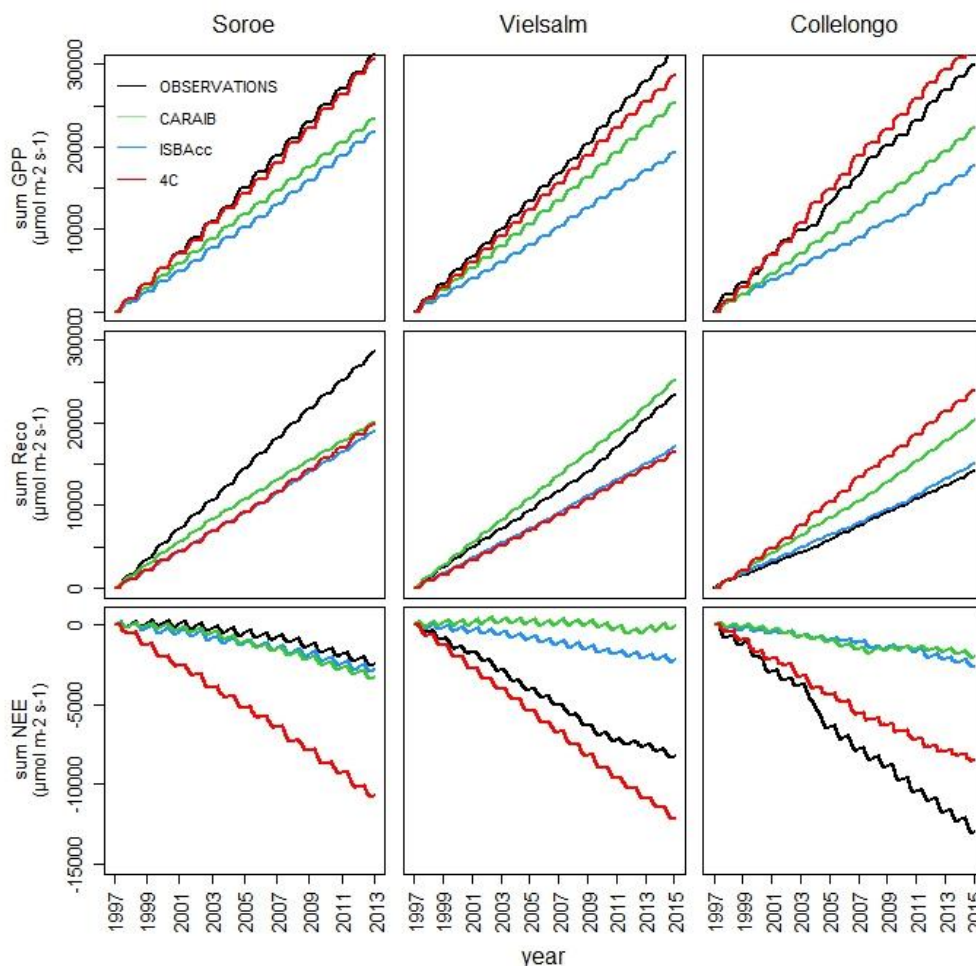


Figure 9: Cumulative plots of the daily observed and simulated gross primary production (GPP; top), ecosystem respiration (R_{eco} ; middle) and net ecosystem exchange (NEE; bottom) for the study sites Soroe (1997-2012), Vielsalm and Collelongo (both 1997-2014).

Table 6: Observed and simulated average values of daily net ecosystem exchange (NEE), gross primary production (GPP) and ecosystem respiration (R_{eco}) with their range (of averages over different years; within brackets). The simulations were made with three different models, i.e. 4C, CARAIB and ISBA_{CC} for the three forest sites. All values are in $\mu\text{mol CO}_2 \text{ m}^{-2} \text{ s}^{-1}$. The dimensionless ratio of R_{eco}/GPP is also indicated.

		NEE		GPP		Reco		R_{eco}/GPP
Soroe								
	Observations	-0.42	[-0.88,0.24]	5.32	[4.29,6.75]	4.9	[4.31,5.59]	0.92
	4C	-1.84	[-2.43,-1.41]	5.23	[4.08,6.75]	3.39	[2.65,4.32]	0.65
	CARAIB	-0.56	[-0.97,-0.13]	4	[3.79,4.28]	3.43	[4.01,3.43]	0.86
	ISBA _{CC}	-0.47	[-0.84,-0.13]	3.73	[2.97,4.49]	3.26	[2.77,3.75]	0.87
Vielsalm								
	Observations	-1.26	[-1.89,-0.48]	4.82	[4.18,5.44]	3.57	[2.81,4.65]	0.74
	4C	-1.85	[-2.09,-1.49]	4.35	[3.78,4.93]	3.57	[2.81,4.65]	0.57
	CARAIB	-0.01	[-0.67,0.43]	3.84	[3.25,44.26]	2.5	[2.10,2.85]	1
	ISBA _{CC}	-0.34	[-0.61,-0.01]	2.94	[2.42,3.37]	3.83	[3.56,4.58]	0.89
Collelongo								
	Observations	-1.97	[-3.69,-0.94]	4.55	[1.44,7.71]	2.6	[2.33,2.95]	0.48
	4C	-1.3	[-2.06,-0.66]	4.94	[3.76,6.62]	2.16	[1.72,2.67]	0.74
	CARAIB	-0.3	[-0.73,0.31]	3.39	[2.75,4.01]	3.09	[2.68,3.54]	0.91
	ISBA _{CC}	-0.4	[-1.00,0.07]	2.69	[1.90,4.00]	2.3	[1.89,3.00]	0.85

Residual analysis

For none of the models the daily residuals were normally distributed, with skR and sdR depending on the site. The density distribution of the daily residuals showed high kurR, indicating that a large part of the variance was explained by more extreme values. Overall, the sdR values were highest for Soroe, while skR and kurR were maximum for Collelongo for the three models. 4C differed from the other models in Soroe by producing very high kurR and skR values here, too (Table 6; Figure 10, top row). The correlations between the daily NEE residuals of the different models were high for some model-site combinations, but not very consistent over sites and models within each site (CorrE in Table 7).

The average yearly residuals changed with time and had a large range including both negative and positive biases (Figure 10, middle row). The mean yearly bias differed between the models, but the relative size of the residuals fluctuated in parallel. In other words, the models reacted with a comparable magnitude and in the same direction to inter-annual environmental changes. Overall, the average yearly residuals of all models were negatively correlated with the average yearly observed NEE (Table 7; Figure 11, bottom row). When high yearly carbon storages were observed, the models consistently underestimated this sink performance of the forests, while, in contrast, at low or negative carbon storage capacity, the models tend to overestimate the carbon uptake.

Table 7: Scalar statistical measures (SSM) for simulated (S) versus observed (O) net ecosystem exchange (NEE), moments of the residual distribution (for abbreviations see Table A1) and correlation coefficients between the residuals and the observed values (CorrO) and the residuals of the other models (CorrE) for the three models run for the three sites.

		Soroe			Vielsalm			Collelongo		
SSM	Interpretation	4C	CARAIB	ISBA _{CC}	4C	CARAIB	ISBA _{CC}	4C	CARAIB	ISBA _{CC}
Scalar fit statistics: how well does S reproduce O?										
R ²	Fraction of the variance in O explained by linear relation between S and O; the closer to 1 the better	0.53	0.74	0.7	0.41	0.47	0.52	0.39	0.66	0.44
bR ²	Fraction of the variance in O explained by linear relation between S and O taking into account systematic error; the closer to 1 the better	0.44	0.44	0.59	0.35	0.25	0.34	0.23	0.22	0.15
NSE	S predicts better the O than the mean of O if NSE>0; the closer to 1 the better	0.22	0.7	0.67	0.17	0.11	0.27	0.3	0.37	0.29
Scalar error estimates: how large is the relative error of the models?										
NRMSE	Measure of the relative error between S and O; the closer to 0 the better	13.8	8.6	8.9	13.9	14.4	13	19.1	18.2	19.3
NMEE	Measure of the relative error between S and O; the closer to 0 the better	0.47	0.28	0.26	0.48	0.61	0.48	0.28	0.28	0.31
Moments of the distribution of the daily residuals: how are the model errors distributed?										
ME	Value far from 0 indicates a probable systematic bias or at least many more or more extreme errors in one direction	-1.42	-0.14	-0.05	-0.59	1.25	0.92	0.53	1.48	1.37
sdR	Expresses the variability in the model errors; high variability means high random error	2.69	1.66	1.74	0.41	0.33	0.52	0.55	0.61	0.54
skR	The more negative the heavier the tail of the negative errors; the more positive the more heavy the tail of the positive errors	-26.19	0.58	-0.34	-9.81	13.37	8.12	37.85	48.35	56.79
kurR	The more negative the less peaks in the distribution and the more the variance is dominated by many, but not very extreme errors. The more positive the more peaks; the more the variance is dominated by some rare extreme errors	232.7	36.22	46.46	92.3	81.09	58.45	390.7	300.0	405.7
Are model errors correlated with the observed NEE value and the errors of other models?										
CorrO	Correlation between the residuals and the observed values. The higher the more the error is dependent on the value of the observed flux	-0.65	-0.5	-0.8	-0.93	-0.81	-0.94	-0.84	-0.93	-0.93
CorrE	Correlation between the residuals and the residuals of the other models The higher the more the errors between two models are correlated	4C	0.65	0.43		0.75	0.4		0.42	0.4
		CARAIB		0.35			0.17			0.75

The observed NEE value for which NEE was correctly simulated differed between models. Minimum yearly average residuals were observed for mean yearly NEE values around $-1.5 \mu\text{mol m}^{-2} \text{s}^{-1}$ for 4C and around $-0.5 \mu\text{mol m}^{-2} \text{s}^{-1}$ for ISBA_{CC} and CARAIB. This similar model behaviour indicated some degree of equifinality in the model results on a yearly time scale. Remarkably, for all models, at the onset of the growing season, Res_{cn} started to increase and reached a maximum when NEE

values were at half their minimum yearly value, to be low during the small period of minimum NEE (highest carbon uptake). In full summer (July-September), the carbon storage rate slowed down and Res_{cn} decreased sharply (Figure 11). However, neither average yearly simulated NEE values nor average yearly NEE residuals were directly correlated with the average yearly or seasonal T, RAD, VPD and DRI (correlations not shown).

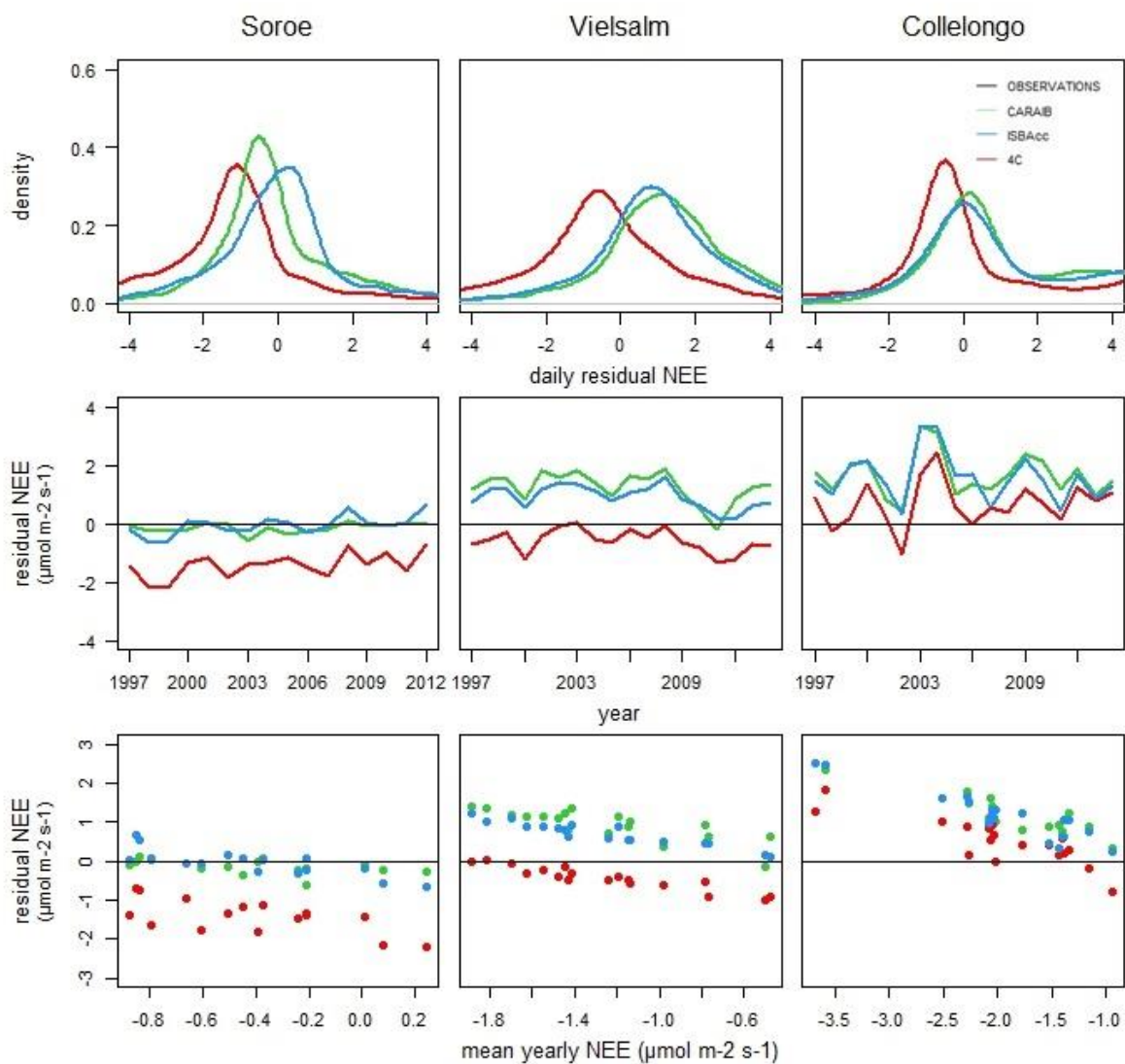


Figure 10: For the three study sites: (i) the distribution density of the daily net ecosystem exchange (NEE) residuals (top row), (ii) the yearly averaged residuals over the whole study period (middle row), and (iii) yearly average residuals versus average yearly observed values (bottom row).

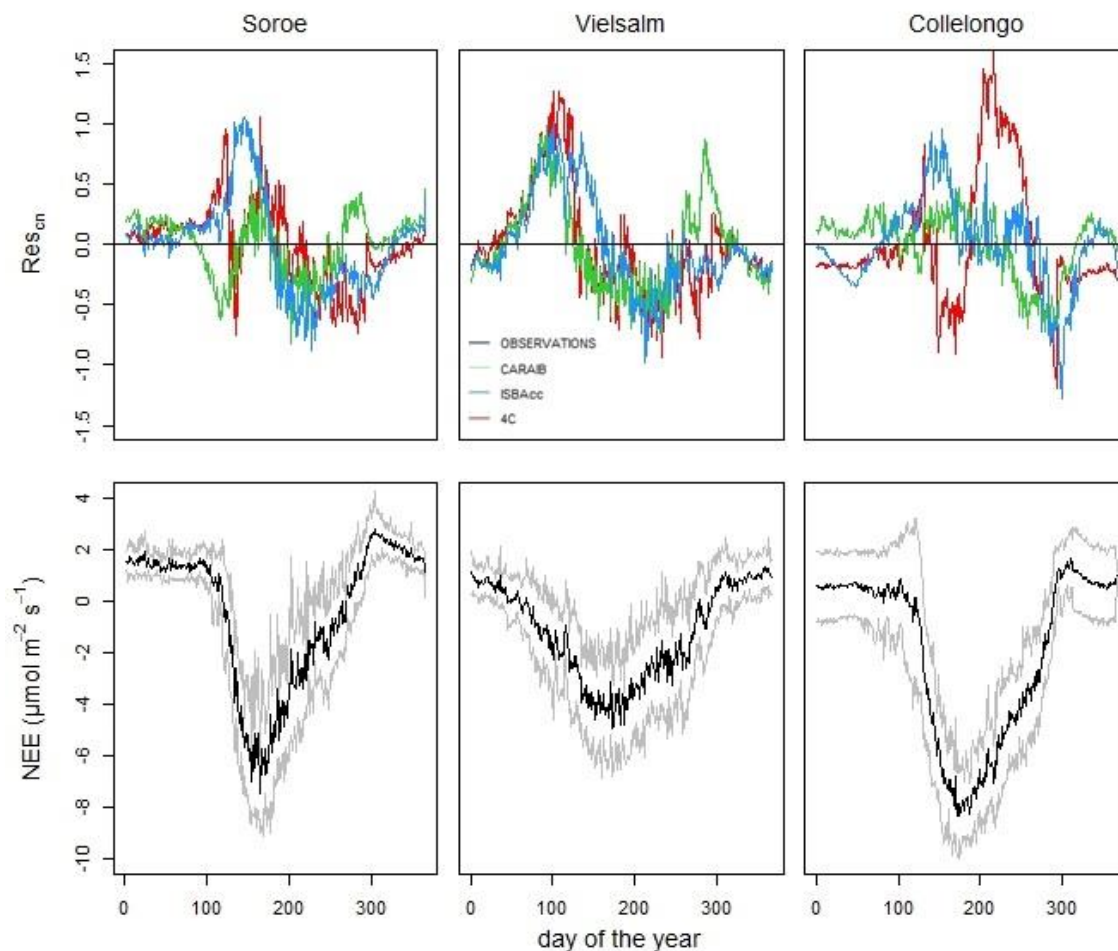


Figure 11: Day of the year averages of the residuals of the centered and normalized simulations and observations (1997-2012 for Soroe; 1997-2014 for Vielsalm and Collelongo) for the three study sites and for each of the models (top row) and the day of the year averages of the NEE observations (black line) with their standard deviations (grey lines). NEE: net ecosystem exchange.

On a daily time scale the univariate relation between the NEE residuals and the observed climate variables, i.e. T, RAD, VPD and DRI could not be unambiguously interpreted. These relations were neither consistent between models, nor for each model between sites (Figure 12). The effect of T on the residuals was low up to temperatures of 10 °C. For higher T, site and model dependent changes in residuals were observed. For Collelongo all models strongly overestimated NEE for high temperatures. The relation between residuals and RAD was less site dependent, although in Collelongo the summer days with high RAD values led again to underestimations of net carbon storage (Figure 12). Site-to-site inconsistency was also observed for the dependence of the model residuals on VPD observations. However, for each site individually, the models largely reacted in the same way. ISBA_{CC} and CARAIB performed independently of DRI, while 4C residuals varied as a function of DRI.

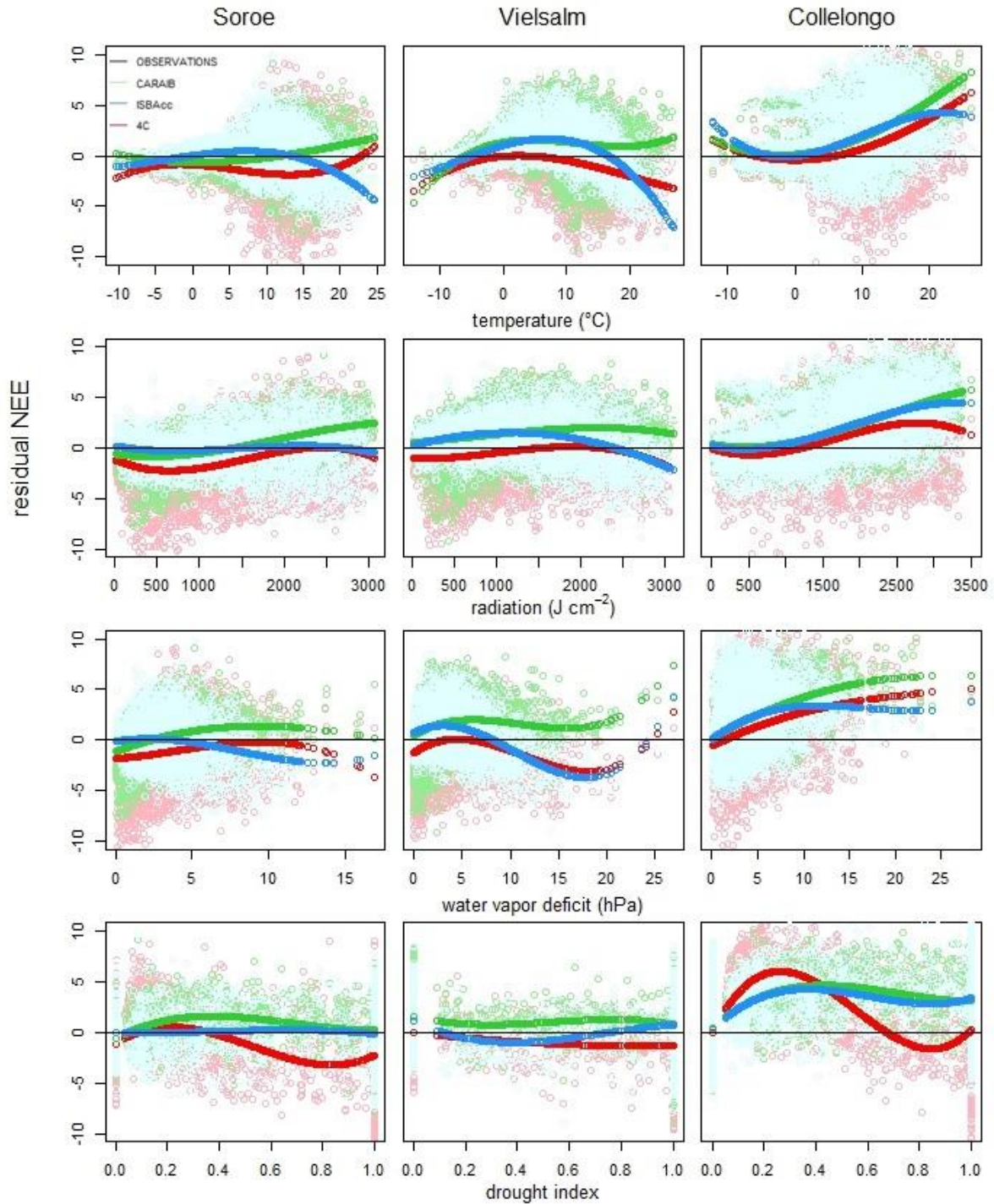


Figure 12: Daily residuals (light colored circles) of net ecosystem exchange (NEE) as a third order polynomial function (the dots represent the individual daily values) of daily observations of air temperature (top row), incoming radiation (second row from top), vapor pressure deficit (third row from top) and drought index (bottom row) for the three models at the three study sites.

Wavelet analysis

The meteorological variables T, RAD, u, VPD, as well as the DRI, all gave, as expected, a significant yearly signal, being least pronounced for u and VPD. For u there was a significant recurrent pattern for higher frequencies (between a few days and two weeks), reflecting the well-known 4-day peak of meteorological processes (Vinnichenko 1970). The DRI showed a significant signal around 128 days meaning that there was a pattern in drought peaks approximately three times a year. In Collelongo, a significant half-yearly VPD signal was present (Figure 13, top row).

The strong power of the yearly signal in NEE observations was depicted by all models (Figure 13, middle row). 4C and ISBA_{CC} underestimated the strength of this yearly signal for Collelongo; CARAIB slightly overestimated its strength at all sites as did 4C for Vielsalm. The strength of the signal simulated by ISBA_{CC} seemed exactly right in Soroe and Vielsalm. A recurrent half-yearly pattern in NEE was furthermore simulated for all sites and was observed in Soroe and Collelongo (Figure 13, middle row). The inter-site differences in intra-annual observed NEE variability were obvious from the power spectra plotted in the time-frequency domain (Figure 14). In Vielsalm there was a higher power at the half-yearly time scale in some of the years, while for the other two sites it was present every year. For Collelongo, the strength of the half-yearly signal simulated by ISBA_{CC} and 4C seemed to be close to the observed one, while CARAIB underestimated this temporal variability (Figure 13, middle row). For Soroe, 4C underestimated the half-yearly signal and in Vielsalm all models overestimated the intra-annual variability leading to a false half-yearly signal in the simulations. 4C overestimated the strength of the spectral power in the NEE time series at higher frequency (inter-monthly to inter-weekly) at all sites, but especially for Collelongo. There was also a significant NEE signal for Soroe and for Collelongo at four months (period approximately 128 days). For periods below one month there were no significant signals for any of the sites.

The results of the WA for the observed and simulated values showed that the yearly peak, driven by the annual solar cycle, was properly modeled, but the same analysis on the Res_{cn} showed a dominating asynchrony between simulations and observations on this time scale (Figure 14, bottom row). The annual signal as well as the half-yearly and the quarterly signal observed for NEE and the meteorological variables were clearly visible in the power spectra of Res_{cn}. The spectral power of the half-yearly asynchronies between simulations and observations were almost as important as that on the yearly time scale. This could not directly be linked to the seasonal pattern of drought neither to the power spectrum of any other environmental variable studied here. Also on higher frequencies (inter-monthly and inter-weekly), where more precipitation related processes and time lagged responses occurred, the model results all significantly deviated from the observed power spectrum. At a frequency of approximately 128 days, where a drought peak was present on all sites, significant shortcomings in model performance were found at two of the three sites, but not in Vielsalm. Since the Res_{cn} for evapotranspiration (data not shown) did not show this 128 days signal but NEE did, the model shortcoming might be linked to an incorrect incorporation of the effects of drought on NEE. For periods between 16 and 64 days, where T, RAD as well as the observed NEE values lacked significant power, unexplained significant periodicity in Res_{cn} still remained. For time periods shorter than 16 days the power spectra were no longer significant. The calculated scaling exponents were between -1 and -1.16 meaning that there was no memory of errors over time scales, i.e. errors were independent on different time-scales.

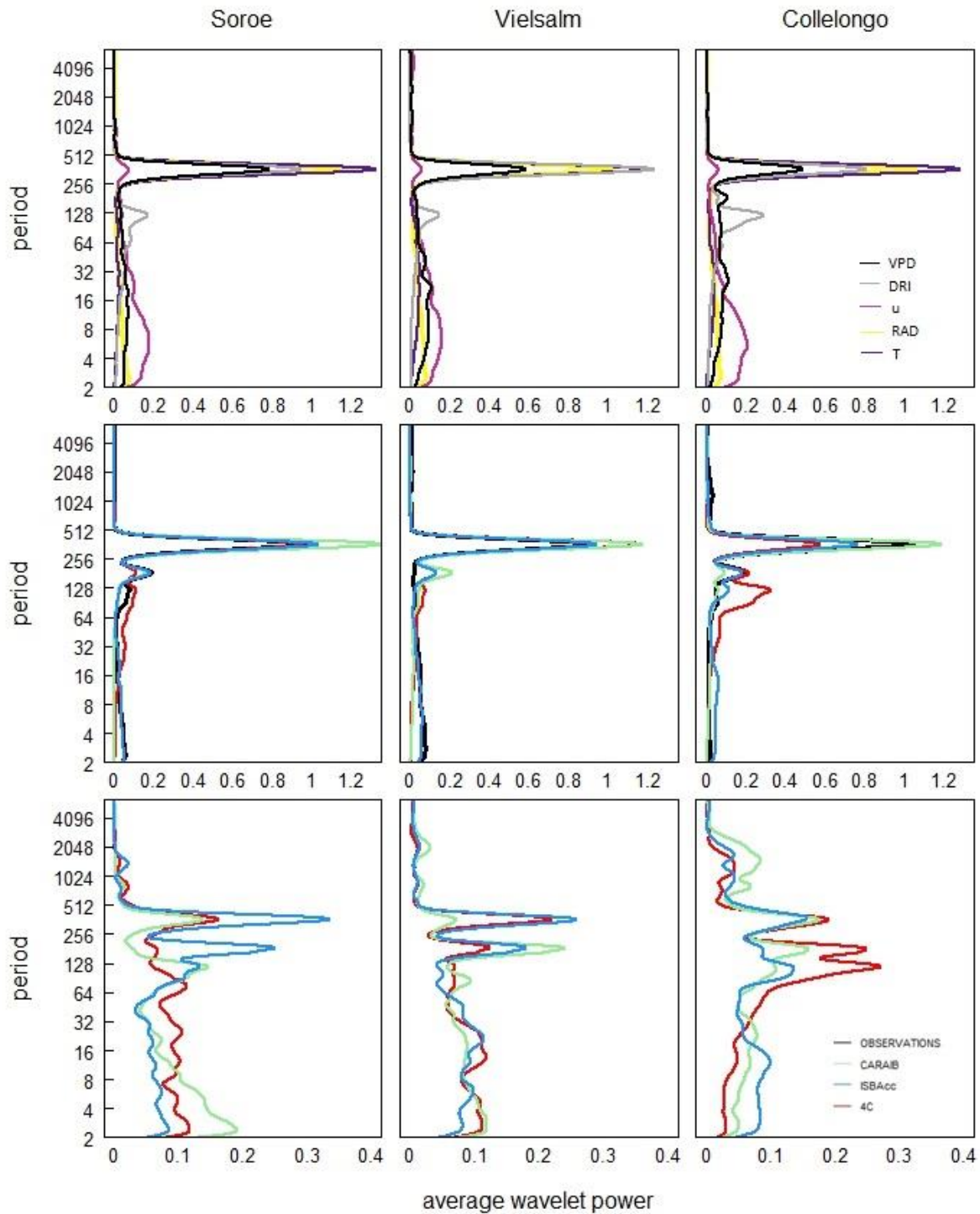


Figure 13: Average power of the wavelet transform for the three study sites. Top row: as a function of the period for the observed meteorological variables, i.e. temperature (T), incoming radiation (RAD), wind speed (u), vapor pressure deficit (VPD) and drought index (DRI). Middle row: for net ecosystem exchange (NEE) simulated by the three models and from observations. Bottom row: power spectra of the wavelet analysis of the residuals of the centered and normalized simulated and observed values of NEE for the three models.

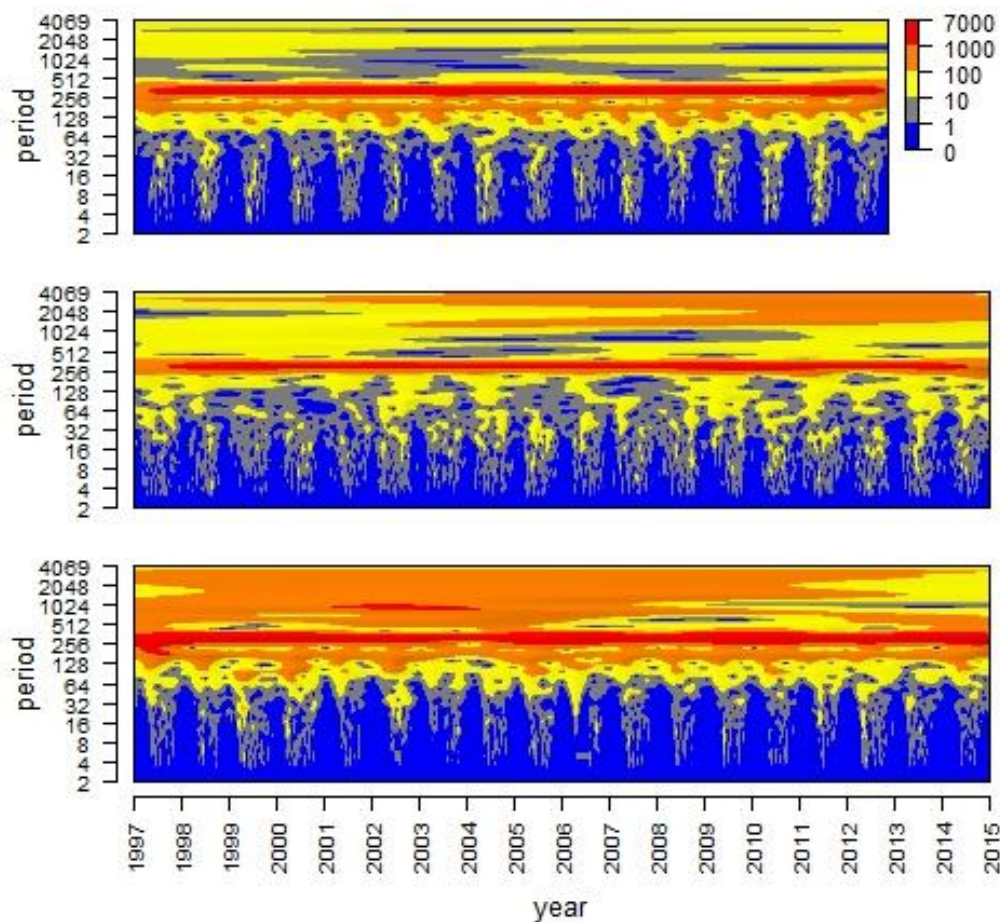


Figure 14: Plots of the spectral power (colors) as a function of time and period for the three models for the observed net ecosystem exchange at the three study sites i.e. Soroe (top), Vielsalm (middle) and Collelongo (bottom).

Singular spectrum analysis

The red noise test showed that there was no significant recurrent pattern on the multi-annual NEE time series, but the SSA allocated high variabilities to bin 1. The variability on this time scale was poorly assessed by the models: the variance that was attributed to this bin was incorrect (Figure 15) and the NMEE values between the bin specific simulations and the observations were large (Table 8). For Soroe less variance was explained by the multi-annual variability than for the other sites. For this site, the variance explained by the multi-annual signal was overestimated by 4C, leading to high NMEE values (Table 8). For Vielsalm and Collelongo, the variance attributed to long-term changes in NEE was generally underestimated, but less by 4C than by the DVMs. For each site, 4C attributed more variance to this bin 1 than the other models. For other frequency bins the NMEE values were site and model dependent without clear patterns. Approximately half of the total variance of the observed NEE time series could be attributed to the annual variability at all sites (bin 2; Figure 15). CARAIB always overestimated the contribution of the annual variability. However, this did not lead to very high NMEE values (Table 8). ISBA_{CC} overestimated the percentage explained by the yearly signal for Soroe and Vielsalm, while 4C underestimated it for Soroe and Collelongo. Bin 3 (the half-yearly signal) was significant for the observations in Soroe (10.12%) and Collelongo (7.80%). In Vielsalm this bin only explained 0.45% of the observed variance in the NEE time series. Nevertheless, the models did simulate a significant half-yearly signal for Vielsalm. While in the WA the half-yearly

signal seemed to be better simulated by ISBA_{CC} and 4C, the variance they attributed to bin 3 was not closer to the observed variance than the variance of that bin estimated by CARAIB. In Soroë bin 4 (inter-monthly or seasonal variability) was significant, even if it explained only 3.90% of the total variance. Higher frequency bins explained small parts of the variance and were not significant for the observations at any of the sites. 4C, giving significant signals for bin 4 and 5 systematically overestimated the variance explained by high frequency bins. CARAIB and ISBA_{CC} had no significant signal in bins 4, 5 and 6.

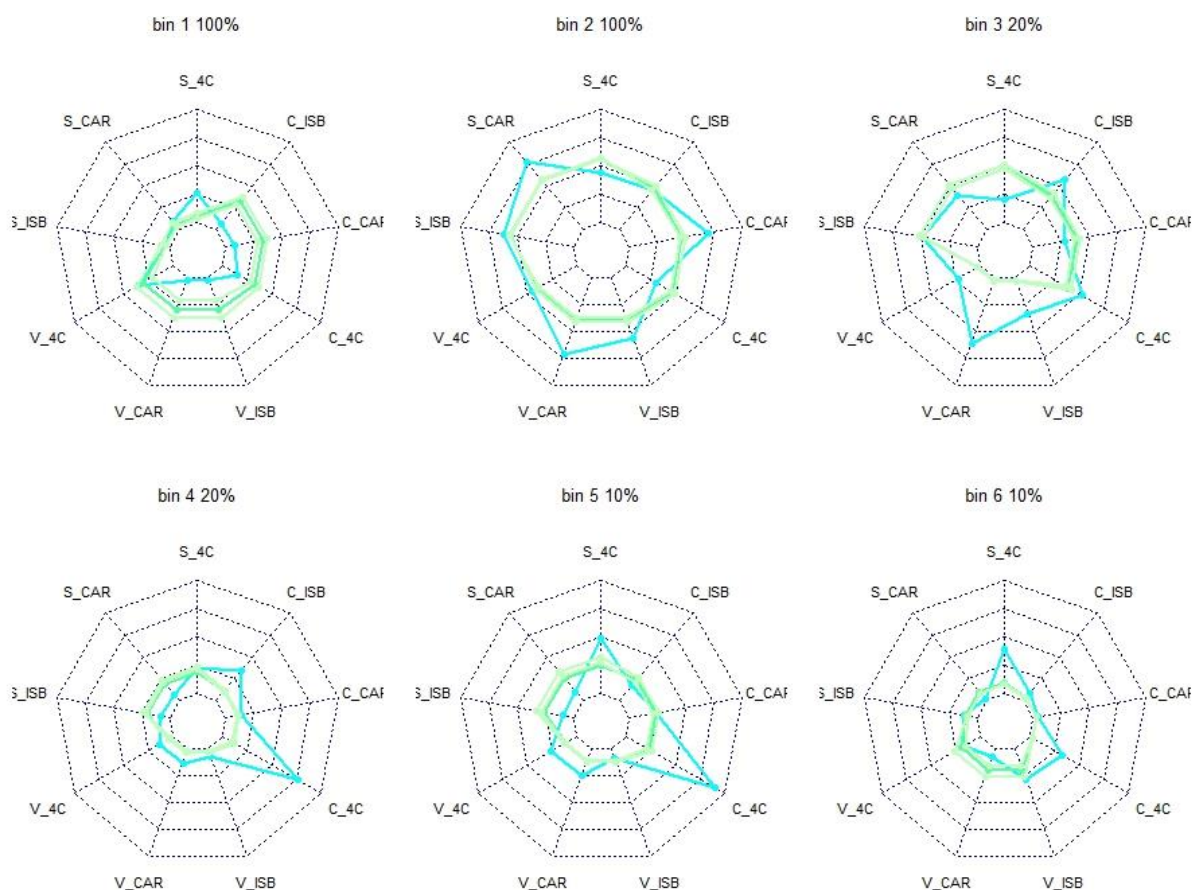


Figure 15: Radar plot of the singular spectrum analysis for the simulated net ecosystem exchange (NEE) in blue, for the observed NEE (green), and for the observed NEE plus and minus the joint uncertainty (light green). S: Soroë, V: Vielsalm, C: Collelongo, CAR: CARAIB, ISB: ISBA_{CC}.

Table 8: Normalized median Euclidean error (NMEE) for the six bins of the singular spectrum analysis for the three models at the three sites.

	Soroë			Vielsalm			Collelongo		
	4C	CARAIB	ISBA _{CC}	4C	CARAIB	ISBA _{CC}	4C	CARAIB	ISBA _{CC}
bin 1	4.52	0.5	0.52	1.38	3.28	2.37	1.26	1.84	1.78
bin 2	0.27	0.19	0.31	0.42	0.15	0.36	0.44	0.5	0.54
bin 3	0.3	0.35	0.63	3.43	4.18	3.45	0.7	0.66	0.5
bin 4	0.38	0.72	0.59	1.89	1.02	0.98	1.75	0.46	0.73
bin 5	0.73	0.63	0.6	1.14	0.97	0.67	1.03	0.59	0.75
bin 6	1.61	0.68	0.93	1.04	0.76	0.98	2.32	0.46	0.99

Interpretation and discussion of the evaluation results

NEE values and scalar statistical measures

The evaluation of the models was focused on NEE. This variable was directly measured by eddy covariance techniques but the models computed NEE as the net result of R_{eco} and GPP. The NEE values were not always correctly simulated by the models, but the observed model errors for NEE could be caused by either wrongly simulated GPP or R_{eco} values or both. Sometimes NEE values seemed to be adequately simulated, while it was actually the net result of simulated GPP and R_{eco} values, both not completely correctly simulated.

A combination of SSMS showed that the model's predictive ability and their relative error compared to the other models were dependent on the site. None of the models had the best or the worst fit for all three sites. This could partly be due to auto- and heterotrophic respiration processes incorporated in the models. The former is modelled by 4C using the fixed fraction calculation method (Landsberg and Waring 1997), that yields important differences in model results as compared to models (e.g. ISBA_{CC} and CARAIB) incorporating maintenance respiration separate from photosynthesis (Hickler et al. 2015). Generally, there is a lack in our understanding of the soil C-climate interactions, especially over the longer term (Crowther et al. 2016). The models simulated soil respiration in different ways. Other processes as the coupling of transpiration and photosynthesis, allocation rules and the sink activity of the trees, as well as the effect of nutrient availability are also of prominent importance for reliable carbon exchange simulations (Hickler et al. 2015). Although some SSMS are more robust than others (Li and Zhao 2006) and give a first impression of how well the simulations fit with the observations, none of them provides information about the specific timing of these model errors and the environmental situations in which they occur. Therefore, more advanced evaluation methods as the ones discussed below, should be used in addition to SSMS for more reliable model evaluations.

Residual analysis

The different model-data asynchronies between the models partly resulted from the different ways in which the evolution of LAI and of phenology is represented in the different models. Although the included processes were different, all three models showed high NEE residuals at moments of transition phases. Another reason for the asynchronies could be that parameter values are often representing adult leaves and the physiological responses of both young or senescing leaves were not well represented.

Surprisingly, the correlations between residuals and yearly NEE were negative for all models. The models overestimated NEE in periods of extreme large carbon uptake and mostly underestimated in periods of carbon release. This could cause problems for predicting NEE in more extreme environments and under future climate change scenarios. Since the residuals of the three models were not systematically cross-correlated, we could not conclude that the observed NEE values contained errors caused by the assumptions in data processing.

Since the modelled processes and the errors on their outcome are neither linearly nor univariately related to climate variables, we might get incomplete and possibly misleading information using univariate relations. Responses to environmental input variables are hard to interpret due to multicollinearity between model structure and parameters; a univariate study could reflect the result of the multicollinearity rather than the cause of model errors. The dependence of the model error on the meteorological input variables were highly site dependent, meaning that such relations were strongly affected by the quality of the site characteristic data, the model context and by the inherent differences of the different forest systems. This site dependency calls for caution in the interpretation of such univariate relations and clearly illustrates the need to evaluate models

for several sites, even more with the ambition for long-term prediction. Responses to meteorological variables do not only directly influence modelled NEE, but also leaf development and senescence. A thorough improvement of the physiological and phenological process description during these periods and also of winter activity will be helpful. Further, residual analysis techniques including bivariate plots, added variable plots (Medlyn et al. 2005) or principal component analysis, could improve our understanding of the environmental dependency of the model errors on NEE simulations.

Spectral analyses

Spectral analyses are in use to detect and to quantify temporal patterns in model simulations, in observations (cfr. Stoy et al. 2005), in their dissimilarities (cfr. Dietze et al. 2011) and to test the statistical significance of those patterns (Mahecha et al. 2010). On the multi-annual time scale, we found high bin-specific model errors (NMEE), as did also other authors (e.g. Braswell et al. 2005, Siqueira et al. 2006), which were linked to the correlation between residuals and observed NEE values. Apparently, certain modelled negative feedback mechanisms affecting NEE were overestimated with respect to reality, where more extreme values occurred. The effect of nitrogen limitation or of stimulation on photosynthesis is very important on the long-term time-scale and needs further investigation. Models not incorporating this effect might overestimate GPP values as a result of CO₂ fertilization, an effect that is often overestimated by PVMs (Anav et al. 2015). Nitrogen limitation effects were only incorporated by 4C, as was also the effect of forest management during the model evaluation period. Eventual forest disturbances (e.g. pest plagues) were included in none of the models. On stand scale, such local high impact events and their lag-effects have a high impact on the long-term evolution of the carbon balance (Anav et al. 2015). On the multi-annual time scale, the spectral power was shown to be often improperly simulated by PVMs (e.g. Braswell et al. 2005). Furthermore, the extraction reliability of the SSA method for low-frequency modes is low (Mahecha et al. 2010). Finally, the time series were not centered before the SSA analysis; the NMEE values did thus not only reflect asynchronies but the entire model error including the model bias.

Regarding the observed and simulated half-yearly spectral peaks, a link to phenology and LAI development was suggested because it more often appears in deciduous forests than in evergreen forests (Mahecha et al. 2010; Dietze et al. 2011). Indeed, Vielsalm consists for one third of conifers. During this evaluation study however, the stand was modelled as a mono-species beech forest. Our results, using the longest available eddy covariance time series, supports the hypothesis that the asynchrony between simulations and observations was large in spring and autumn, dropping to lower levels in full summer and full winter (see Figure 10). Inter-annual phenology variability might explain a large part of yearly NEE fluctuations (Keenan et al. 2012) and the way it is incorporated in simulation models affects model performance (Richardson et al. 2012). Further research on this intra-annual variability of carbon exchange and especially on the effect of both transition phases, remains necessary to improve model performance.

4C often overestimated the importance of high frequency variability (inter-monthly to inter-daily) in NEE. The dependence on T which is used to redistribute weekly simulated NEE values to daily values could be too sensitive. Other reasons for asynchrony on smaller frequency bins, by all models, could possibly be ascribed to the simplifications of the forest structure and the vertical radiation partitioning through the canopy, affecting photosynthesis as well as respiration on small time scales. One possible cause for the significant periodicity in Rescn for periods between 16 and 64 days, could be the influence of VPD (Dietze et al. 2011). Also, NEE observations and model input variables measured at the site are prone to random and/or systematic measurement errors. The former might have large effects on the time scale specific analyses of the highest frequencies (Hollinger and Richardson, 2005). An important part of the uncertainty in NEE observations is ascribed to the assumptions in the NEE calculation procedure (Aubinet et al. 2012). Since observational data are often incomplete and models show context errors, it is important to evaluate

the models for several sites to discover the real systematic problems in the model structure. While model residuals were shown to maintain a certain temporal correlation structure varying over sites (Richardson et al. 2008), the scaling exponent from our WA of the normalized residuals did not give evidence for a lingering effect of errors over time scales.

4.1.2. VALIDATION OF THE CARAIB CROP MODULE

The crop module implemented into the CARAIB DVM was largely built within this project. Its validation was carried out at two scales: at the local and at the Belgian scales.

At the local scale, we have used data from sites equipped with eddy covariance measurements systems. This technique allows the assessment of different fluxes, and for the CARAIB validation, we focus on three of them: the gross primary productivity (GPP), the evapotranspiration (ET) and the net ecosystem productivity (NEP). Depending on the additional data available for some sites, we were able to compare other parameters, especially for the site of Lonzée (Buysse et al., 2017, Dufranne et al., 2011 and Aubinet et al., 2009) and Grignon (Loubet et al., 2011), regarding yields and leaf area index (LAI).

After some model adaptations for each site (soil parameters, crop management, etc.), we have compared the CARAIB outputs with the data available at the site. Globally, the determination coefficient between data and measurements are relatively good (Table 9), especially for GPP with the minimum absolute determination coefficient of 0.59 for cereals (in Grignon) and a maximum absolute R^2 of 0.95 for sugar beets (in Lonzée). If we have a more detailed look at the results from the Belgian Lonzée site (Figure 16), which may influence the calibration at the Belgian scale, we could highlight some observations (also relevant for the other eddy covariance sites):

- CARAIB tends to globally underestimate the GPP ;
- the underestimation is particularly large for maize, which is possibly linked to the simplified photosynthetic scheme used for C4 plants in the model ;
- the model suffers of a lack of development of the different crop development stages. As we can see for cereals, the important senescence phase is not reproduced by CARAIB. Indeed, the GPP calculated by CARAIB falls abruptly at the time of harvest, while the GPP should gradually decrease during the senescence phase at the end of the vegetative period.

Table 9: Coefficients of determination R^2 and relative RMSE (%) for the 3 parameters (GPP – gross primary productivity, ET – evapotranspiration and NEP – Net Ecosystem Productivity) for each of the 2 simulated crop sites where eddy covariance data are available (Lonzée, Belgium, and Grignon, France)

		2004	2005	2006	2007	2008	2009	2010	2011	2012	2013	2014	
Lonzée (Belgium)	Crops	S. Beets	Wheat	Potatoes	Wheat	S. Beets	Wheat	Potatoes	Wheat	Maize	Wheat	Potatoes	
	GPP	R^2	0.91	0.70	0.91	0.57	0.95	0.69	0.88	0.62	0.88	0.71	0.83
		relative RMSE	40	74	56	86	34	75	127	95	101	83	85
	ET	R^2	0.35	0.41	0.60	0.50	0.71	0.65	0.35	0.21	0.43	0.41	0.65
		relative RMSE	61	88	65	71	128	66	89	105	81	90	55
	NEP	R^2	0.91	0.63	0.84	0.45	0.86	0.66	0.76	0.57	0.78	0.60	0.85
		relative RMSE	-136	-190	-384	-235	-139	-260	267	-270	-249	-230	440
		Crops	Barley	Maize	Wheat	Barley	Maize	Wheat	Tritical	Maize	Wheat	Rapeseed	
Grignon (France)	GPP	R^2	0.69	0.83	0.67	0.52	0.83	0.59	0.59	0.46	0.58	0.44	
		relative RMSE	69	86	87	93	75	97	88	133	102	132	
	ET	R^2	0.02	0.44	0.52	0.38	0.44	0.60	0.41	0.46	0.58	0.65	
		relative RMSE	86	63	55	60	59	59	61	64	72	60	
	NEP	R^2	0.26	0.77	0.76	0.49	0.53	0.65	0.67	0.16	0.52	0.49	
		relative RMSE	-157	-344	-257	-246	-144	-143	-131	-183	-240	-343	

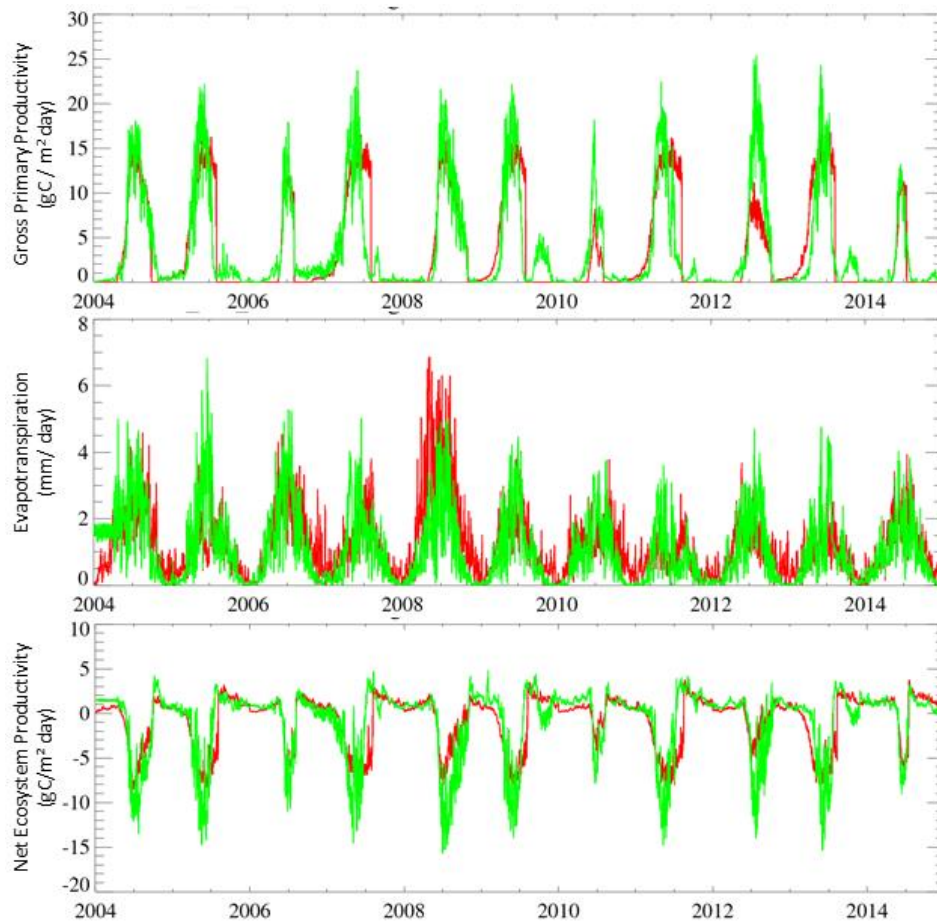


Figure 16: Comparison of (a) gross primary productivity (GPP), (b) evapotranspiration (ET) and (c) net ecosystem productivity (NEP) outputs from CARAIB with measurements at the eddy covariance sites of Lonzée (Belgium)

At the Belgian scale, the challenge was quite different, as we have to associate the spatial and the temporal variability. The model was adapted thanks to the information provided by the use of the eddy covariance data, but also thanks to the country statistics on crop yields (FPS Economy). The disadvantage of these data is that they are not available at the km^2 scale but at the scales of the country or of the agricultural regions, while the spatial variability can be important. For this validation, CARAIB was run over the Belgian territory for crops with ALARO daily climate forcing (1 km climate derived from 4 km-ALARO simulation) and compared with the yearly average yields for Belgium and agricultural regions. Here, we propose simulations performed with a LC dataset providing the 6 crops proportions for each municipality: this implies that the spatial distribution is less accurate than a LULC at 1 km provided by the agent-based model, but this one is based on the Belgian agricultural statistics (Figure 2).

While Figure 17 gives the inter-annual variation of the average Belgian yield, Table 10 presents a summary of the results obtained both, at the Belgian and for the main agricultural region for each crop. In Table 10, for each of the 6 crops selected, we list the coefficient of determination for whole Belgium as a whole and for the 2 agricultural regions with the highest area dedicated to the crop. These results must be analysed with these factors in mind:

- we do not know exactly which sampling method has been used to compute the agricultural statistics, while here, we consider every parcel/pixel where the crop is cultivated ;
- differences observed over the country can be partially explained by differences in the crop management (new techniques, sowing density, fertilizer, etc.) that we are not able to take into account in the model ;

- some natural hazards (crop laying, diseases, etc.) cannot be simulated by the DVM.

Table 10: Coefficients of determination R^2 obtained (and, in grey, area in km^2) between the observed and simulated average yields of each of the 6 crops over Belgium and the main agricultural regions.

	Sum of pixels fractions (1 pixel = 1km^2)	Belgium (temporal ; spatial)	Loamy (temporal)	Sandy- Loamy (temporal)	Sandy (temporal)	Condroz (temporal)
	Total area	31243	4701	5437	3823	2611
	Total cultivated area	8264.5	2620.9	1920.5	990.0	784.0
Wheat	R^2	0.11 ; 0.09	0.13	0.14		
	Cultivated area	2671.2	1121.2	555.0		
Maize	R^2	0.26 ; 0.66		0.00	0.27	
	Cultivated area	2809.4		629.7	628.6	
S. Beets	R^2	0.27 ; 0.88	0.13	0.24		
	Cultivated area	1326.1	691.6	345.7		
Potatoes	R^2	0.32 ; 0.17	0.13	0.16		
	Cultivated area	786.4	226.0	292.4		
Barley	R^2	0.00 ; 0.00	0.01			0.02
	Cultivated area	588.6	208.3			127.7
Rapeseed	R^2	0.00 ; 0.40	0.07			0.02
	Cultivated area	82.8	12.0			45.1

Figure 18 allows us to have a better idea of the spatial pattern given by the DVM. For the two winter cereals, the model can reproduce quite well the spatial distribution presented in Figure 5. For both crops, the model seems to slightly overestimate the yield in the Kempen region and in the south of the country. The winter wheat average yield shows a good consistency with the distribution observed on Figure 2. With their quite good determination coefficient, potatoes and sugar beets show a good distribution over the country, especially in the west of the country for potatoes and in the centre for sugar beets (the most important region for each crop given in Figure 1). Rapeseed presents quite uniform yield over (the south of) the country and, if we are in the good range of values with the model, the spatial distribution could be improved. As already highlighted in the validation at the site level, the maize shows less good results, with yield being quite low compared to the expected values, but with a satisfactory spatial distribution. Finally, we compare each pixel with the respective agricultural region average yield to get the correlation coefficient (Figure 19), but only for the pixels with more than 5% of agricultural area (Figure 2). The coefficient is positive for three of the four most important crops in Belgium, winter wheat, potatoes and sugar beets while, once again, maize shows the worst results.

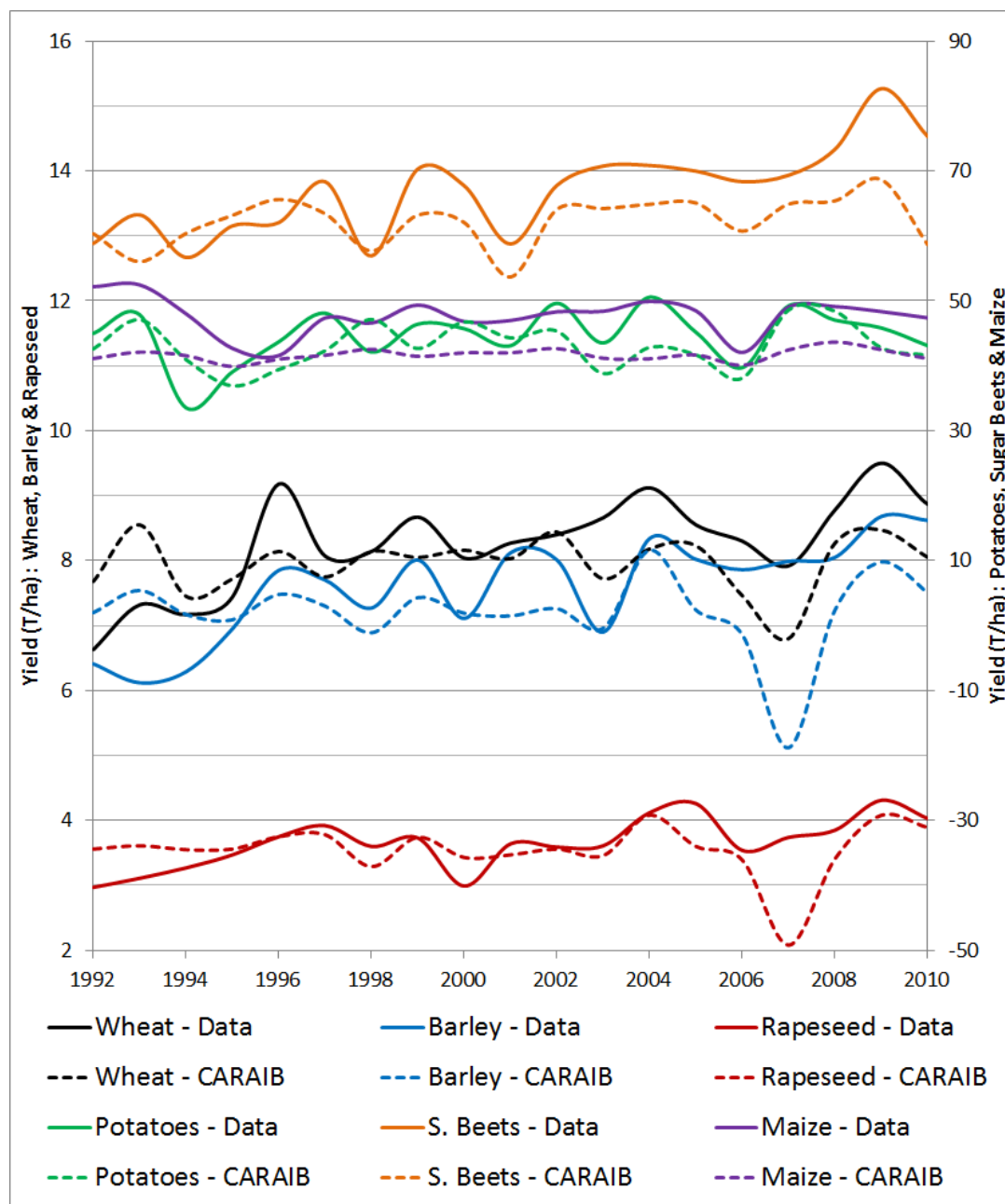


Figure 17: Average yield for Belgium calculated by CARAIB (forced by ALARO outputs itself forced by climate reanalyses) and compared to yield statistics between 1991 and 2010

In conclusion, at the beginning of the project, the simulations over Belgium provided almost uniform results over Belgium with only a slight yield increase in the south of the country. The average Belgian yield was quite far from the one given in the agricultural statistics. These figures illustrate the progresses made during this project, but they also highlight the need to better catch the processes which take place in the different regions of the country.

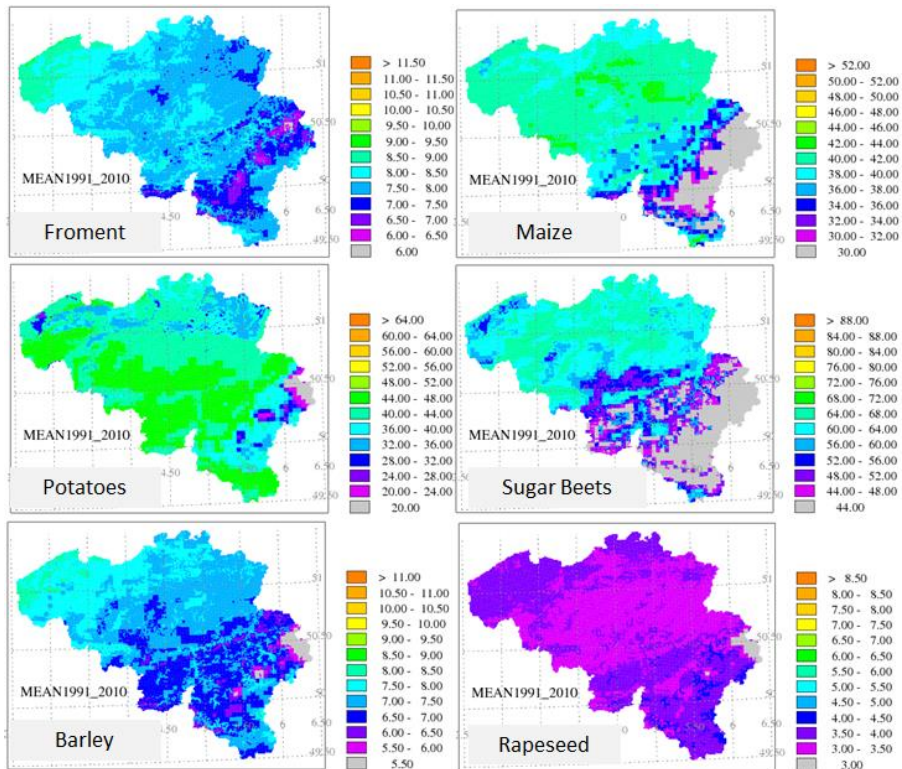


Figure 18: Average yield over Belgium calculated by CARAIB between 1992 and 2010 (forced by ALARO outputs, using climate reanalyses)

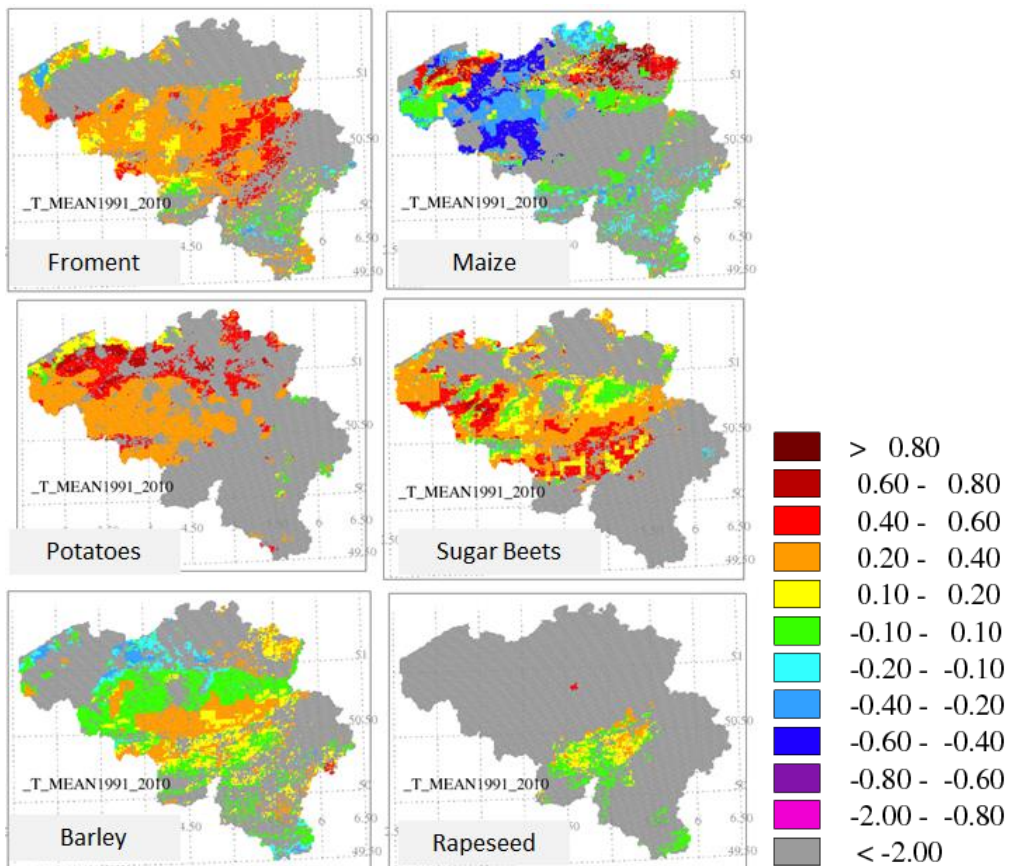


Figure 19: Yield correlation coefficient and relative RMSE for period 1991 and 2010 (forced by ALARO outputs, using climate reanalyses)

4.1.3. CALIBRATION AND VALIDATION OF THE ADAM AGENT-BASED MODEL

Most parameters used in the ADAM model are based on empirical data (number of farmers per municipality, mortality rates) or were defined through discussions with experts in the field (profitability). Data on the percentage of farmers that retire after passing the legal retirement age (65) are not available. In order to calibrate this percentage, the model was run for Belgium for percentages between 15 and 35%. The results for the evolution of the farmer population between 2000 and 2010 were compared to the evolution of the population according to the observed values from the Agricultural Surveys (Statistics Belgium, 2015) for half of the municipalities (uneven NIS code). The other half of the municipalities was used to validate the model. Comparison has only been done between 2000 and 2010. Data after 2010 are available but from 2011 onwards, in order to simplify administration, farmers could choose to be registered collectively in the survey, leading to a direct decrease of the number of farmers provided in the survey results and of the average farm size, which is derived from the number of farmers (Departement Landbouw en Visserij, 2014). This change in methodology makes a comparison between the number of farmers that are observed and predicted, difficult from 2011 onwards.

The predicted and observed data were evaluated by the means of a relative root mean square error (RRMSE). The RRMSE, is based on the root mean square error (RMSE) but relative to the mean of the observed values.

$$RMSE = \sqrt{\frac{1}{n} \sum_{i=1}^n (m_i - o_i)^2}$$

$$RRMSE = RMSE \times \frac{100\%}{o_{avg}}$$

with n the number of observations, m the modelled value, o the observed value and o_{avg} the average of the observed values.

The RRMSE gives an idea about the difference between the modelled and the observed values, the lower the RRMSE value, the better the model performs.

The different percentages of retirement after legal retirement age, result in a minimum RRMSE of 1.7% for a retirement percentage of 20% (Figure 20). For subsequent runs, a percentage of 20 was used.

The model was validated by comparing the predicted results obtained for 2000 to 2010 with the observed data for half of the municipalities in the dataset (even NIS code, the other municipalities were used to calibrate the model). An RRMSE of 1.6% for the number of farmers was obtained, showing that the model is capable of simulating the evolution of the farmer population.

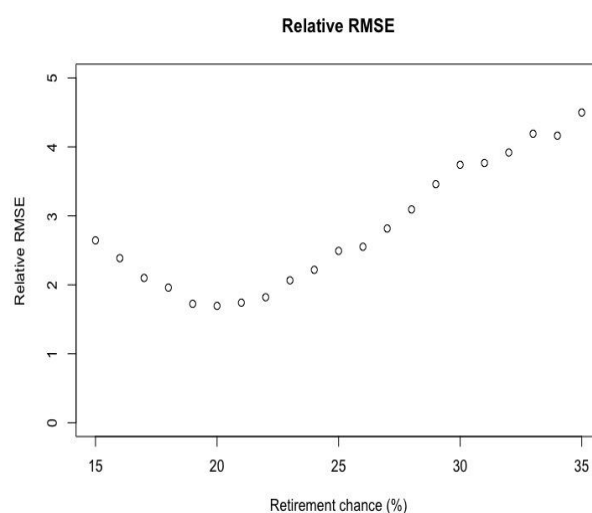


Figure 20: Calibration through the relative RMSE for different percentages of retirement after legal retirement age

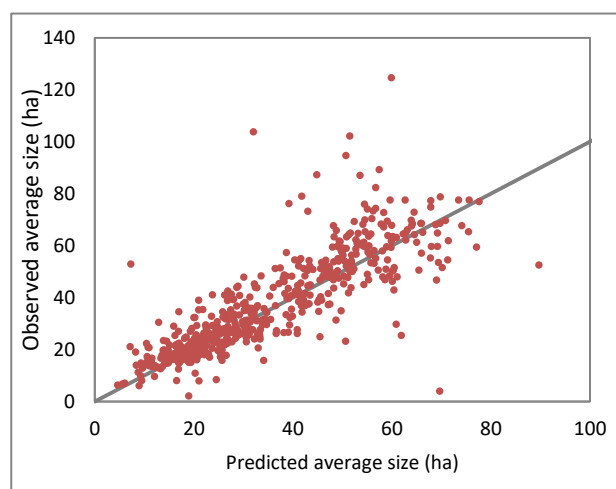


Figure 21: Predicted average farm size versus observed size in hectares for municipalities in 2010

A comparison between the predicted and observed average farm size per municipality shows that the predictions are close to the observed averages with both over- and underestimations (Figure 21). The error according to the RMSE equals 10.6 ha for 2010.

4.2 SPATIAL SIMULATIONS FOR THE PRESENT

4.2.1 ADAM SIMULATIONS

Given the successful calibration and validation for 2000-2010. Spatial simulations with the model until 2015 were performed. The number of farmers further decreases and the average farm size continues to increase with small farms leaving the system, being taken over by bigger farms. These trends differ throughout the country. A spatial visualisation of the results for Belgium shows that the biggest farms, located in the centre of Belgium, continue to grow and increase in size (Figure 22).

Figure 23 shows the modelled evolution between 2000 and 2015 of the total number of farmers, and each farming type. The biggest decrease of farmers is predicted for the north of the country, which is related to the on average smaller farm sizes in the region. An evolution that can also be observed for land based animal farming and farming focussed on yearly crop rotations. For this last type of farming, the strong decrease is not only limited to the north. Strong decreases can also be observed in the most southern part, the Ardens, where soils are less fertile than in other parts of the country. The decrease for this type of farming is noticeably less in the central part of Belgium, the fertile loam area, where farms are on average larger. The decrease of greenhouse farming can be predominantly observed in the north, mostly due to a lack of this type of farming in other parts of the country. Decreases in permanent crop farming can be observed everywhere in the country, but are clearly less heavy in the Hesbaye area, in the east of the country, which is specialized in apples, pears and cherries and where farms focussing on permanent crops are on average bigger than elsewhere. Barn based animal decreases in the entire country, whereby no specific geographic trend can be observed, since barn based animal farming is independent of the physical conditions of its environment.

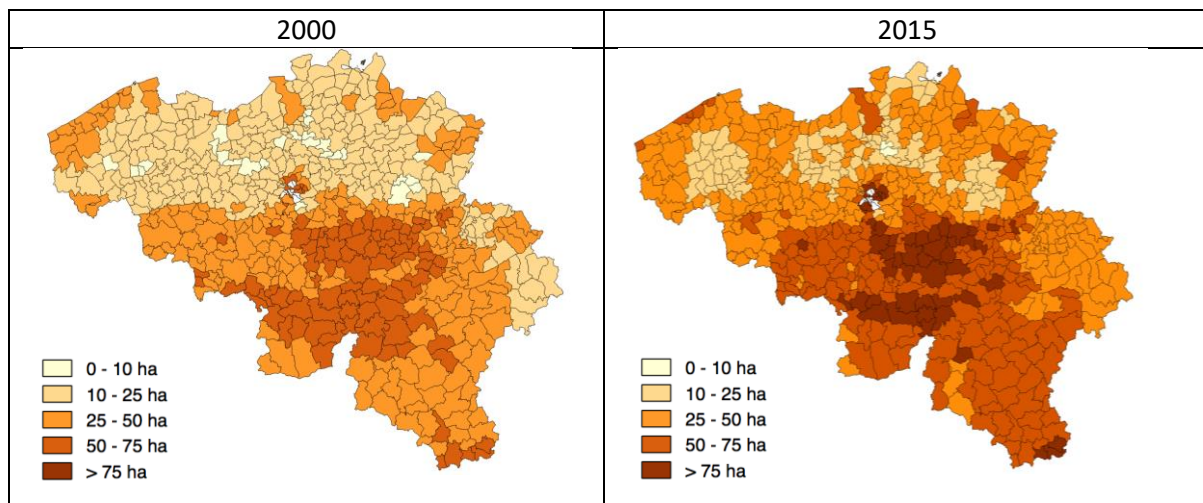


Figure 22: Modelled average farm size in Belgium for 2000 (left) 2015 (right).

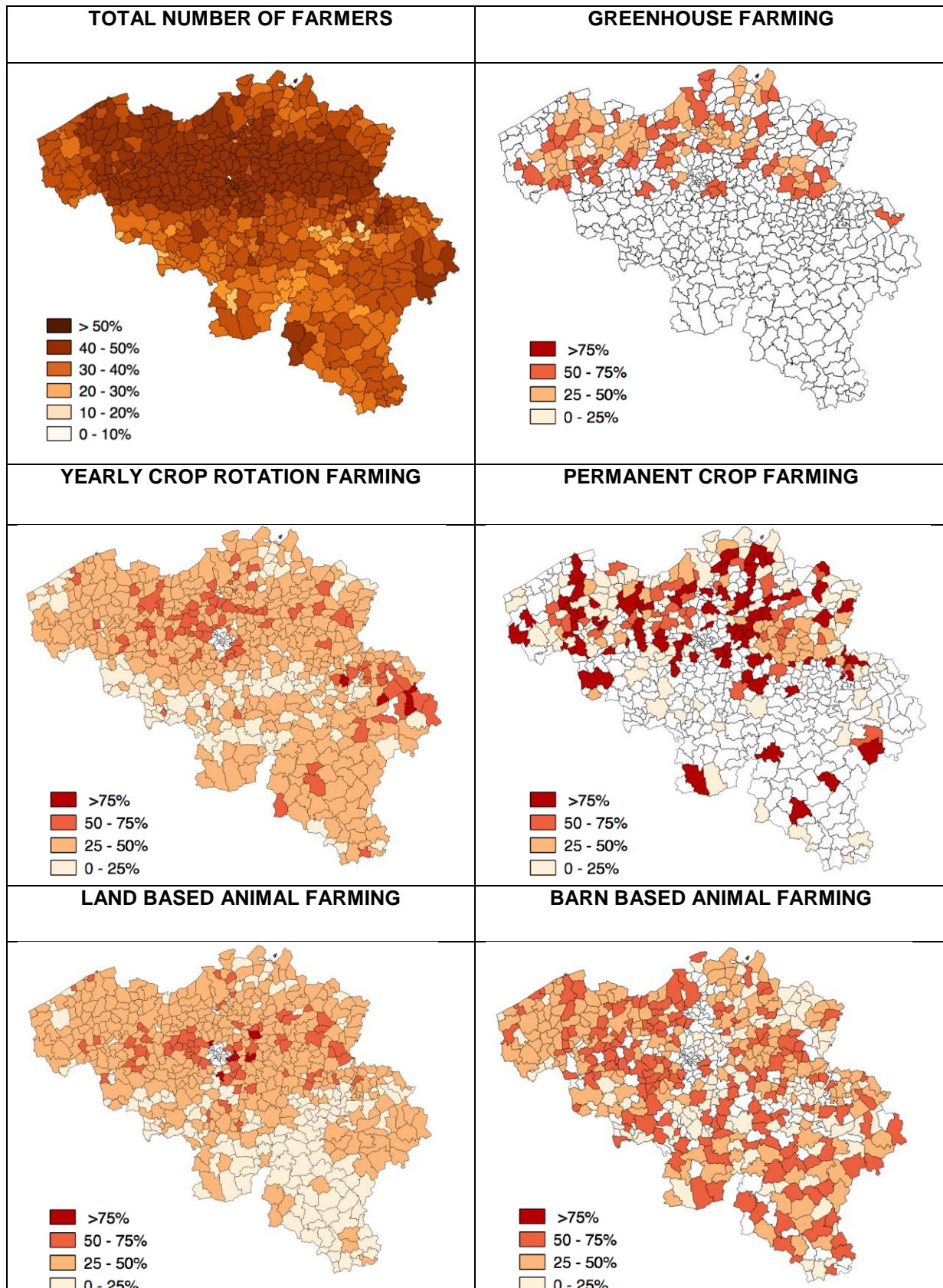


Figure 23: Predicted percentage decrease of the number of farmers in total and for each type between 2000 and 2015

4.2.2 TESTS OF THE REGIONAL CLIMATE MODEL IN THE PRESENT CLIMATE

Added value of using SURFEX

The performance of SURFEXv5 within ALARO-0 has been evaluated next to the configuration with ISBA. Both simulations are performed at 20 km horizontal resolution, using the ACRANEB scheme in a long-term model experiment, with lateral boundary conditions from ERA-Interim and in a forecast-mode update frequency of the initial conditions. The results were validated against E-OBS, a daily high-resolution gridded dataset (Haylock et al., 2008). For Belgium, the differences using SURFEX with respect to ISBA in winter occur mainly in the minimum temperature ranges below -10 °C. In contrast to winter, the configuration with SURFEX gives much improvement in summer for the minimum temperature. The use of ISBA within ALARO results in a general warm bias of 1-2 °C and for some regions in Spain, France and the east of the domain values up to 3 °C. The use of SURFEX diminishes this warm bias with 1-3 °C resulting in very small biases of -0.5 to +0.5 °C, despite a worsening over high elevated terrain with cold biases up to -5 °C. For Belgium, the summer minimum temperatures lower than 5 °C are underestimated by the model and the minimum temperatures above 5 °C are overestimated. The largest improvement using SURFEX with respect to ISBA occurs for the minimum temperature range above 20 °C. In contrast to temperature, the precipitation is not as sensitive to the surface scheme.

Relevance? To understand the results for the future using this model setup, to motivate the use of this model setup for the future climate projections.

Update frequency of the initial conditions

An assessment of three downscaling approaches has been performed using the regional climate model ALARO-0 coupled to the land surface model SURFEXv5, with lateral and initial boundary conditions from ERA-Interim. The simulations were applied for a 10-yr period from 1991 to 2000, for a Western European domain. The performance of ALARO-0 with SURFEX has already been validated for NWP applications (Hamdi et al., 2014), and here we present an evaluation for long-term climate simulations.

We compared the commonly used approach of a continuous climate simulation with two alternative methods of frequently reinitialising the RCM boundary conditions, combined with either a daily reinitialised or continuous land surface. The use of a daily reinitialised atmosphere outperformed the continuous (CON) approach for winter and summer 2 m temperature, and deteriorated the summer precipitation. However, the use of a continuous land surface (FS) with a daily reinitialised atmosphere improved the summer precipitation relative to the full continuous approach. Furthermore, it improved the winter 2 m temperature, whereas it resulted in a neutral impact on the summer 2 m temperature and the winter precipitation, despite a slight deterioration over the Mediterranean. The SSTs were reinitialised daily together with the atmosphere, as compared to the monthly updated SSTs in the continuous approach.

In conclusion, this study demonstrated that the approach of a daily reinitialised atmosphere was superior over the full continuous approach. The use of a continuous surface next to a daily reinitialised atmosphere improved the winter temperature and summer precipitation. We recommend using FS in a setup with GCM forcing for climate simulations with ALARO-0.

Relevance? To motivate the use of the FS approach for the future climate projections.

Urban Heat Island

The UHI in Brussels was enhanced under heat wave conditions both for the dense urban areas as the suburban areas. The increased nighttime urban temperatures suggested a feedback between a heat wave and the UHI, which was in agreement with other studies. Moreover, the vegetated areas experienced a large increase in the UHI under heat wave conditions because of the lack of radiative

cooling. Even though the UHI is predominantly a nighttime phenomenon, an increase in UHI was still present during daytime. The reduced wind speed under heat wave conditions confined the UHI effect to the urban area instead of further downwind under climatological conditions.

The state-of-the-art simulation over Belgium at 1 km horizontal resolution allowed us to compare different rural and urban regions with the purpose of analysing urban climate. More heat waves occurred in urban areas than in rural areas in the 20-yr period of 1991-2010. The heat wave duration was also impacted by the urbanisation resulting in the longest lasting heat waves occurring in the dense urban area. Besides, a larger number of heat waves was found in the northern part compared to the southern part. However, the cities in the southern part demonstrated larger number of heat waves because they were located more inland and at low elevation levels in the river valley. In correspondence to larger UHI during the night, the cumulated nighttime intensity was larger than the cumulated daytime intensity. The intensity was twice as large in the urban areas than the rural areas.

The four cities in Belgium were evaluated with respect to their UHI effect. Brussels and Liège illustrated a higher UHI intensity during nighttime and daytime than Antwerp and Ghent. On the one hand, this could be explained by the location of the cities of Brussels and Liège that are more inland. On the other hand, Antwerp and Ghent are closely located to the sea and host large water bodies (the ports) that can cool the surface.

Relevance? Identify the Belgian cities that are most vulnerable to climate change, that have a large UHI effect today. We put particular focus on these cities when disseminating the results at the end of the project.

4.3 SPATIAL SIMULATIONS FOR THE FUTURE

4.3.1 EVOLUTION OF FARM SIZES

Simulations with ADAM show the continuing decrease of farmers and the increase of farm size (Figure 24). When categorized, the results show a clear decrease in the relative importance of the smallest farm sizes. It is mostly the category of 30-50 ha that gains the most relative importance in the total farm size distribution. The largest farm sizes (>50ha) only increase slightly (Figure 25).

Spatial visualisation of these results shows a clear increase in the average farm size in 2035, when compared to 2010. Especially in the central south of Belgium, the model predicts important increases. This can be attributed to the low fertility of the soil and the, in general, lower succession rate in this part of the country. Patterns from 2010 persist in 2035, with in general smaller farms in the north of the country than in the south (Figure 26).

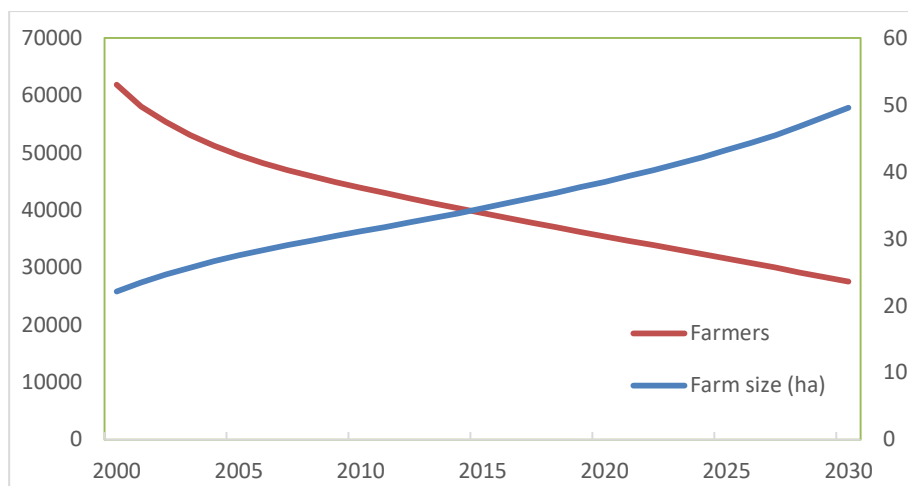


Figure 24: Evolution of the number of farmers and the average farm size in hectares according to simulations in ADAM

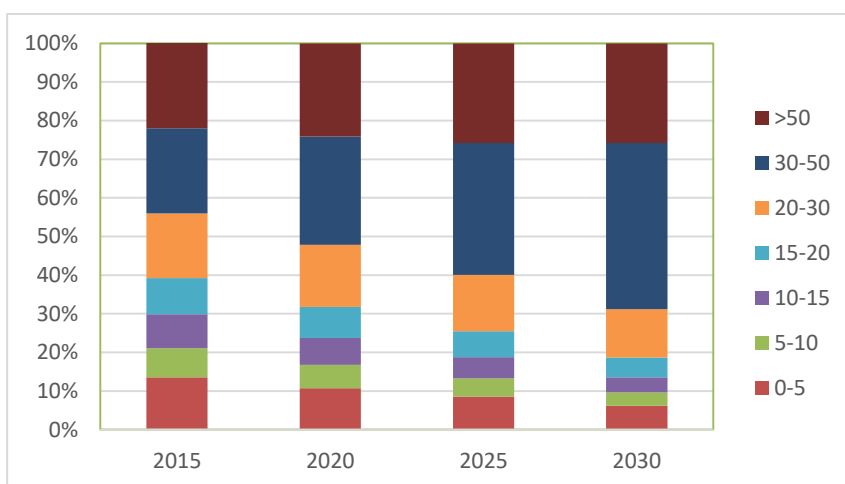


Figure 25: Evolution of the farm size distribution as a percentage of the total amount of farms in Belgium based on ADAM simulations

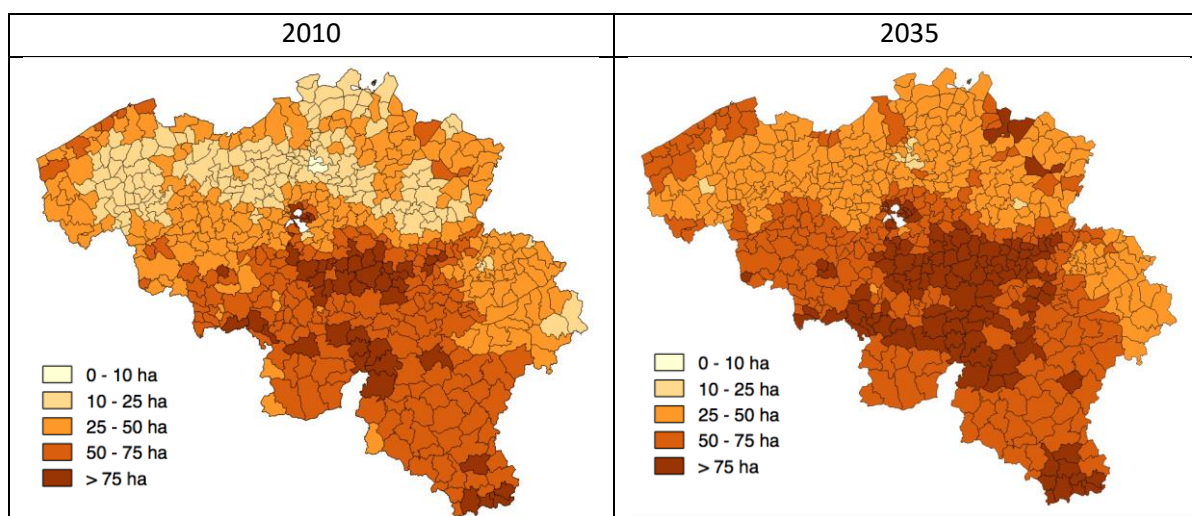


Figure 26: Observed average farm size in Belgium for 2010 (left) and predicted farm size for 2030 (right) by ADAM.

4.3.2 LAND USE CHANGE SIMULATIONS

Compared to the version used for the validation, the model was slightly adapted to the context of the MASC project :

- The coupling requirements lead to the simplification of the growing season, with a growing taking place over only one civil year (the sowing date of winter cereals and rapeseed is thus done the first day of the year). Other parameters were adapted consistently with that change ;
- Globally, the use of different climate scenarios leads to a slight recalibration of the crop model parameters.

Basic ADAM model version and coupled simulation under RCP8.5

These simulations lead to a fully coupled cycle with the final use of the LU maps produced by the LSD module imported into the ALARO model, in order to study the impacts of LU changes on climate. First of all, let us note that the LU map produced by the LSD module is quite different from the initial one used previously in ALARO (which came from the ECOCLIMAP-SURFEX module), due to several LU conversions and simplifications between the surface schemes of the models (Figure 27). The most perceptible impact can be observed for forests with a very different distribution between the three forest types, which is mainly due to the simplified forest composition used in the project. The coupling strategy between LSD and ALARO, now based on the LU, leads to the choice of the socio-economic and climate scenario RCP 8.5 & Global Economy, which gives the stronger LU changes through time. Under that scenario, the main changes are related to the dense urban and temperate sub-urban classes (Table 11 and Figure 28).

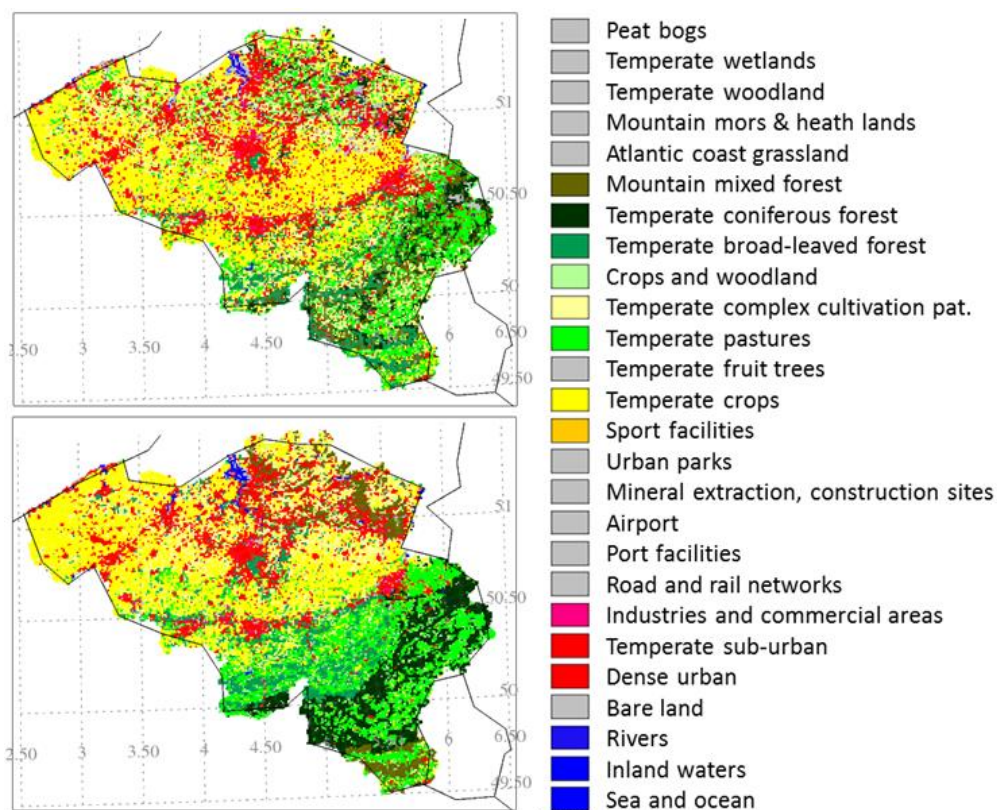


Figure 27: Top, initial LU map from ECOCLIMAP; bottom, new LU map produced by the LSD module (colored classes represent more than 95% of the simulated area).

Class Number	Class	% of change
151	Dense urban	+210%
153	Temperate sub-urban	+21%
166	Temperate crops	-4%
182	Temperate pastures	-13%
218	Mountain mixed forest	-6%

Table 11 : Evolution of the main LU classes (from SURFEX-ECOCLIMAP)

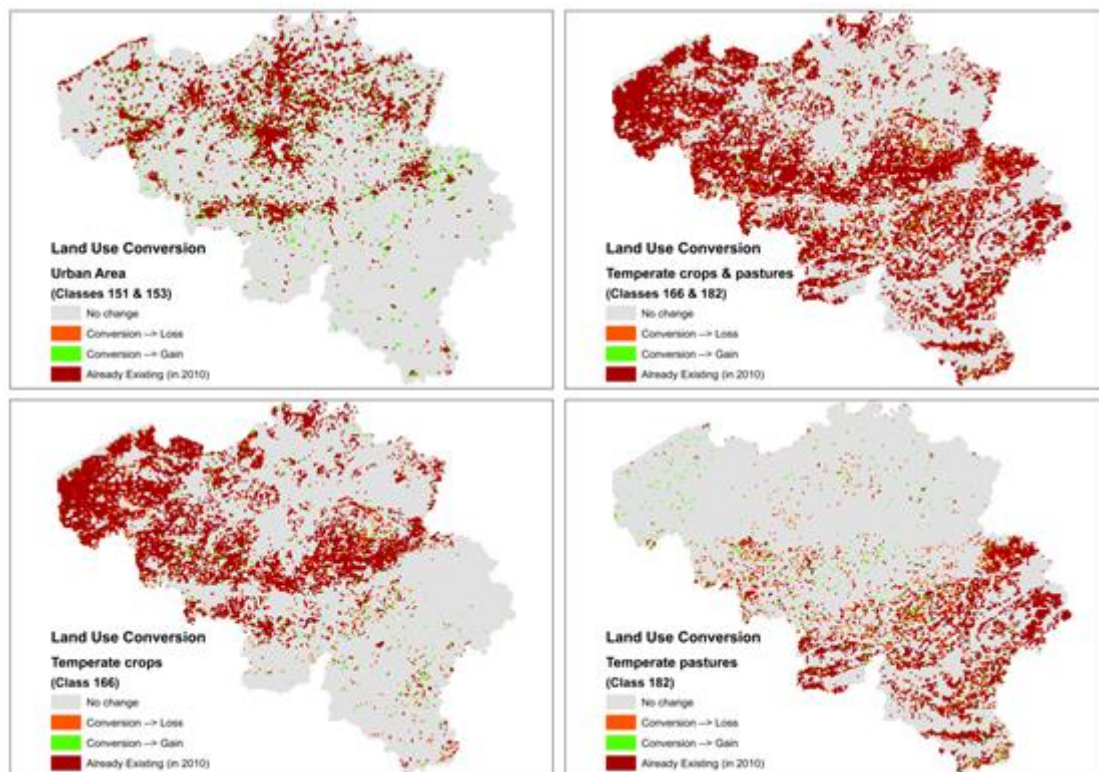


Figure 28: Cells conversion (gain for and loss from) the main LU classes impacted, given to the LSD module under RCP8.5.

Improved ADAM model and new coupled simulations under RCP8.5 and RCP4.5

While the previous simulations (full coupled LSD-ALARO) were sensitive to LU changes, they were clearly less sensitive to LC changes within the agricultural areas. With an improved ADAM version (for agricultural areas), we propose here a more detailed analysis of the LULC changes for LSD simulations under socio-economic and climate scenarios RCP 8.5 and 4.5. We propose to compare mainly two coupled simulations, RCP 8.5 associated by socio-economic scenario “Global Economy” (GE) and the climate scenario RCP 4.5, associated with the scenario “Strong Europe” (SE).

First, CARAIB was forced with the two climate scenarios in order to analyse the climate impact on the productivity and especially on crop yield, to which the agent-based model is sensitive. Under the two scenarios, the productivities and yields are very slightly positively impacted by climate change, but also by the fertilisation effect of the rising atmospheric CO₂ (Figure 29). Even if the 2035 time horizon used in this study is relatively limited (at the climate scale), we could however observe a

difference in the model response under these two climate forcings. Nevertheless, while the inter-annual variability remains reasonable with the climate scenario used for the validation (Figure 17), we have to note that inter-annual variability is higher in these simulations. Its increasing through time probably needs to be put into perspective. As a whole, and as expected, the global Belgian yields of the 6 selected crops increase in the future, but it is likely that they will potentially suffer more frequent and more intense extreme events which significantly reduce crop yields during these extreme years.

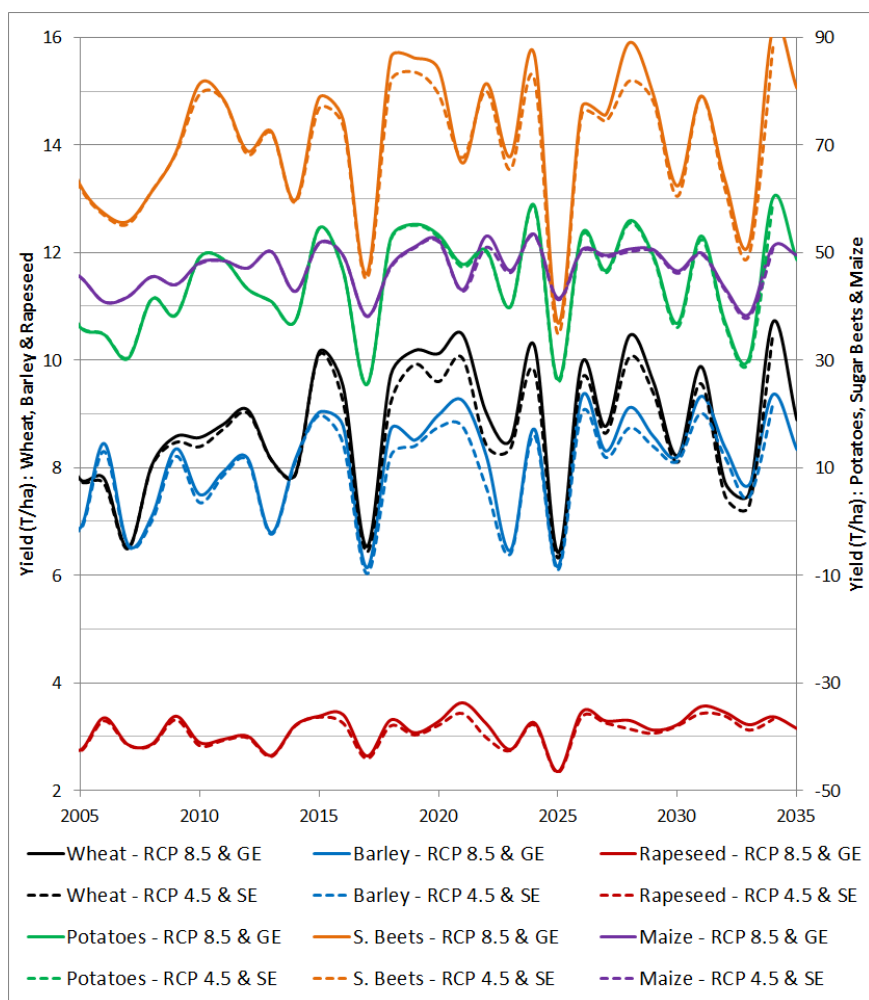


Figure 29: Average yield for Belgium calculated by CARAIB between 2005 and 2035, under climate scenario RCP 4.5 and RCP 8.5 (associated respectively with socio-economic “Strong Europe” and “Global Economy”).

These yields, calculated under climate changes, were used by the ABM to produce LULC outputs, according to their associated socio-economic scenarios (Table 12). As expected, “bare soil” and “water” already relatively limited in the area are not much modified under the two combined scenarios. After all, natural vegetation and crops remain relatively stable through time; it is the pasture class which shows a relatively more important decrease under the combined scenario “RCP8.5&GE”, with a reduction larger than 3%. But all these small decreases benefit to the urban class which strongly increases, especially, as expected, under the scenario “RCP8.5 & GE”. Within the area of agricultural crops, the relative changes are more important, with a nearly disappearance of sugar beets under the 4 combined scenarios, while potatoes and rapeseed also significantly decrease. This is probably due to the high yield variation through time, linked to the market price,

under both combined scenarios. Rapeseed is reduced strongly, while winter cereals increase, especially under the scenario “RCP8.5 & GE”.

The examination of the yearly LULC evolution (Figure 30), e.g., for the coupled scenarios “RCP8.5&GE”, shows that the evolution is smooth for the LU change, while the variations are well-marked for LC. Obviously, the ABM is sensitive to the yield variation (which are especially well-marked with these climate scenarios), and the important decreases explain the increase of the maize cover, which shows a more stable evolution in the future. Spatially, if we compare the LU maps used in CARAIB (dominant class) per pixel in 2000 and the LU maps under both combined scenarios (Figure 31), the differences are not obvious, but if we carefully analyze the north of the country we can notice a significant urban sprawl, especially under combined scenario “RCP8.5 & GE”.

	RCP 8.5		RCP 4.5	
	GE	BAU	SE	RC
Natural Vegetation	-1.7	-1.5	-0.2	0.2
Crops	-2.0	-2.7	-1.0	-1.0
Pasture	-3.7	-0.7	-1.5	-0.8
Urban area	9.6	7.5	3.6	2.2
Bare soil	-1.5	-1.8	0.2	-0.2
Water	-0.7	-1.2	0.0	0.0
W. Barley	13.9	14.2	15.9	16.6
W. Wheat	14.5	14.0	16.1	15.6
Potatoes	-23.1	-23.3	-22.5	-22.4
Sugar Beets	-85.6	-86.0	-86.1	-86.0
Maize	19.0	17.8	20.2	20.0
Rapeseed	-31.8	-32.3	-32.2	-31.4

Table 12: Relative area change (%) between the average 2006-2015 and 2026-2035 for the 6 land use classes and the 6 crop covers (within the agricultural crop area).

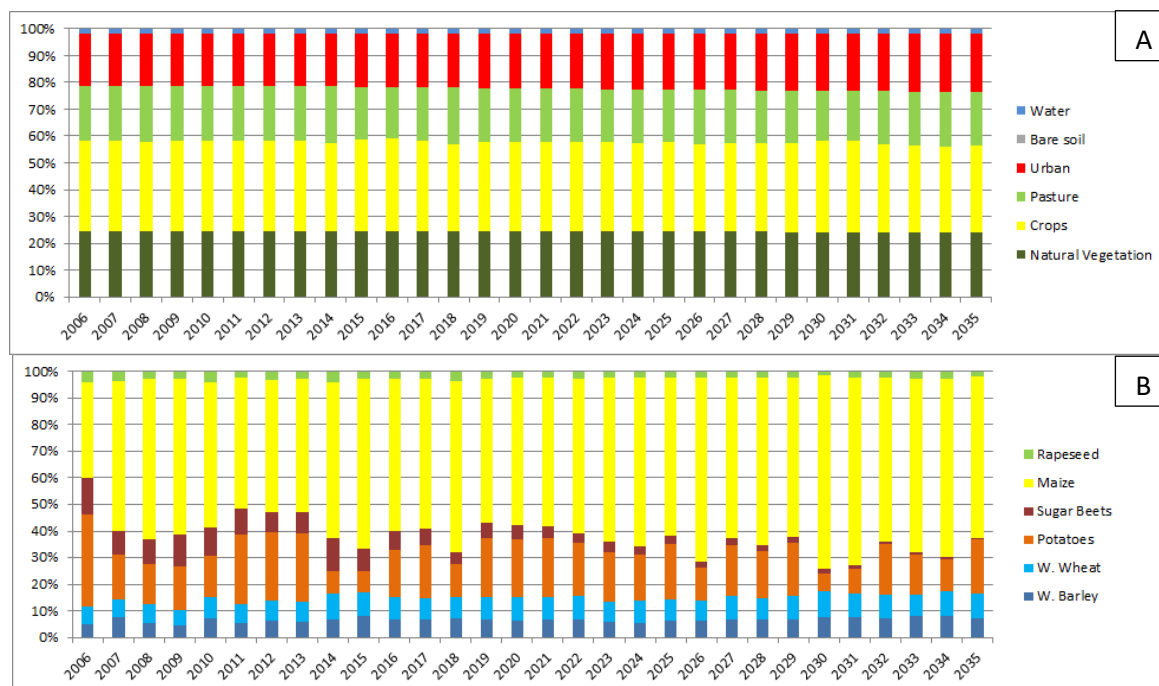


Figure 30: Yearly evolution of the 6 LU class proportions (A) and of the 6 selected crop covers within the agricultural area (B), under combined scenario “RCP8.5 & GE”

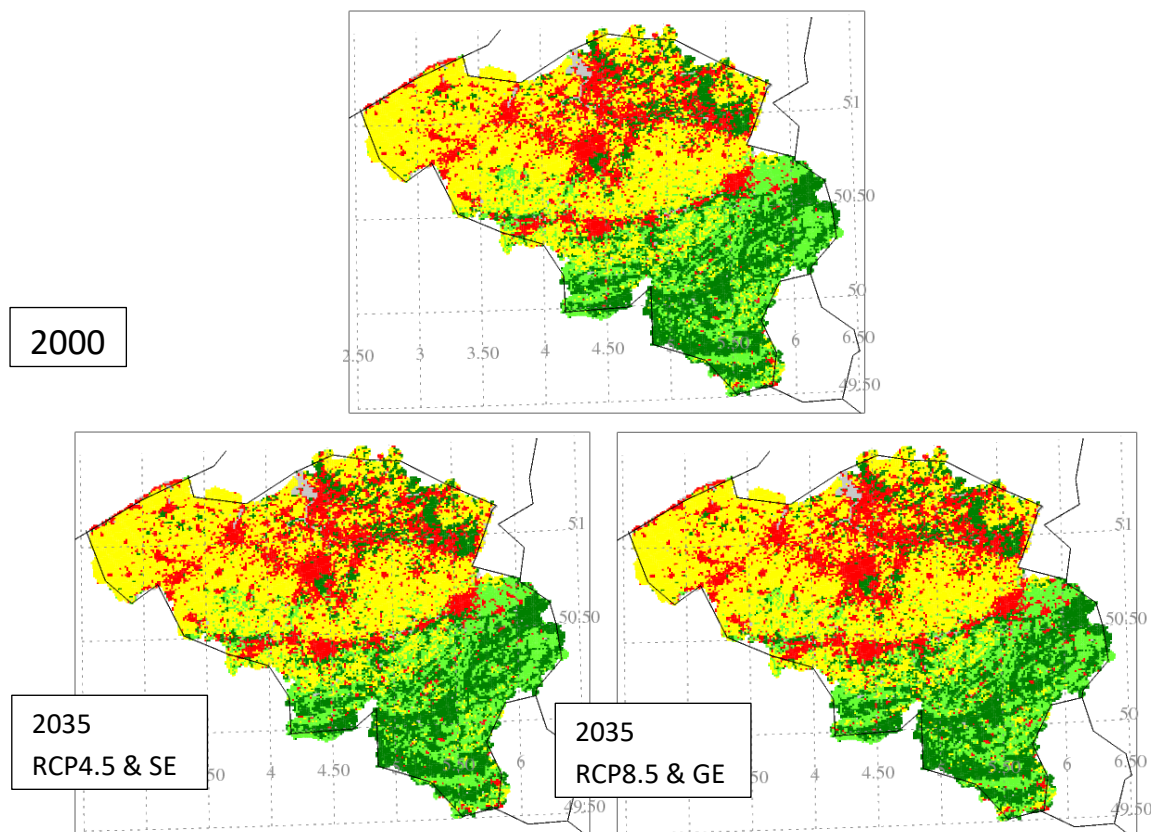


Figure 31 : LU dominant classes (CARAIB) in 2000, compared with LU dominant class per pixel in 2035 under combined scenarios RCP4.5 & SE, and under RCP 8.5 & GE.

All these changes will obviously impact the ecosystems (Figure 32), but also parameters influencing the climate (Figure 33). For the recent past (2006-2015), the net primary productivity (NPP) is as expected, higher in the south of the country, clearly linked to more abundant vegetation. Overall for the future, NPP will remain quite stable in the future, but vegetated areas will be positively impacted by the climate change and the increasing atmospheric CO₂, and the increase is more important under the scenario “RCP8.5 & GE”. This is particularly true for the south of the country which is clearly more vegetated. For both scenarios (but obviously, in a larger extent under scenario “RCP8.5 & GE”), we could observe some patches with a net decreasing NPP, located in the center of the country and linked to the LULC changes with increased urban area.

The net sequestration of organic matter, or the net gain or loss of carbon for a region, can be evaluated with the Net Biome Production (NBP - Figure 32). The NBP is defined as the NPP reduced by the heterotrophic respiration (it can include the losses by herbivores, but in the model, it is mainly the decomposition of organic matter in the soil), the losses through rivers, the losses due to fires and, more important, the harvest losses; the NBP can illustrate the changes in the carbon cycle induced by land use. In the largest part of the country, the NBP is negative, due to the removal of carbon on the agricultural area (harvesting). On the contrary, forested areas show largely positive values, but in the future, it seems that NBP could be reduced in these areas (blue area – Figure 32) in the south of the country. The coniferous forests and meadows (Figure 27 – bottom) seem to be negatively impacted, with a gain of NPP unable to counterbalance the losses.

Regarding the soil water content, the reference period (2006-2015) logically presents drier conditions in the north with the sandy soils, while the south is wetter thanks to higher rainfall. For the future, we could not identify a significant trend, but the sandy region and High Ardennes present slightly drier conditions, while, in lesser extent, the opposite region along the French border have a slightly wetter soil.

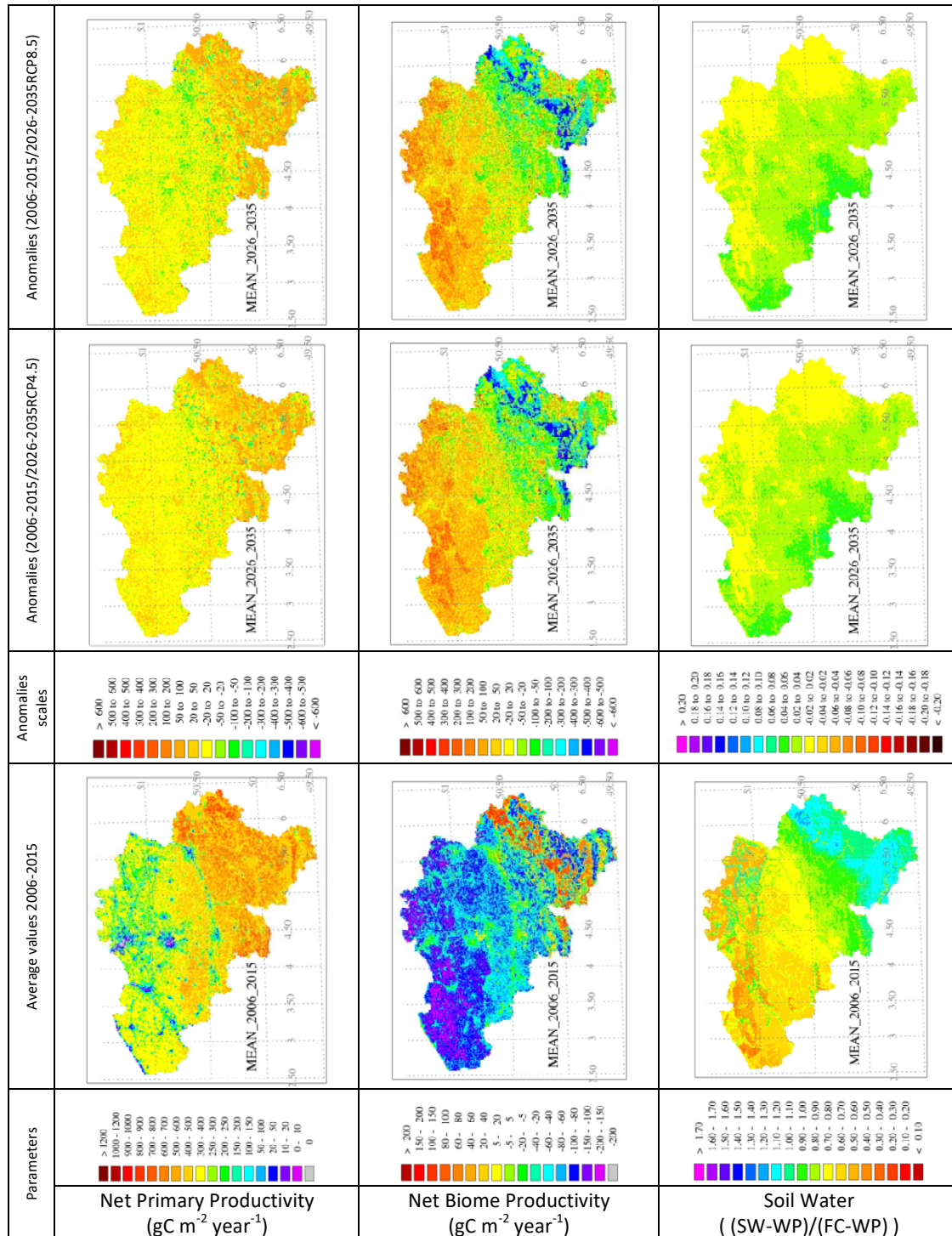


Figure 32: Average values (2006-2015) of the Net Primary Productivity, the Net Biome Productivity and the Soil Water content, with their anomaly maps for the future (average 2026-2035) under combined scenarios “RCP4.5 & SE” et “RCP8.5 & GE”.

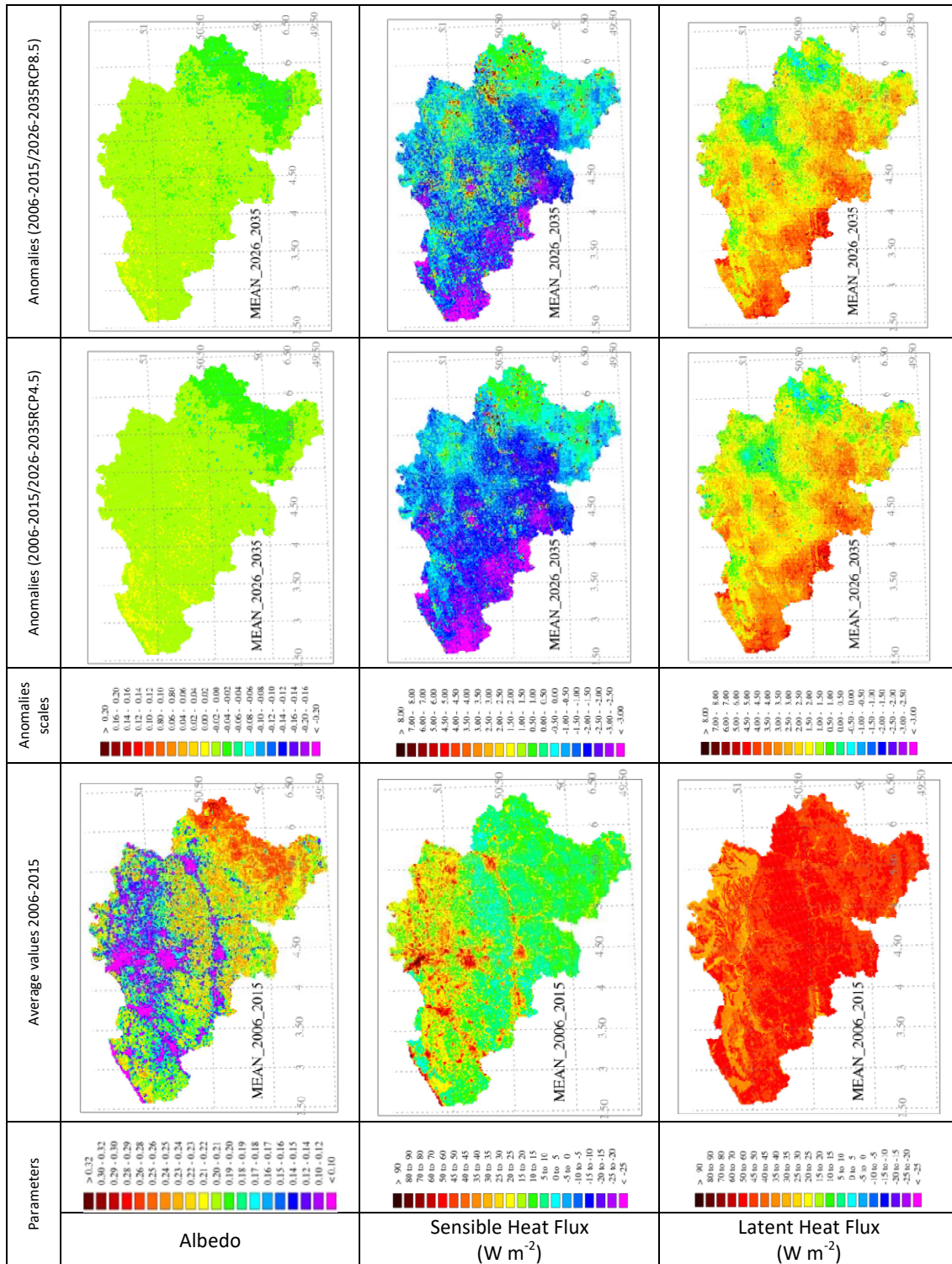


Figure 33: Average values (2006-2015) of the albedo, the sensible heat flux and the latent heat flux, with their anomaly maps for the future (average 2026-2035) under combined scenarios “RCP4.5 & SE” et “RCP8.5 & GE”.

Beyond these relatively positive impacts observed for ecosystems, we can now have a look on the potential feedbacks of these changes on the climate (Figure 33), and the first parameter we can analyze is the albedo. Its average value for the period 2006-2015 is quite high in the south of the

country due to the snow cover in winter. During spring and summer, the forested areas show values under 0.20 (around 0.18/0.19 for deciduous forests and 0.16/0.17 for coniferous forests). In the future, the snow cover decrease leads to a lower albedo in the south of the country. But, as a whole, due to the LULC conversions, some areas (mainly in the north) show a slight increase of the albedo, while in the center the opposite evolution is observed. This dominant slight decrease could reinforce the climate change effect over the country.

Regarding the latent and sensitive heat fluxes, they react in opposite directions, with a global increase for latent heat flux and thus a decrease for the sensible heat flux. At the regional level, the pattern (linked to the soil water) shows (1) slightly stronger sensible heat fluxes in Kempen and in high Ardennes (where soil is becoming slightly drier) and (2) the opposite is observed along the French border (where the soil is becoming slightly wetter). In the Ardennes and in Kempen, this could lead to the reinforcement of the climate change (in addition to the albedo changes). At the coast and near the south border, the fluxes changes could lead to counteract the effects of the climate changes (in addition to the albedo increase).

4.3.3 NEAR FUTURE CLIMATE PROJECTIONS

An assessment of the near future climate changes in Western Europe has been performed using ALARO-SURFEX driven by boundary conditions from CNRM-CM5.1, with a particular focus on Belgium. We illustrated the changes that occurred in the projected period (2006-2035) compared to the control period (1976-2005) under the assumptions of two greenhouse gas concentration trajectories resulting from the IPCC Fifth Assessment Report, namely the scenarios RCP4.5 and RCP8.5. The focus of the analysis was particularly on the near-surface daily temperature and daily precipitation totals. The mean global climate changes in the near future have been diagnosed as being small with respect to the extremes (Kirtman et al., 2013). Therefore, this analysis covered both mean changes of the temperature and precipitation as well as changes in their extremes. In addition, a good understanding of the changes in the near future is of high interest to stakeholders, as they can help society in designing adaptation strategies in function of the extreme events.

The projected mean change over Western Europe of the daily 2 m temperature was found to increase in the range of 0.3 to 0.6 °C. This projection was valid for the two RCP scenarios, as the differences among them were very small. The differences in space were also small except for the Alps that simulated a higher increase during autumn and winter and a north-south gradient in summer. The minimum temperatures increased at a faster rate than the maximum temperatures, except for autumn. In fact, the increase in maximum temperature in autumn was the largest modelled change in the near future with 0.58 °C. A particular focus on Belgium revealed largest increases in summer in the north of the country, but largest increase in winter in the south of the country. Despite a decrease in variability in spring, the other seasons demonstrated an increase in variability in the temperature.

The changes in extreme temperature were similar to the mean temperature changes at low resolution. However, a large spatial variability was present with increases of extreme temperature up to 2 °C for widespread regions in our domain (Figure 34). Increasing the resolution over Belgium revealed an urban-rural contrast of 1.2 °C with respect to 0.6 °C. Consequently, these results confirmed the added value of SURFEX and its urban parameterisation. Besides, they confirm that extreme temperatures warm faster than the mean temperatures in the near future (Kirtman et al., 2013). The spatial variability in summer was also reflected by the number of heat waves. Although the change in the number of heat waves was small, the number of heat wave days will likely increase with +6 to +13 days depending on the future scenario. Besides, the scenarios agreed on an increase in the maximum duration of 1 to 3 days and an increase in minimum cumulated intensity of 0.2-2 °C. The modelling of heat waves was less sensitive to the choice of the resolution than to the choice of the scenario.

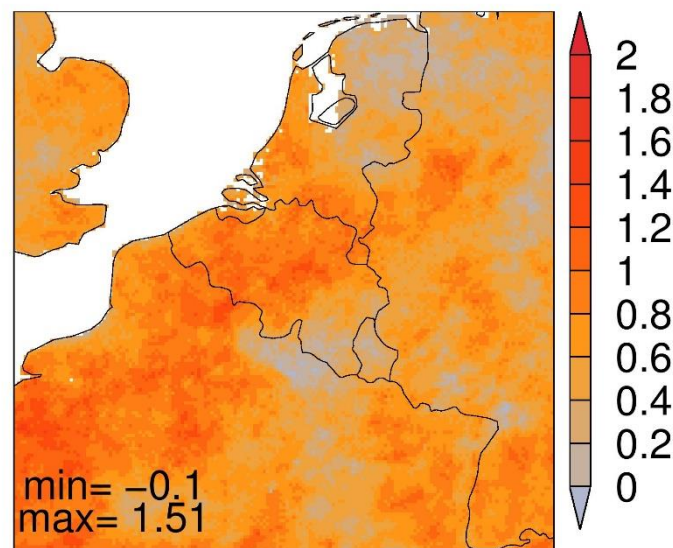


Figure 34: The projected change in the 90th percentile of the maximum daily temperature at 4 km horizontal resolution.

The projected mean changes over Western Europe of the daily precipitation totals were found to be small in the range of 2-5%. However, the extreme precipitation changes were larger during spring, autumn and winter than the mean precipitation changes with values of 4-6% and local increases up to 20% and more. The winter showed a consistent signal under both scenarios and model resolutions with decreasing frequency and intensity of extreme precipitation events and increasing extreme precipitation amounts in accordance to the higher return values.

Relevance? The previous results for mean and extreme temperature and precipitation changes in the near future give the framework for assessing the regional climate model with changed land use and land cover.

Land use and land cover changes

We performed an experiment with changing the underlying land cover in the model with a scenario for the land use changes in the near future. The simulations were performed for a 30-yr period in the near future (2006-2035) and compared to the same period but with the original land cover, to disentangle the effects of LULCC only. The previous results were used for the sensitivity test of the climate change effects. The comparison of the future period with changed land cover and the historical period (1976-2005) with the original land cover was used to reveal the combined effect of climate change and land use change.

The results are demonstrated (Figure 35) for three boxes in the region of Western Europe that correspond to regions with large portions of grid cells experiencing a conversion from one land cover type to another land cover type: (Box 1) from grassland to arable, (Box 2) from arable to built-up, (Box 3) from arable to forest (Berckmans et al., 2019).

We demonstrate the effect of LULCC in the future climate by averaging the entire domain and the grid boxes in the three boxes. The changes in the mean temperature by LULCC are largest for box 2 and box 3 with an average warming of 0.35 °C and 0.13 °C. This increase is mainly determined by an increase in minimum temperature of 0.56 °C and 0.53 °C. Furthermore, the LULCC increase the maximum temperature in box 2, but inhibit decreases in maximum temperature for the other boxes. The mean and minimum temperature decreases in box 1 under LULCC with -0.19 °C and -0.38 °C respectively, while the maximum temperature change is slightly positive with 0.01 °C. All domains

display significant decreases in the diurnal temperature range by LULCC. The precipitation change caused by LULCC in the future is negligible.

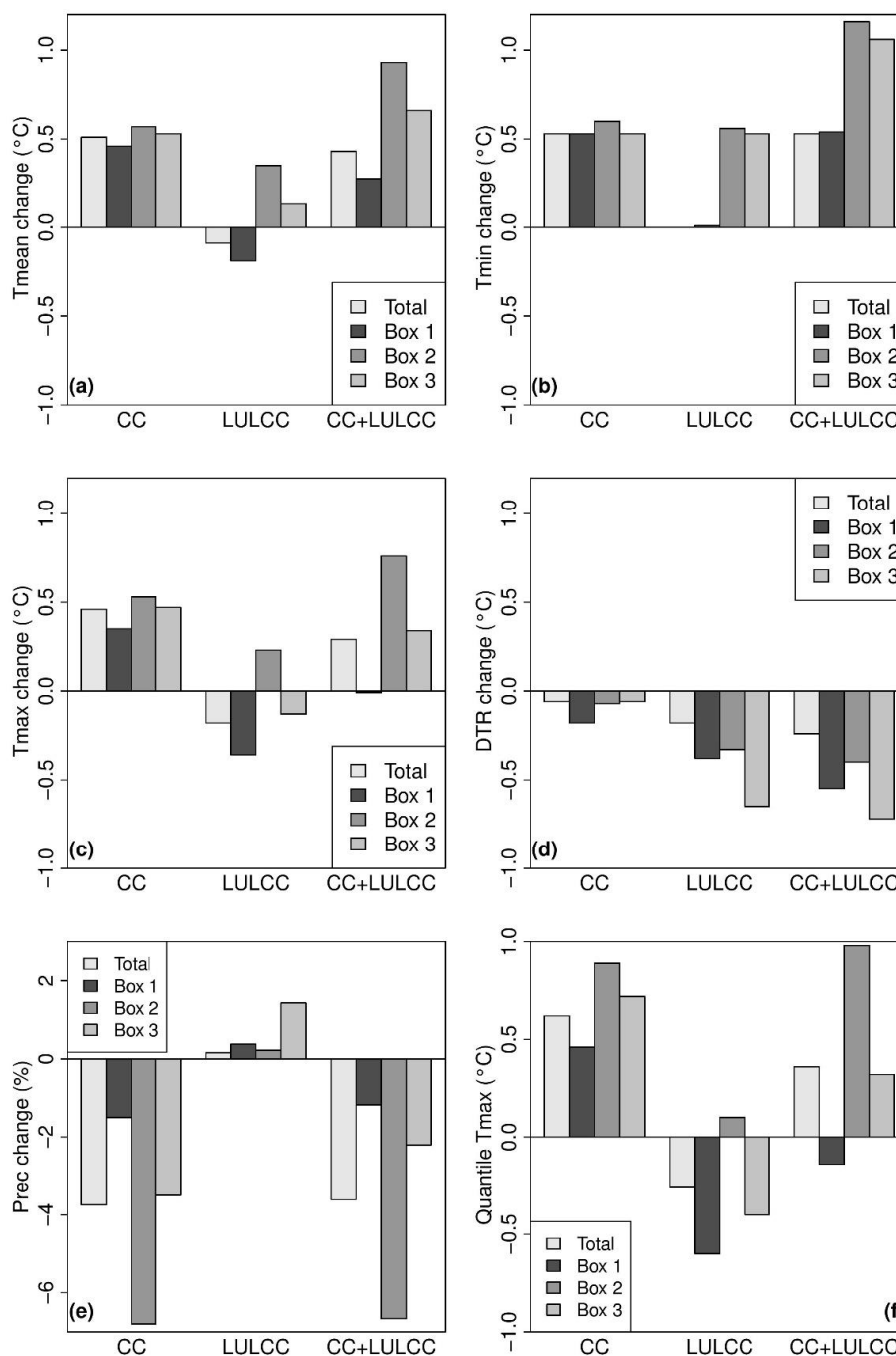


Figure 35: Projected climate changes (CC) in the 30-yr period (2006-2035) with respect to the 30-yr control period (1976-2005) in the summer (June-July-August), projected LULCC under RCP8.5 and the combined effect of both for (a) mean 2 m temperature (°C), (b) minimum 2 m temperature (°C), (c) maximum 2 m temperature (°C), (d) diurnal temperature range (°C), (e) precipitation(%), and (f) 90th percentile of maximum 2 m temperature (°C).

The combined effect of climate change and LULCC results in an amplified minimum temperature compared to the climate change only (Figure 35b) that reaches positive changes above 1 °C when averaged over the grid boxes of box 2 and 3. The maximum temperature is reduced when considering climate change and LULCC for the region in box 1 and 3 and the averaged total domain

(Figure 35c). Both increased minimum temperatures and decreased maximum temperatures lead to a stronger reduction of the diurnal temperature range in the near future combined with LULCC (Figure 35d). The negative precipitation changes under climate change are only slightly reduced by the small positive precipitation changes under LULCC (Figure 35e).

Dynamic vegetation

We demonstrate the impact of dynamic vegetation for the near future using the CARAIB model on the country-scale of Belgium. Figure 36 presents the daily minimum 2 m temperature changes due to LULCC (Figure 37) in comparison to the near future without LULCC. Largest positive changes occur over the urban areas. Only small locations show a decrease in temperature. On average, the temperature is projected to rise from 0.4 °C to locations that will convert to more urban fraction. The main warming occurs around the city of Liège and Charleroi. Not much at the coast or in the Province of Luxembourg.

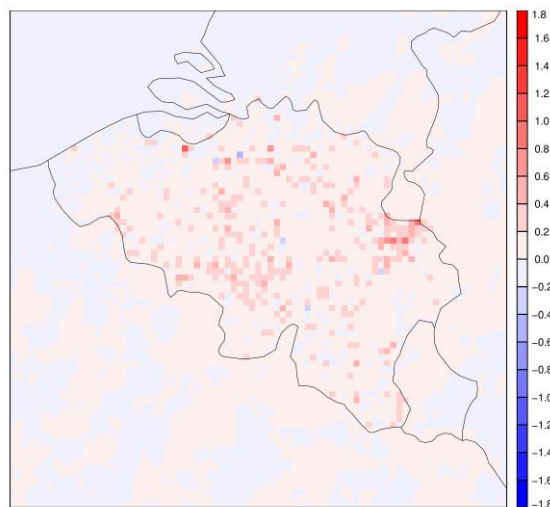


Figure 36: Projected summer change of the daily minimum 2 m temperature in the 16-yr period 2020–2035 under RCP8.5 and with dynamic LULCC with respect to the projected period without LULCC.

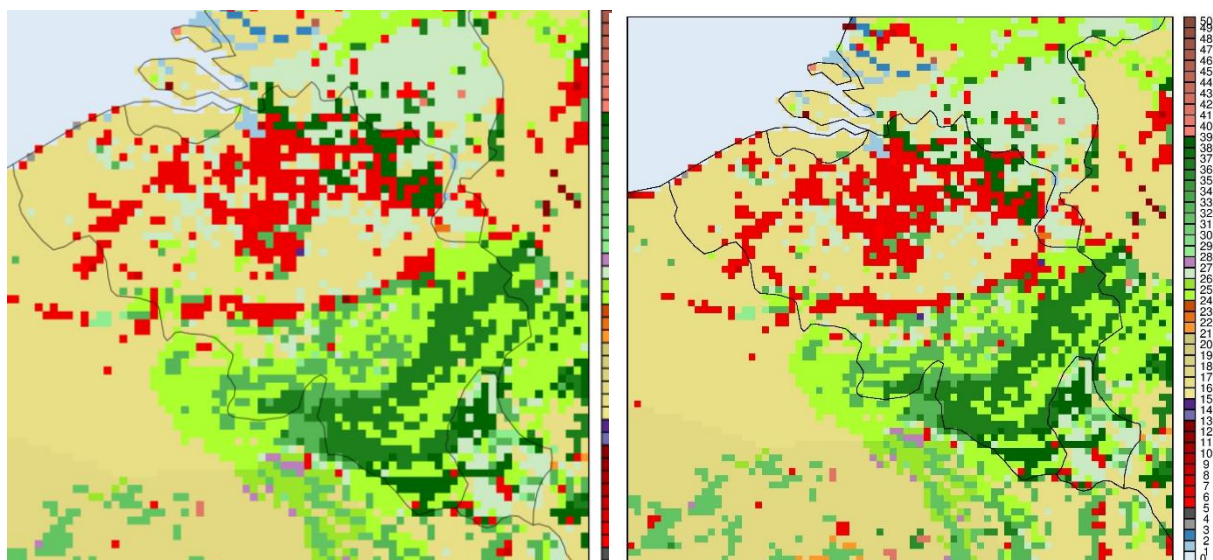


Figure 37: Land cover types by left) CARAIB year 2005 and right) CARAIB year 2035. Blue colors = water surfaces, red colors = urban areas, yellow = crops, lightgreen = grassland, bluegreen = pasture, green = forest, brown = others

4.3.4 PHENOLOGICAL CHANGES

The applicability of the method developed by Laanaia et al. (2016) to analyze the uncertainties of the impact of climate change on vegetation over France was demonstrated over the Euro-Mediterranean area. Phenology indicators (leaf onset, leaf senescence) were produced for four plant functional types (grasslands, straw cereals, broadleaf tress, coniferous trees). Figure 38 shows the results for grassland leaf onset at the end of the 21st century.

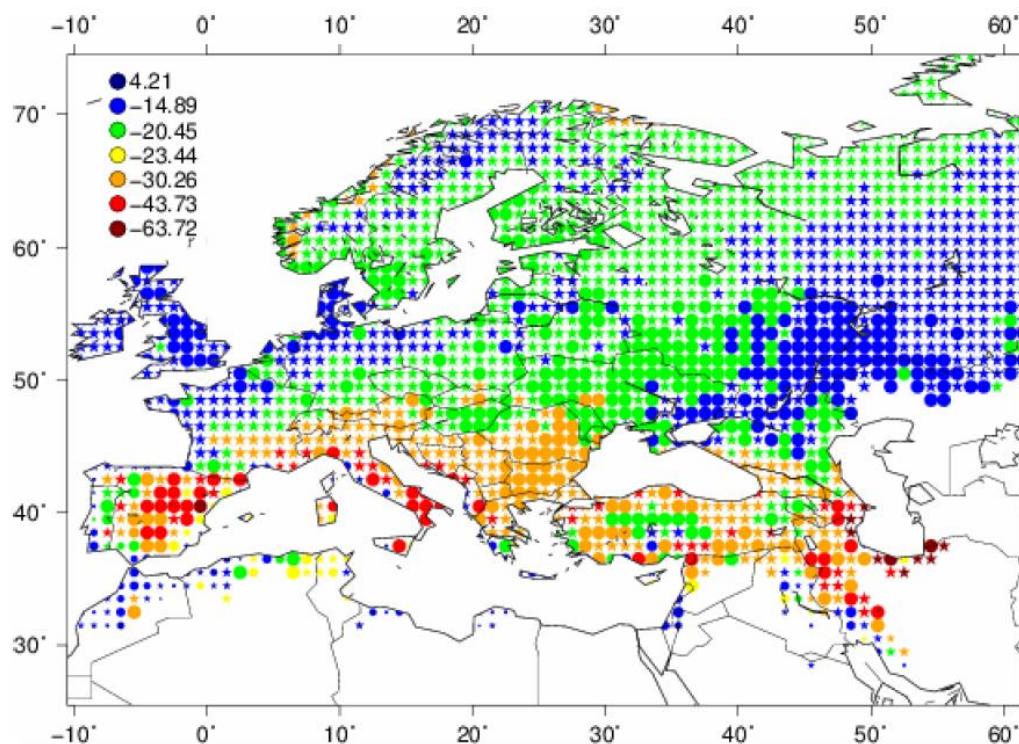


Figure 38: Grassland mean leaf onset difference (days) in 2070-2099 with respect to present (1985-2015) over the Euro-Mediterranean area, under the RCP8.5 climate scenario. Atmospheric variables from four climate model simulations (CNRM-CM5, HADGEM2, IPSL-CM5A-MR, CanESM2) are used to produce ISBacc simulations. Leaf onset is derived from the simulated LAI. Symbols size corresponds to the number of ISBacc simulations presenting a significant trend. Circles mean that all ISBacc simulations indicate a significant trend. Stars mean that at least one ISBacc simulation trend differs from the other simulations.

4.4 POLICY RELEVANCE AND RECOMMENDATIONS

The main objective of this project was to evaluate the impacts of land surface changes on climate at a regional scale. The tiny changes that affect land use and land cover from one year to the next are generally thought as unimportant, in terms of climate. Thus, they generally have been disregarded in climate studies and models, which generally consider land use and land cover patterns, but not their changes over time. However, the cumulated effects of these changes over a specific region may have substantial effects on climate and reinforce or mitigate climate change, depending on the type of land use/land cover conversion.

Simulations on agricultural population and farm size evolution in Belgium under the assumption that recent trends continue, predict an ever-increasing average farm size for the future (up to the 2035 horizon). The increase in farm size results in an increase of average parcel size (Figure 38). The

enlargement of parcels results in a decrease in linear elements (ditches, edges and hedges) and point elements (tree islands), grasslands and wetlands (Harms et al., 1984; Ihse, 1995; Poudevigne and Alard, 1997). These landscape changes have an effect on regional climate and these effects might be even more pronounced under the different scenarios of climate change. A focus on conserving these point and linear elements in the agricultural landscape might mitigate the effects of climate change. This can be achieved through an active conservation policy on these elements in the process of farm size increases, or through the active support of smaller farms that contribute to a more diverse landscape.

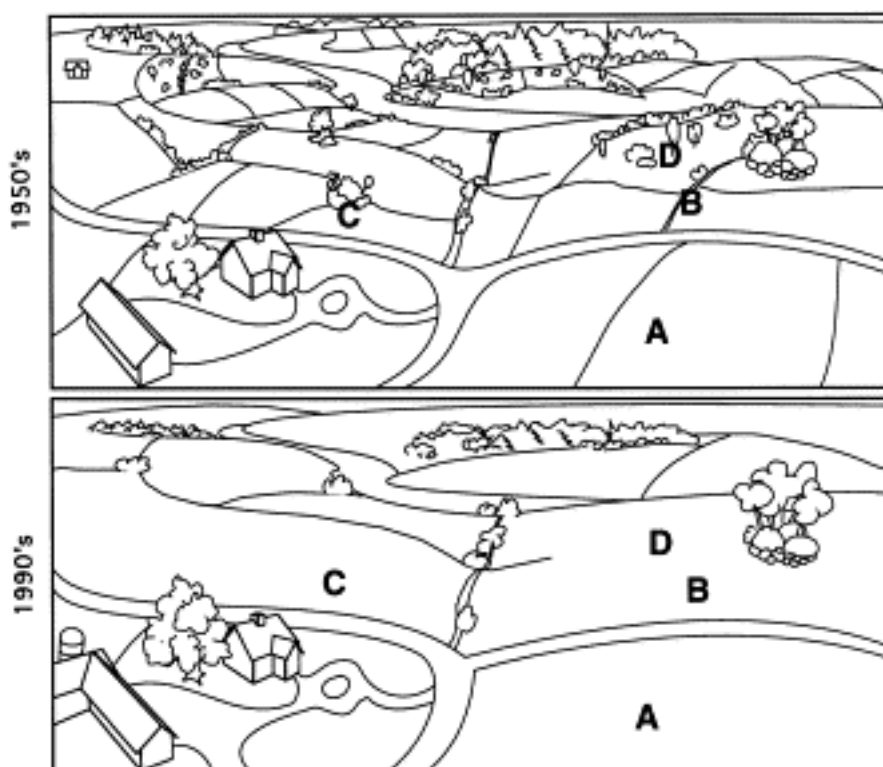


Figure 38: Example of agricultural landscape changes: (A) enlargement of fields; (B) removal of linear elements; (C) removal of point elements; (D) cultivation of natural grasslands (Björklund et al., 1999).

At a slightly larger scale, the simulations of the regional climate model performed in this project show which regions will be most vulnerable to land use change in the near future and where mitigation and adaptation strategies should be applied. Depending on the type of conversion involved, projected land use/land cover changes can reinforce or reduce climate change. In the scenarios that were developed in this project, a reinforcement of climate change is generally observed. This is because expected land use change in the near future is dominated by conversions from grasslands or crops to urban areas. The associated warming adding to climate change is about 0.4°C on average for the summer season. The effect is particularly important around the cities of Liège and Charleroi. It may even be more important during extreme events, such as heat waves.

Another interesting result of these projections is the fact that the inter-annual variability of crop yield can be expected to increase in the future. This increased variability is associated with more frequent extreme events, such as droughts, which decrease the net primary productivity of vegetation during these years, while the productivity increases during the years not affected by these events, in response to warmer climatic conditions and higher atmospheric CO₂ levels. Phenological changes can also be expected, with for instance a significant advance of leaf onset in the spring.

Many of these results should be useful to landscape planners, urban planners, forest managers, farmer agencies and local governments. There are, however, large uncertainties. The land use/land cover change scenarios have been obtained in a dynamic way, i.e., by using an agent-based model where the agents are farmers who react not only to the socio-economic context, but also to the modelled climate impacts on crop yields. The involved processes are complex and so the uncertainties are high. For instance, the reactions of the farmers in such a scheme strongly depend on the calculated variation of crop yields from one year to the next. However, the uncertainties on inter-annual variations of gross primary productivities and crop yields calculated by dynamic vegetation models are still very large, particularly in regions like Belgium, where yield inter-annual variability is only of the order of 5-10 % of the yield value. Thus, it is quite important to assess the quality of dynamic vegetation models and to evaluate the uncertainties on their projections. In the MASC project, we thus devoted much time to the evaluation of vegetation models. This evaluation was performed at eddy covariance sites, both for crop and forest ecosystems. It proved the added value of using a set of different statistical evaluation methods and data from multiple sites (without site-specific calibration) for long-term model evaluations. The evaluation methods not only confirmed each other, but also led to new insights. Aspects for which one method only provided speculative evidence can be specified using another method. Our model evaluation exercise at forest sites highlighted the need for reviewing the accuracy of the models at the time of canopy closure in spring and canopy shed in autumn and points to other processes to be reconsidered. We confirmed the confining effect of model complexity on the model evaluation process. In order to evaluate each proposed model process in depth, we advise to perform additional techniques including parameter sensitivity tests and the evaluation of structural changes in the models on long-term data across different sites.

5. DISSEMINATION AND VALORISATION

Several methods were used for the dissemination and the valorisation of the results, depending on the target audience (scientific community, stakeholders or general public).

Dissemination among the scientific community

The main channels used to disseminate the results within the scientific community were publications in international journals and presentations at international scientific conferences, such as the annual General Assembly of the European Geosciences Union (EGU), the “Facing the future” conference in Giessen, Germany, the annual meeting of the European Meteorological Society (EMS), the “Ecosystem Services Partnership” (ESP) conference, etc. The latest results of the project have not been finalized yet in the form of scientific articles, but this should be done in a near future.

A web-based platform and a ftp site have also been established. They have been mainly used within the MASC network to exchange data, but were also accessible to a wider audience. Also, a training course on ISBA-NCB was organized by CNRM in Toulouse for RMI staff in October 2016.

Dissemination among stakeholders and general public

Some stakeholders or scientists in close contact with stakeholders have been chosen in the follow-up committee of the project. Regular meetings of this follow-up committee have been organised. Many questions/suggestions resulted from these meetings and these have significantly impacted the orientation of MASC research.

A publication presenting the project was organised in *PanEuropean Networks* to publicize the project among European stakeholders.

Several interviews for media or conferences for general public were also given by my MASC scientists. For instance, a conference was given by Ingrid Jacquemin to the “Fédération Wallonne de l’Agriculture”.

Valorisation

There have been various types of valorisation of the project.

First, the project produced four doctoral theses, two of which have been defended in the last year of the contract, while the others are still to be defended.

The project also enabled some of the MASC teams to participate in international projects, such as the PROFOUND COST Action and the Inter-Sectoral Impact Model Intercomparison Project (ISIMIP; <https://www.isimip.org>). The upgrades of the models performed within MASC, especially the implementation of land use/land cover change in the CARAIB model, have enabled the participation in ISIMIP2a and ISIMIP2b. The spatial scale of the ISIMIP simulations were quite different from MASC (global versus Belgium territory), but code development performed within MASC allowed the participation within ISIMIP. Several co-authored papers have resulted from our participation in PROFOUND and ISIMIP.

Finally, the project has also allowed two of the MASC teams (ULiège and UNamur) to write a successful proposal (MAPPY) in the framework of the AXIS call of JPI-Climate. The European-wide MAPPY project is led by Prof. L. François, coordinator of MASC. It exploits the tools upgraded (the CARAIB DVM) or built (the ADAM ABM) within MASC to analyse the dynamics of land use change and the associated feedbacks on regional climate in several European countries (Austria, Belgium, Germany, The Netherlands and Spain). Moreover, this new transnational project will also analyse the feedbacks of land use dynamics and climate change on pollination, a topic which was not studied within MASC. This new project involves many stakeholders in the participating countries. It would not have been possible without the expertise developed within the MASC project.

Some attempts of project valorisation for the stakeholders have also been made. For instance, in the fall of 2018, a call for proposal has been released by the Belgian Science Policy, aiming at the valorisation of BRAIN-Be funded projects. In this framework, contacts have been taken with the “*Institut de Conseil et d’Etudes en Développement Durable (ICEDD)*”, who was member of the follow-up committee of MASC. The objective was to translate the results of the MASC project in a form useful, understandable and exploitable for the stakeholders (of which the municipalities) and the general public. One idea was to produce, from MASC climate scenarios, a climate layer to be added in the online land registry maps. The idea looks quite interesting, but the estimated costs were far too high with respect to the maximum budget available per project in the above-mentioned call. So, the idea was abandoned. This is really sad, but we hope that in the future, there will be other opportunities to develop such initiatives of result valorisation for the stakeholders, for instance, in connection with the MAPPY project, that will start in a near future and will extend MASC results.

6. PUBLICATIONS

Publications in peer-reviewed journals

- Balzarolo M., Vicca S., Nguy-Robertson A., Bonal D., Elbers J.A., Fu Y.H., Grünwald T., Horemans J.A., Papale D., Peñuelas J., Suyker A., Veroustraete F. 2016. Monitoring the phenology of Net Ecosystem Carbon uptake using MODIS and in-situ vegetation indices derived from FLUXNET radiation measurements. *Remote Sensing of Environment*, 174, 290-300. Doi: 10.1016/j.rse.2015.12.017.

- Bloemen J., Fichot R., Horemans J.A., Broeckx L., Verlinden M.S., Zenone T. and Ceulemans R. 2017. Water use of a multi-genotype poplar short-rotation coppice from tree to stand scale. *GCB-Bioenergy*, 9, 370-384. Doi: 10.1111/gcbb.12345.
- Dreesen F.E., De Boeck H., Horemans J.A., Janssens I. A. and Nijs I. 2015. Recovery dynamics and invasibility of herbaceous plant communities after exposure to experimental climate extremes. *Basic and Applied Ecology*, 16, 583-591. Doi: 10.1016/j.baae.2015.05.002.
- Horemans J.A., Bosela M., Dobor L., Barna M., Bahyl J., Deckmyn G., Fabrika M., Sedmak R. and Ceulemans R., 2016. Variance decomposition of stem biomass increment predictions for European beech: contribution of selected sources of uncertainty. *Forest Ecology and Management*, 361, 46-55. Doi: 10.1016/j.foreco.2015.10.048.
- Horemans, J.A., Van Gaelen, H., Raes, D., Zenone, T., Ceulemans, R., 2017. Can the agricultural AquaCrop model simulate water use and yield of a poplar short rotation coppice? *Global Change Biology Bioenergy* , 9, 1151-1164. Doi: 10.1111/gcbb.12422.
- Horemans, J.A., Henrot A., Delire, C., Kollas, C., Lasch-Born,, P., Reyer, C.P.O., Suckow, F., Francois, L., Ceulemans, R., 2017. Combining multiple statistical methods to evaluate the performance of process-based vegetation models across three forest stands, *Central European Forestry Journal*, 63, 253-272. DOI: 10.1515/forj-2017-0025.
- Horemans, J.A., Janssens, I.A., Gielen, B., Roland, M., Verstraeten, A., Neiryneck, J., Ceulemans, R., 2018. Unraveling the temporal variation in a 16-year net ecosystem exchange time series of a Belgian mixed forest. Resubmitted for publication in *Agricultural and Forest Meteorology*.
- Van Sundert, K., Horemans, J.A., Stendahl, J., Vicca, S., 2017. Investigating nutrient availability of Swedish conifer forests: important soil factors and evaluation and update of a nutrient availability metric. *Biogeosciences Discussion*. Doi: 10.5194/bg-2017-372.
- Beckers, V., Beckers, J., Vanmaercke, M., Van Hecke, E., Van Rompaey, A., Dendoncker, N. 2018. Modelling farm growth and its impact on agricultural land use: a country scale application of an agent-based model. *Land*, 7 (3), 109. Doi: 10.3390/land7030109.
- Berckmans J., O. Giot, R. De Troch, R. Hamdi, R. Ceulemans, P. Termonia (2017): Reinitialised versus continuous regional climate simulations using ALARO-0 coupled to the land surface model SURFEXv5, *Geosci. Model Dev.*, Vol. 10, 223-238, doi:10.5194/gmd-10-223-2017.
- Berckmans J., R. Hamdi, N. Dendoncker (2019): Bridging the gap between policy-driven land use changes and regional climate projections, *J. Geoph. Res.: Atmospheres*, 124. doi: 10.1029/2018JD029207
- Hamdi R., F. Duchêne, J. Berckmans, A. Delcloo, C. Vanpoucke, P. Termonia (2016): Evolution of urban heat wave intensity for the Brussels Capital Region in the AREPGE-Climat A1B scenario, *Urban Climate*, Vol. 17, 176-195, doi:10.1016/j.uclim.2016.08.001.
- Dewaele, H., Munier, S., Albergel, C., Planque, C., Laanaia, N., Carrer, D., and Calvet, J.-C., 2017. Parameter optimisation for a better representation of drought by LSMs: inverse modelling vs. sequential data assimilation, *Hydrol. Earth Syst. Sci.*, 21, 4861–4878. Doi: 10.5194/hess-21-4861-2017.

The following peer-reviewed publications from ISIMIP, COST/PROFOUND and FACCE-JPI/MACSUR, co-authored by MASC scientists, have used the version of CARAIB (with the crop module and land use) developed within the MASC project:

- Bugmann, H., Seidl, R., Hartig, F., Bohn, F., Brůna, J., Cailleret, M., François, L., Heinke, J., Henrot, A.-J., Hickler, T., Hülsmann, L., Huth, A., Jacquemin, I., Kollas, C., Lasch-Born, P., Lexer, M. J., Merganič, J., Merganičová, K., Mette, T., Miranda, B. R., Nadal-Sala, D., Rammer, W., Rammig, A., Reineking, B., Roedig, E., Sabaté, S., Steinkamp, J., Suckow, F., Vacchiano, G., Wild, J., Xu, C., Reyer, C. P. O., 2019. Tree mortality submodels drive simulated long-term

- forest dynamics: assessing 15 models from the stand to global scale. *Ecosphere*, 10(2). Doi : 10.1002/ecs2.2616.
- Schewe, J., Gosling, S. N., Reyer, C., Zhao, F., Ciais, P., Elliott, J., François, L., Huber, V., Lotze, H. K., Seneviratne, S. I., van Vliet, M. T. H., Vautard, R., Wada, Y., Breuer, L., Büchner, M., Carozza, D. A., Chang, J., Coll, M., Deryng, D., de Wit, A., Eddy, T. D., Folberth, C., Frieler, K., Friend, A. D., Gerten, D., Gudmundsson, L., Hanasaki, N., Ito, A., Khabarov, N., Kim, H., Lawrence, P., Morfopoulos, C., Müller, C., Müller Schmied, H., Orth, R., Ostberg, S., Pokhrel, Y., Pugh, T. A. M., Sakurai, G., Satoh, Y., Schmid, E., Stacke, T., Steenbeek, J., Steinkamp, J., Tang, Q., Tian, H., Tittensor, D. P., Volkholz, J., Wang, X., Warszawski, L., 2019. State-of-the-art global models underestimate impacts from climate extremes. *Nature Communications*, 10(1), 1005. Doi : 10.1038/s41467-019-08745-6.
 - Wartenburger, R., Seneviratne, S.I., Hirschi, M., Chang, J., Ciais, P., Deryng, D., Elliott, J., Folberth, C., Gosling, S.N., Gudmundsson, L., Henrot, A.-J., Hickler, T., Ito, A., Khabarov, N., Kim, H., Leng, G., Liu, J., Liu, X., Masaki, Y., Morfopoulos, C., Müller, C., Schmied, H.M., Nishina, K., Orth, R., Pokhrel, Y., Pugh, T.A.M., Satoh, Y., Schaphoff, S., Schmid, E., Sheffield, J., Stacke, T., Steinkamp, J., Tang, Q., Thiery, W., Wada, Y., Wang, X., Weedon, G.P., Yang, H., Zhou, T., 2018. Evapotranspiration simulations in ISIMIP2a Evaluation of spatio-temporal characteristics with a comprehensive ensemble of independent datasets. *Environmental Research Letters*, 13 (7) 075001. Doi :10.1088/1748-9326/aac4bb
 - Cantú, A. G., Frieler, K., Reyer, C. P. O., Ciais, P., Chang, J., Ito, A., Kazuya, N., François, L., Henrot, A.-J., Hickler, T., Steinkamp, J., Rafique, R., Zhao, F., Ostberg, S., Schaphoff, S., Tian, H., Pan, S., Yang, J., Morfopoulos, C., Betts, R., 2018. Evaluating changes of biomass in global vegetation models: the role of turnover fluctuations and ENSO events. *Environmental Research Letters*, 13(7), 075002. Doi : 10.1088/1748-9326/aac63c
 - Fronzek, S., Pirttioja, N., Carter, T. R., Bindi, M., Hoffmann, H., Palosuo, T., Ruiz-Ramos, M., Tao, F., Trnka, M., Acutis, M., Asseng, S., Baranowski, P., Basso, B., Bodin, P., Buis, S., Cammarano, D., Deligios, P., Destain, M.-F., Dumont, B., Ewert, F., Ferrise, R., François, L., Gaiser, T., Hlavinka, P., Jacquemin, I., Kersebaum, K. C., Kollas, C., Krzyszczak, J., Lorite, I. J., Minet, J., Minguez, M. I., Montesino, M., Moriondo, M., Müller, C., Nendel, C., Öztürk, I., Perego, A., Rodríguez, A., Ruane, A. C., Ruget, F., Sanna, M., Semenov, M. A., Slawinski, C., Stratonovitch, P., Supit, I., Waha, K., Wang, E., Wu, L., Zhao, Z., Rötter, R. P., 2018. Classifying multi-model wheat yield impact response surfaces showing sensitivity to temperature and precipitation change. *Agricultural Systems*, 159, 209-224.
 - Chang, J., Ciais, P., Wang, X., Piao, S., Asrar, G., Betts, R., Chevallier, F., Dury, M., François, L., Frieler, K., Garcia Cantu Ros, A., Henrot, A.-J., Hickler, T., Ito, A., Morfopoulos, C., Munhoven, G., Nishina, K., Ostberg, S., Pan, S., Peng, S., Rafique, R., Reyer, C., Rödenbeck, C., Schaphoff, S., Steinkamp, J., Tian, H., Viovy, N., Yang, J., Zeng, N., Zhao, F., 2017. Benchmarking carbon fluxes of the ISIMIP2a biome models. *Environmental Research Letters*, 12, 045002. Doi :10.1088/1748-9326/aa63fa
 - Chen, M., Rafique, R., Asrar, G. R., Bond-Lamberty, B., Ciais, P., Zhao, F., Reyer, C. P. O., Ostberg, S., Chang, J., Ito, A., Yang, J., Zeng, N., Kalnay, E., West, T., Leng, G., François, L., Munhoven, G., Henrot, A.-J., Tian, H., Pan, S., Nishina, K., Viovy, N., Morfopoulos, C., Betts, R., Schaphoff, S., Steinkamp, J., Hickler, T., 2017. Regional contribution to variability and trends of global gross primary productivity. *Environmental Research Letters*, 12(10), 105005. Doi : 10.1088/1748-9326/aa8978
 - Ito, A., Nishina, K., Reyer, C. P. O., François, L., Henrot, A.-J., Munhoven, G., Jacquemin, I., Tian, H., Yang, J., Pan, S., Morfopoulos, C., Betts, R., Hickler, T., Steinkamp, J., Ostberg, S., Schaphoff, S., Ciais, P., Chang, J., Rafique, R., Zeng, N., Zhao, F., 2017. Photosynthetic productivity and its efficiencies in ISIMIP2a biome models: benchmarking for impact assessment studies. *Environmental Research Letters*, 12(8), 085001. Doi : 10.1088/1748-9326/aa7a19

Publication advertising MASC project for stakeholders

- Unmasking the climate system - A Belgian project is implementing surface land use and socioeconomic feedbacks in high-resolution climate projections over Belgium and western Europe, PanEuropean Networks, Government 14, 115, May 2015.

Theses

- Horemans, J., 2017. Tackling challenges in process-based forest modelling: from concept to uncertainty. PhD thesis defended at the University of Antwerp, December 19, 2017. Pp 186.
- Berckmans, J., 2017. Modelling land-atmosphere interactions: Impact of near future land use and climate change over Western Europe. PhD thesis defended at the University of Antwerp, March 22, 2018. Pp 227.
- Beckers, V., University of Namur, thesis on ADAM ABM, still to be defended.
- Jacquemin, I., University of Liège, thesis on CARAIB crop module and its coupling with the ABM, still to be defended.

Conference abstracts

- Jacquemin, I., Dury, M., Henrot, A.-J., Beckers, V., Berckmans, J., Dendoncker, N., Hamdi, R., Hambuckers, A., Tychon, B., & François, L. (2017, November 17). High-resolution simulations of natural and agricultural ecosystems over Belgium with the CARAIB Dynamic Vegetation Model. Paper presented at 7th Belgium Geography Day, Liège, Belgium.
- Dury, M., Henrot, A.-J., Jacquemin, I., Steinkamp, J., Hickler, T., Reifenberg, S., & François, L. (2017, October 09). How do individual species and Plant Functional Type responses to environmental change differ in Dynamic Vegetation Models? - A forest stand analysis. Poster session presented at PROFOUND Final Event "Robust projections of forests under climate change - data, methods and models", Potsdam, Germany.
- Jacquemin, I., Beckers, V., Henrot, A.-J., Berckmans, J., Hamdi, R., François, L., & Dendoncker, N. (2017, May 23). Land surface interactions modeling (Agent-Based-Model - Dynamic Vegetation Model) over Belgium: current state and crop yield assessment for future (at the Belgian and European scales). Poster presented at MACSUR Scientific Conference, Berlin, Germany.
- Jacquemin, I., Henrot, A.-J., Fontaine, C. M., Dendoncker, N., Beckers, V., Debusscher, B., Tychon, B., Hambuckers, A., & François, L. (2016, April 22). Using a dynamic vegetation model for future projections of crop yields : application to Belgium in the framework of the VOTES and MASC projects. Poster session presented at EGU General Assembly 2016, Vienna, Austria.
- Jacquemin, I., Henrot, A.-J., Beckers, V., Berckmans, J., Debusscher, B., Dury, M., Minet, J., Hamdi, R., Dendoncker, N., Tychon, B., Hambuckers, A., & François, L. (2016, April 21). High-resolution climate and land surface interactions modeling over Belgium: current state and decennial scale projections. Poster session presented at EGU General Assembly 2016, Vienna, Austria.
- Jacquemin, I., Dury, M., Henrot, A.-J., Berckmans, J., Hamdi, R., Hambuckers, A., Tychon, B., & François, L. (2016, September 29). Using a dynamic vegetation model for future projections of crop yields: simulations from the plot scale to the Belgian and European scales. Paper presented at FACEing the future : food production and ecosystems, Giessen, Germany.
- Dury, M., Hambuckers, A., Henrot, A.-J., Jacquemin, I., Munhoven, G., & François, L. (2016, September 26). Assessing the impact of climate change on terrestrial plants in Europe using

- a Dynamic Vegetation Model driven by EURO-CORDEX projections. Poster session presented at FACEing the future: food production and ecosystems, Giessen, Germany.
- Jacquemin, I., Henrot, A.-J., Fontaine, C. M., Dendoncker, N., Beckers, V., Debusscher, B., Tychon, B., Hambuckers, A., & François, L. (2016, April 22). Using a dynamic vegetation model for future projections of crop yields : application to Belgium in the framework of the VOTES and MASC projects. Poster session presented at EGU General Assembly 2016, Vienna, Austria.
 - Jacquemin, I., Henrot, A.-J., Beckers, V., Berckmans, J., Debusscher, B., Dury, M., Minet, J., Hamdi, R., Dendoncker, N., Tychon, B., Hambuckers, A., & François, L. (2016, April 21). High-resolution climate and land surface interactions modelling over Belgium: current state and decennial scale projections. Poster session presented at EGU General Assembly 2016, Vienna, Austria.
 - François, L., Henrot, A.-J., Dury, M., Jacquemin, I., Munhoven, G., Friend, A., Radermacher, T. T., Hacket-Pain, A., Hickler, T., Tian, H., Morfopoulos, C., Ostberg, S., Chang, J., Rafique, R., & Nishina, K. (2016, April). Response to droughts and heat waves of the productivity of natural and agricultural ecosystems in Europe within ISI-MIP2 historical simulations. Paper presented at EGU General Assembly 2016, Vienna, Austria.
 - Henrot, A.-J., Dury, M., Hambuckers, A., Munhoven, G., Jacquemin, I., & François, L. (2015, July). Modelling ecosystem response to present and future drought events in Western Europe with the CARAIB dynamic vegetation model. Poster session presented at Our Common Future Under Climate Change, CFCC 2015, Paris, France.
 - Henrot, A.-J., François, L., Dury, M., Hambuckers, A., Jacquemin, I., Minet, J., Tychon, B., Heinesch, B., Horemans, J., & Deckmyn, G. (2015, April). Modelling carbon fluxes of forest and grassland ecosystems in Western Europe using the CARAIB dynamic vegetation model: evaluation against eddy covariance data. Poster session presented at EGU General Assembly 2015, Vienna, Austria.
 - François, L., Jacquemin, I., Fontaine, C., Minet, J., Dury, M., & Tychon, B. (2014). Implementing agricultural land-use in the CARAIB dynamic vegetation model. Paper presented at FACCE-JPI MACSUR Mid-term Scientific Conference, Sassari, Italy.
 - Beckers, V. & Dendoncker, N. (2017, May) Creating a dynamical farmer population model at country scale level. MACSUR Science Conference, Berlin, Germany.
 - Beckers, V. & Dendoncker, N. (2015, November 13) Analysing agriculture in Belgium to define agents for investigation future agricultural land use changes through ABM, Belgium Geography Days 2015, C1: Spatial modelling of environmental processes. Oral presentation.
 - Beckers, V., Dendoncker, N., Fontaine, C. M. (2014, September) Improving the decision making in agent-based modelling framework for land use dynamics through ecosystem services changes monitoring. ESP Conference, Costa Rica, 2014.
 - Berckmans J., R. Hamdi: Designing mitigation strategies for Belgian cities in the near future under climate change and land use changes, Geophysical Research Abstracts, Vol. 20, EGU2018-7902 (poster presentation)
 - Berckmans J., R. Hamdi, N. Dendoncker, R. Ceulemans: Bridging the gap between policy-driven land use changes and regional climate projections, Geophysical Research Abstracts, Vol. 20, EGU2018-277 (oral presentation)
 - Berckmans J., R. Hamdi, N. Dendoncker, R. Ceulemans: Modelling the impact of land use and climate changes at the regional scale, EMS Annual Meeting Abstracts, Vol. 14, EMS2017-750 (oral presentation)
 - Berckmans J., O. Giot, R. De Troch, R. Hamdi, R. Ceulemans, P. Termonia (2017): Reinitialised versus continuous regional climate simulations using ALARO-0 coupled to the land surface model SURFEXv5, Geosci. Model Dev., Vol. 10, 223-238, doi:10.5194/gmd-10-223-2017

- Berckmans J., A.-J. Henrot, I. Jacquemin, R. Hamdi: Sensitivity of the regional climate model ALARO-0 to land surface changes: a conceptual framework, EMS Annual Meeting Abstracts, Vol. 13, EMS2016-533 (poster presentation)
- Hamdi R., F. Duchêne, J. Berckmans, A. Delcloo, C. Vanpoucke, P. Termonia (2016): Evolution of urban heat wave intensity for the Brussels Capital Region in the AREPGE-Climat A1B scenario, Urban Climate, Vol. 17, 176-195, doi:10.1016/j.uclim.2016.08.001
- Berckmans J., O. Giot, R. De Troch, R. Hamdi: Reinitialised versus continuous regional climate simulations using ALARO coupled to the land surface model SURFEX: investigating the land-atmosphere feedback, Stockholm, Sweden, 17-20 May 2016 (poster presentation)
- Berckmans J., R. Hamdi: The decadal projection of the Belgian urban heat island under changing climate and land use, Toulouse, France, 20-24 July 2015 (poster presentation)
- Berckmans J., R. Hamdi, R. De Troch, O. Giot: Validation of the regional climate model ALARO with different downscaling approaches and different horizontal resolutions, Geophysical Research Abstracts, Vol. 17, EGU2015-11175 (poster presentation)
- Berckmans J., R. Hamdi, L. François, P. Termonia: The decadal projection of the Belgian and Western European climate under changing land cover, land use and socio-economic factors, Brussels, Belgium, 23-26 September 2014 (poster presentation)
- Berckmans J., R. Hamdi, L. François, P. Termonia: The decadal projection of the Belgian and Western European climate under changing land cover, land use and socio-economic factors, Grindelwald, Switzerland, 31 August – 5 September 2014 (poster presentation)
- Pottiaux E., J. Berckmans, C. Bruyninx: Advanced multi-GNSS troposphere modeling for improved monitoring and forecasting of severe weather, Geophysical Research Abstracts, Vol. 16, EGU2014-11730 (poster presentation)
- Berckmans J., R. Hamdi, R. De Troch, O. Giot: Validation of the regional climate model ALARO with different downscaling approaches and different horizontal resolutions, Geophysical Research Abstracts, Vol. 17, EGU2015-11175 (poster presentation)
- Laanaia, N., Calvet, J.-C., Carrer, D., and Seferian, R. (2016, April) Mapping climate change impact on vegetation and the associated uncertainties in the Euro-Mediterranean area, Geophysical Research Abstracts, 18, EGU2016-4247-1, EGU General Assembly, 2016.

7. ACKNOWLEDGEMENTS

We are grateful to the members of the follow-up committee of our project, as well as to Martine Vanderstraeten, our project officer, for the very fruitful discussions that we had during the follow-up committee meetings. These discussions significantly impacted the orientation of our research.

ANNEXES

Table A1. Short description of the processes included in the CARAIB dynamic vegetation model

Plant functional types	Plant functional type or species level. In this study parameters for beech.
Spatial scale	Grid cell containing different PFTs or point scale
Soil input initialisation	Sand fraction, clay fraction, rooting depth per PFT/species, soil color
Forest structure and carbon pools initialisation	Grid cell with one layer of trees and one layer containing herbs and shrubs.
Climate input	CO ₂ , air temperature, amplitude of air temperature (T _{day_{max}} -T _{day_{min}}), precipitation, air relative humidity, short-wave incoming radiation, wind velocity. [Daily]
Spin-up	Yes, by using ERA-interim re-analysis (Uppala et al. 2005) [Daily]
Photosynthesis	Light interception by big leaf approach with separation of sun and shaded leaves (De Pury and Farquhar 1997). Time step subdivided into sunny and non-sunny portions, depending on the percentage of sunshine hours. Photosynthesis thus calculated 3 times in each time step for each PFT/species: for sun and shaded leaves during the sunny portion and for all leaves during the non-sunny portion. Light use efficiency calculated by the model of Farquhar et al. (1980), as simplified by Collatz et al. (1991). Radiative transfer through the canopy according to Goudriaan et al. (1985) with radiation attenuation by Beer's law. Gross primary production only calculated when air temperature >-10°C and if LAI >0. [2-hourly]
Respiration	Autotrophic respiration subdivided into growth respiration, as a fixed fraction of the carbon allocated to the growth of carbon pools, and maintenance respiration, as a Q ₁₀ function of temperature and proportional to the biomass and the C:N ratio of that pool (Warnant, 1999) and decreasing with the average air temperature of the previous 2 months for leaves and the previous 4 years for wood/roots to mimic temperature acclimation process (Wythers et al. 2005). Heterotrophic respiration dependent on soil temperature and soil moisture (Nemry et al. 1996) [2-hourly]
Allocation	Photosynthetic products (GPP) are allocated to the metabolic (leaves and fine roots) and structural (wood and coarse roots) carbon reservoirs. The carbon partitioning between the two pools is species-specific and depends on environmental conditions (temperature and soil water) (Otto et al. 2002).
Carbon nitrogen balance	Constant C:N ratio prescribed at initialisation. Turnover of litter and organic matter vary with temperature and soil water. Three carbon reservoirs are considered: leaf litter, wood litter and humus. [Daily]
Soil water balance	Soil water budget modelled in the root zone. Soil hydraulic conductivity is calculated from soil texture, using the parameterization of Saxton et al. (1986). Soil water can vary from wilting point to saturation. [Daily]
Water interception storage	Parameterization from leaf bucket model run at very high temporal resolution (~1 minute), depending on precipitation, potential evapotranspiration and LAI. [Daily]
Evapotranspiration	Actual evapotranspiration calculated as the sum of snow sublimation, the evaporation of intercepted rain and the evaporation/transpiration from the soil-vegetation system. This sum cannot exceed the potential evapotranspiration calculated over the pixel from Penman's equation (e.g., Mintz and Walker 1993). Transpiration is considered as a supply function for the water transpired by the PFT/species growing on the pixel. [Daily]
Phenology	Regulated purely by evolution of LAI. LAI growth (resp. leaf fall) is initiated when the air temperature is above (resp. below) a prescribed species-dependent threshold. [Daily]
Regeneration/planting	Amount of seeds proportional to NPP. Seeds (here only beech) can colonize gaps in the canopy caused by mortality. [yearly]
Management	A prescribed fraction of biomass (leaf or wood) can be removed. [Daily] Not used in this study.
Mortality	Age dependent natural mortality and mortality caused by thermal and water deficit stress as well as by fire disturbance. [Daily]

Table A2. Short description of the processes included in the ISBA_{CC} dynamic vegetation model

Plant functional types	Several plant functional types in one gridcell possible, not interacting and each having their own soil. Here only temperate deciduous forest.
Spatial scale	Grid or point scale.
Soil input initialisation	Per layer: saturation, field capacity, permanent wilting point, sand fraction, clay fraction, carbon content, General: rooting depth, ground water depth.
Forest structure and carbon pools initialisation	Grid cell with one layer of trees.
Climate input	CO ₂ , air temperature, precipitation, air relative humidity, short-wave incoming radiation, long-wave incoming radiation, wind velocity. [Hourly]
Spin-up	Yes by cycling through the available meteorological data. [Hourly]
Photosynthesis	Semi-empirical parametrization of net carbon assimilation and mesophyll conductance following the photosynthesis model of Jacobs (1994) based on Goudriaan et al. (1985) and implemented by Calvet et al. (1998). 10-layer radiative transfer scheme taking into account direct and diffuse radiation and sunlit and shaded leaves to calculate photosynthesis in the canopy (Carrer et al.2013). [Hourly]
Respiration	Maintenance respiration rates of twigs, sapwood and fine root carbon pools depending linearly on biomass of the pool and its temperature, calculated by the Arrhenius temperature function (Lloyd and Taylor, 1994; Joetzjer et al. 2015). Growth respiration proportional to the photosynthetic capacity of the leaves (Jacobs, 1994). Heterotrophic respiration based on the CENTURY model (Parton et al. 1987). [Hourly]
Allocation	Assimilated carbon directly allocated to leaves, twigs, aboveground and belowground wood and fine roots following the daily carbon balance of the leaves (Gibelin et al. 2008). [Daily]
Carbon nitrogen balance	Nitrogen not simulated.
Soil water balance	Multilayer (14 layers) solution of the Fourier law and the mixed-form of the Richards equation to calculate the soil energy and water budgets including freezing/thawing (Decharme et al. 2011. [Hourly]
Water interception storage	Depending on LAI, precipitation and a maximum interception pool. [Hourly]
Evapotranspiration	Sum of snow sublimation, evaporation of intercepted rain, transpiration and soil evaporation (Noilhan and Planton 1989). [Hourly]
Phenology	Directly resulting from the leaf carbon balance. A minimum LAI at all time (0.3 for deciduous trees). Leaves start to grow when the amount of assimilated carbon is larger than the amount of lost carbon through respiration and turnover. This depends on the incoming radiation, the temperature and is only possible when the soil moisture is not limiting. At the end of the growing season the inverse happens. [Daily]
Regeneration/planting	Not explicitly modelled, presence of a minimum LAI allowing plant functional types to grow when climatic conditions are favorable. [Daily]
Management	Not modelled
Mortality	Not explicitly modelled, except for leaves. Biomass decreases through turnover. [Daily]

Table A3. Short description of the processes included in the 4C forest model

Plant functional types	No plant functional types. Fixed parameters available for 13 tree species, here Beech.
Spatial scale	Stand-scale
Soil input initialisation	Per layer: field capacity, permanent wilting point, soil density, pH, stone fraction, sand fraction, clay fraction, humus fraction, carbon and nitrogen content in the humus fraction, NH ₄ and NO ₃ content. General: rooting depth, ground water depth, evaporation depth, mineralization constant of humus in litter layer and in mineral soil, nitrification constant.
Forest structure and carbon pools initialisation	Per cohort: species, foliage biomass, fine root biomass, sapwood biomass, heartwood biomass, cross sectional area of heartwood at stem base, tree height, bole height, tree age, number of trees, diameter at crown base, diameter at breast height. Cohorts compete for light and for water and nutrients in the soil.
Climate input	CO ₂ , air temperature, precipitation, air relative humidity, net radiation, wind velocity. [Daily]
Spin-up	No.
Photosynthesis	Net photosynthesis as function of environmental drivers and physiological capacity depending on light use efficiency calculated according to Haxeltine and Prentice (1996) based on the mechanistic model of Farquhar et al. (1980) as simplified by Collatz et al. (1991) and limited by water and nitrogen availability and maximum nitrogen uptake per cohort. Net photosynthetic fraction per cohort proportional to its share in the absorbed photosynthetic active radiation, adapted when forest structure changes and with phenology (Lambert-Beer law). [Weekly, redistributed to daily values by a Q ₁₀ function of air temperature]
Respiration	Autotrophic respiration proportional to photosynthetic capacity (Landsberg and Waring, 1997). Heterotrophic respiration calculated by the carbon dynamics of the soil, dependent on soil temperature and soil moisture. [Weekly, redistributed to daily values by a Q ₁₀ function of air temperature]
Allocation	Theory of Mäkelä (1990), functional balance hypothesis (Davidson 1969), pipe model theory (Shinozaki, 1964) and mass-conservation law. Allometric relationships dynamically responding to water and nutrient limitations. [Yearly]
Carbon nitrogen balance	Decomposition of primary organic matter to humus described by first order reactions (Grote et al. 1998). Turnover from organic matter depending on water content, soil temperature and pH (Franko 1990; Kartschall 1989). Soil carbon/nitrogen depending on the percentage in the organic matter and their turnover rates (Running and Gower 1991). Outflow of nitrogen from the root zone by plant uptake and it's transport by water. [Daily]
Soil water balance	Soil water balance per soil horizon by percolation model, bucket model, water leaching and conductivity parameter depending on soil texture (Glugla 1969; Koitzsch 1997). Link to vegetation is plant available water versus transpiration demand and limited when more than 10 percent difference from field capacity (Chen, 1993), divided per cohort depending on its share in fine root biomass. [Daily]
Water interception storage	Depending on precipitation and evapotranspiration (Jansson 1991) and proportional to LAI. [Daily]
Evapotranspiration	Potential evapotranspiration by equation of TURC if air temperature > 5°C and by an equation of IVANOV if air temperature < 5°C (Dyck and Peschke 1989). Calculation of potential transpiration takes into account the interception evaporation and partitioned to cohorts considering their relative conductance. [Daily]
Phenology	Interaction of growth-promoting and growth-inhibiting agents driven by temperature and photoperiod (Schaber and Badeck 2003). Leaves appearing and disappearing all together at one time point when the threshold is reached. [Yearly]
Regeneration/planting	Regeneration by seed supply (Rogers and Johnson 1998), seed germination (Jorritsma et al. 1999) Not used in this study. [Yearly]
Management	Thinning (from below or from above), harvest (clear cut, shelterwood) and planting strategies options (method, strength and timing; Lasch et al. 2005). Here used by thinning to target number of trees known during the study period. [Yearly]
Mortality	Intrinsic mortality depending on maximum life span (Botkin 1993) or carbon-based stress mortality, by drought stress or light shortage or by disturbances (Keane et al. 1996; Loehle and LeBlanc 1996; Sykes and Prentice 1996). Not used in this study. [Yearly]

REFERENCES

- Anav, A., Frielingstein, P., Beer, C., Ciais, P., Harper, A., Jones, C. ., Murray-Tortarolo, G., Papale, D., Parazoo, N. C., Peylin, P., Piao, S., Sitch, S., Viovy, N., Wiltshire, A., Zhao, M., 2015: Spatio-temporal patterns of terrestrial gross primary production. *Reviews of Geophysics*, 53:785-818.
- ALADIN International Team, 1997: The ALADIN project: Mesoscale modelling seen as a basic tool for weather forecasting and atmospheric research. *WMO Bulletin*, 46:317–324.
- Aubinet, M., Grelle, A., Ibrom, A., Rannik, U., Moncrieff, J., Foken, T., Kowalski, A. S., Martin, P. H., Berbigier, P., Bernhofer, C., Clement, R., Elbers, J., Granier, A., Grunwald, T., Morgenstern, K., Pilegaard, K., Rebmann, C., Snijders, W., Valentini, R., Vesala, T., 2000: Estimates of the annual net carbon and water exchange of forests: The EUROFLUX methodology, *Advances in Ecological Research*, 30:113-175.
- Aubinet, M., Moureaux, C., Bodson, B., Dufranne, B., Heinesch, B., Suleau, M., Vancutsem, F., Vilret, A., 2009: Carbon sequestration by a crop over a 4-year sugar beet/winter wheat/seed potato/winter wheat rotation cycle. *Agricultural and Forest Meteorology*, 149:407-418.
- Aubinet, M., Vesala, T., Papale, D. (Eds.), 2012: *Eddy Covariance: A Practical Guide to Measurement and Data Analysis*. Springer Atmospheric Sciences, Dordrecht, Netherlands, 424 p. ISBN: 978-94-007-2350-4.
- Bala, G., Caldeira, K., Wickett, M., Phillips, T.J., Lobell, D.B., Delire, C., Mirin, A., 2007: Combined climate and carbon-cycle effects on large-scale deforestation. *Proceedings of the National Academy of Sciences of the United States of America*, 104:6550-6555.
- Beckers, V., Beckers, J., Vanmaercke, M., Van Hecke, E., Van Rompaey, A., Dendoncker, N., 2018: Modelling farm growth and its impact on agricultural land use: A country scale application of an agent-based model. *Land*, 7(3), 109; doi:10.3390/land7030109.
- Berckmans J., Hamdi, R., Dendoncker, N., 2019: Bridging the gap between policy-driven land use changes and regional climate projections. *Journal of Geophysical Research: Atmospheres*, 124, <https://doi.org/10.1029/2018JD029207>
- Best, M. J., Beljaars, A., Polcher, J., Viterbo, P., 2004: A proposed structure for coupling tiled surfaces with the planetary boundary layer. *Journal of Hydrometeorology*, 5:1271–1278.
- Björklund, J., Limburg, K.E., Rydberg, T., 1999: Impact of production intensity on the ability of the agricultural landscape to generate ecosystem services: An example from Sweden. *Ecological Economics*, 29:269–291.
- Bonan, G.B., 2008: *Forests and climate change: forcings, feedbacks, and the climate benefits of forests*. *Science*, 320:1444-1449.
- Botkin, D., 1993: *Forest Dynamics: An Ecological Model*. Oxford University Press, Oxford, New York, UK. 309 p.

Braswell, B. H., Sacks, W. J., Linder, E., Schimel, D. S., 2005: Estimating diurnal to annual ecosystem parameters by synthesis of a carbon flux model with eddy covariance net ecosystem exchange observations. *Global Change Biology*, 11:335-355.

Bubnovà, R., Hello, G., Bénard, P., Geleyn, J.-F., 1995: Integration of the fully elastic equations cast in the hydrostatic pressure terrain-following coordinate in the framework of the ARPEGE/Aladin NWP system. *Monthly Weather Review*, 123:515–535.

Bugmann, H., Grote, R., Lasch, P., Lindner, M., Suckow, F., 1997: A new forest gap model to study the effects of environmental change on forest structure and functioning. In: Mohren, G.M.J., Kramer, K., Sabate, S. (Eds.). *Impacts of Global Change of Tree Physiology and Forest Ecosystem*. Kluwer Academic Publisher, Dordrecht, The Netherlands, p. 255-261.

Buysse, P., Bodson, B., Debacq, A., De Ligne, A., Heinesch, B., Manise, T., Moureaux, C., Aubinet, M., 2017: Carbon budget measurement over 12 years at a crop production site in the silty-loam region in Belgium. *Agricultural and Forest Meteorology*, 246:241-255.

Calvet, J. C., Noilhan, J., Roujean, J. L., Bessemoulin, P., Cabelguenne, M., Olioso, A., Wigneron, J. P., 1998: An interactive vegetation SVAT model tested against data from six contrasting sites. *Agricultural and Forest Meteorology*, 92:73-95.

Carrer, D., Roujean, J. L., Lafont, S., Calvet, J. C., Boone, A., Decharme, B., Delire, C., Astellu-Etchegorry, J. P., 2013: A canopy radiative transfer scheme with explicit FAPAR for the interactive vegetation model ISBA-A-gs: impact on carbon fluxes. *Journal of Geophysical Research Biogeosciences*, 118:1-16.

Chen, C. W., 1993: The response of plants to interacting stresses: PGSM Version 1.3 Model Documentation. EPRI TR-101880. Electric Power Research Institute, Palo Alto, CA, USA, 128 p.

Collatz, G. J., Ball, J. T., Grivet, C., Berry, J. A., 1991: Physiological and environmental regulation of stomatal conductance, photosynthesis and transpiration: a model that includes a laminar boundary layer. *Agricultural and Forest Meteorology*, 54:107-136.

Crowther, T. W., Todd-Brown, K. E. O., Rowe C. W., Wieder, W. R., Carey, J. C., Machmuller, M. B., Snoek, B. L., Fang S., Zhou, G., Allison, S. D., Blair, J. M., Bridgham, S. D., Burton, A. J., Carrillo, Y., Reich, P. B., Clark, J. S., Classen, A. T., Dijkstra, F. A., Elberling, B., Emmett, B. A., Estiarte, M., Frey, S. D., Guo, J., Harte, J., Jiang, L., Johnson, B. R., Kröel-Dulay, G., Larsen, K. S., Laudon, H., Lavallee, J. M., Luo, Y., Lupascu, M., Ma, L. N., Marhan, S., Michelsen, A., Mohan, J., Niu, S., Pendall, E., Peñuelas, J., Pfeifer-Meister, L., Poll, C., Reinsch, S., Reynolds, L. L., Schmidt, I. K., Sistla, S., Sokol, N. W., Templer, P. H., Treseder, K. K., Welker, J. M., Bradford, M. A., 2016: Quantifying global soil carbon losses in response to warming. *Nature*, 540:104-108.

Davidson, R. L., 1969: Effect of root/leaf temperature differentials on root/shoot ratios in some pasture grasses and clover. *Annals of Botany*, 33:561-569.

Decharme, B., Boone, A., Delire, C., Noilhan, J., 2011: Local evaluation of the interaction between soil biosphere atmosphere soil multilayer diffusion scheme using four pedotransfer functions. *Journal of Geophysical Research*, 116:1984–2012.

Departement Landbouw en Visserij, 2014. Landbouwrapport 2014.

De Pury, D.G., Farquhar, G.D., 1997: Simple scaling of photosynthesis from leaves to canopies without the errors of big-leaf models. *Plant, Cell and Environment*, 20:537-557.

De Troch, R., Hamdi, R., Van De Vyver, H., Geleyn, J.-F., Termonia, P., 2013: Multiscale performance of the ALARO-0 model for simulating extreme summer precipitation climatology in Belgium. *Journal of Climate*, 26:8895–8915.

Dewaele, H., Munier, S., Albergel, C., Planque, C., Laanaia, N., Carrer, D., and Calvet, J.-C., 2017: Parameter optimisation for a better representation of drought by LSMs: inverse modelling vs. sequential data assimilation. *Hydrology and Earth System Sciences*, 21:4861–4878.

Dietze, M. C., Vargas, R., Richardson, A. D., Stoy, P. C., Barr, A. G., Anderson, R. S., Arain, M. A., Baker, I. T., Black, T. A., Chen, J. M., Ciais, P., Flanagan, L. B., Gough, C. M., Grant, R. F., Hollinger, D., Izaurrealde, R. C., Kucharik, C. J., Lafleur, P., Liu, S., Lokupitiya, E., Luo, Y., Munger, W., Peng, C., Poulter, B., Price, D. T., Ricciuto, D. M., Riley, W. J., Sahoo, A. K., Schaefer, K., Suyker, A. E., Tian, H., Tonitto, C., Verbeeck, H., Verma, S. B., Wang, W., Weng, E., 2011: Characterizing the performance of ecosystem models across time scales: a spectral analysis of the North American Carbon Program site-level synthesis. *Journal of Geophysical Research*, 116: G04029.

Dufranne, D., Moureaux, C., Vancutsem, F., Bodson, B., Aubinet, M., 2011: Comparison of carbon fluxes, growth and productivity of a winter wheat crop in three contrasting growing seasons. *Agriculture, Ecosystems and Environment*, 141:133-142.

Dury, M., Hambuckers, A., Warnant, P., Henrot, A.-J., Favre, E., Ouberdous, M., François, L., 2011: Response of the European forests to climate change: a modelling approach for the 21st century. *iForest - Biogeosciences and Forestry*, 4:82–99.

Dyck, S., Peschke, G., 1995: *Grundlagen der Hydrologie*. Verlag für Bauwesen, Berlin, Germany, 536 p.

Ewert, F., Rounsevell, M. A. D., Reginster, I., Metzger, M. J., Leemans, R., 2005: Future scenarios of European agricultural land use I. Estimating changes in crop productivity. *Agriculture Ecosystems & Environment*, 107:101-116.

Faloon, P., Betts, R. 2010: Climate impacts on European agriculture and water management in the context of adaptation and mitigation - The importance of an integrated approach. *Science of the Total Environment*, 408:5667-5687.

FAO, 2006: World reference base for soil resources: A framework for international classification, correlation and communication. Technical Report, Food and Agriculture Organisation of the United Nations, 145 pp.

Faroux, S., Kaptué Tchuenté, A. T., Roujean, J.-L., Masson, V., Martin, E., Le Moigne, P., 2013: ECOCLIMAP-II/Europe: a twofold database of ecosystems and surface parameters at 1 km resolution based on satellite information for use in land surface, meteorological and climate models. *Geoscientific Model Development*, 6:563-582.

Farquhar, G. D., von Caemmerer, S., Berry, J. A., 1980: A biochemical model of photosynthetic CO₂ assimilation in leaves of C3 species. *Planta*, 149:78-90.

Fontaine, C. M., Dendoncker, N., De Vreese, R., Jacquemin, I., Marek, A., Van Herzele, A., Devillet, G., Mortelmans, D., François, L., 2014: Towards participatory integrated valuation and modelling of ecosystem services under land-use change, *Journal of Land Use Science*, 9:278-303.

Forster, P., Ramaswamy, V., Artaxo, P., Bernsten, T., Betts, R., Fahey, D. W., Haywood, J., Lean, J., Lowe, D. C., Myhre, G., Nganga, J., Prinn, R., Raga, G., Schulz, M., Van Dorland, R., 2007: Changes in atmospheric constituents and in radiative forcing. In: *Climate Change 2007: The Physical Science Basis. Contribution of Working Group I to the Fourth Assessment Report of the Intergovernmental Panel on Climate Change* [Solomon, S., D. Qin, M. Manning, Z. Chen, M. Marquis, K.B. Averyt, M.Tignor and H.L. Miller (Eds.)]. Cambridge University Press, Cambridge, United Kingdom and New York, NY, USA.

François, L. M., Delire, C., Warnant, P., Munhoven, G., 1998: Modelling the glacial–interglacial changes in the continental biosphere. *Global Planetary Change*, 16–17:37–52.

François, L., Utescher, T., Favre, E., Henrot, A.-J., Warnant, P., Micheels, A., Erdei, B., Suc, J.-P., Cheddadi, R., Mosbrugger, V., 2011: Modelling late Miocene vegetation in Europe: results of the CARAIB model and comparison with palaeo-vegetation data. *Palaeogeography, Palaeoclimatology, Palaeoecology*, 304:359-378.

Franko, U., 1990: C- und N-Dynamik beim Umsatz organischer Substanz im Boden. Akademie der Landwirtschaftswissenschaften der DDR, Dissertation 2, Berlin, Germany, 140 p.

Geleyn, J.-F., 1988: Interpolation of wind, temperature and humidity values from model levels to the height of measurement. *Tellus*, 40A:347–351.

Gérard, J. C., Nemry, B., François, L. M., Warnant, P., 1999: The interannual change of atmospheric CO₂: contribution of subtropical ecosystems? *Geophysical Research Letters*, 26:243-246.

Gerard, L., Piriou, J. M., Brozková, R., Geleyn, J. F., Banciu, D., 2009: Cloud and Precipitation parameterization in a Meso-Gamma-Scale operational weather prediction model. *Monthly Weather Review*, 137: 3960-3977.

Gesch, D., Verdin, K., Greenlee, S., 1999: New land surface digital elevation model covers the earth. *EOS, Transactions American Geophysical Union*, 80:69–70.

Gian-Reto, W., Beissner, S., Burga, C. A., 2005: Trends in the upward shift of alpine plants. *Journal of Vegetation Science*, 16:541-548.

Gibelin, A. L., Calvet, J. C., Viovy, N., 2008: Modelling energy and CO₂ fluxes with an interactive vegetation land surface model, evaluation at high and middle latitudes. *Agricultural and Forest Meteorology*, 148:1611-1628.

Giot, O., Termonia, P., Degrauwe, D., De Troch, R., Caluwaerts, S., Smet, G., Berckmans, J., Deckmyn A., De Cruz, L., De Meutter, P., Duerinckx, A., Gerard, L., Hamdi, R., Van den Bergh, J., Van Ginderachter, M., Van Schaeybroeck, B., 2016: Validation of the ALARO-0 model within the EURO-

CORDEX framework. *Geoscientific Model Development*, 9:1143–1152.

Glugla, G., 1969: Berechnungsverfahren zur Ermittlung des aktuellen Wassergehaltes und Gravitationswasserabflusses im Boden. *Albrecht-Thaer-Archiv*, 13:71-376.

Golyandina, N., Zhigljavsky, A., 2013 (Eds.): *Singular Spectrum Analysis for Time Series*. Springer Briefs in Statistics, Springer, Heidelberg, Germany. 119 p. ISBN: 978-3-642-34912-6. <http://dx.doi.org/10.1007/978-3-642-34913-3>.

Goudriaan, J., van Laar, H. H., van Keulen, H., Louwse, W., 1985: Photosynthesis, CO₂ and plant production. In: Day, W., Atkin, R. K. (eds.). *Wheat Growth and Modelling*. Plenum Press, New York, USA. NATO AS/ Series, Series A, 86:107-122.

Grote, R., Suckow, F., Bellmann, K., 1998: Modelling of carbon-, nitrogen-, and water balances in pine stands under changing air pollution and deposition. In: Hüttel, R. F. and Bellmann, K. (eds.). *Changes of Atmospheric Chemistry and Effects on Forest Ecosystems. A Roof Experiment Without Roof*. Kluwer Publishers, Dordrecht, The Netherlands, 3:251-281.

Hamdi, R., Masson, V., 2008: Inclusion of a drag approach in the Town Energy Balance (TEB) scheme: offline 1D evaluation in a street canyon. *Journal of Applied Meteorology and Climatology*, 47:2627–2644.

Hamdi, R., Van de Vyver, H., Termonia, P., 2012: New cloud and microphysics parameterisation for use in high-resolution dynamical downscaling: application for summer extreme temperature over Belgium. *International Journal of Climatology*, 32:2051–2065.

Hamdi, R., Degrauwe, D., Duerinckx, A., Cedilnik, J., Costa, V., Dalkilic, T., Essaouini, K., Jerczynki, M., Kocaman, F., Kullmann, L., Mahfouf, J.-F., Meier, F., Sassi, M., Schneider, S., Váňa, F., Termonia, P., 2014: Evaluating the performance of SURFEXv5 as a new land surface scheme for the ALADINcy36 and ALARO-0 models. *Geoscientific Model Development*, 7:23–39.

Harms, W.B., Stortelder, a. H.F., Vos, W., 1984: Effects of Intensification of Agriculture on Nature and Landscape in the Netherlands. *Ekológia*, 3:281–304.

Haxeltine, A., Prentice I. C., 1996: A general model for the light-use efficiency of primary production. *Functional Ecology*, 10:551-561.

Haylock, M. R., Hofstra, N., Tank, A. M. G. K., Klok, E. J., Jones, P. D., New, M., 2008: A European daily high-resolution gridded data set of surface temperature and precipitation for 1950-2006. *Journal of Geophysical Research*, 113D:20119.

Henrot, A.-J. , Utescher, T., Erdei, B., Hamon, N., Ramstein, G., Krapp, M., Herold, N., Goldner, A., Favre, E., Munhoven, G., François, L., 2017: Middle Miocene climate and vegetation models and their validation with proxy data. *Palaeogeography, Palaeoclimatology, Palaeoecology*, 467:95-119.

Hewitt, C. D., Griggs, D. J., 2004: Ensembles-based predictions of climate changes and their impacts. *EOS, Transactions American Geophysical Union*, 85:1-566.

Hibbard, K., Janetos, A., van Vuuren, D. P., Pongratz, J., Rose, S. K., Betts, R. Herold, M., Feddema, J. J., 2010: Research priorities in land use and land-cover change for the Earth system and integrated assessment modelling. *International Journal of Climatology*, 30:2118–2128.

Hickler, T., Amming, A., Werner, C., 2015: Modelling CO₂ impacts on forest productivity. *Current Forestry Reports*, 1:69-80.

Hollinger, D.Y., Richardson, A.D., 2005: Uncertainty in eddy covariance measurements and its application to physiological models. *Tree Physiology*, 25:873-885.

Hughes, L., 2000: Biological consequences of global warming: Is the signal already apparent? *Trends in Ecology and Evolution*, 15:56-61.

Ihse, M., 1995: Swedish agricultural landscapes — patterns and changes during the last 50 years, studied by aerial photos. *Landscape and Urban Planning*, 31:21–37.

IPCC, 2007: *Climate Change 2007: Synthesis Report. Contribution of Working Groups I, II and III to the Fourth Assessment Report of the Intergovernmental Panel on Climate Change* [Core Writing Team, Pachauri, R.K and Reisinger, A. (Eds.)]. IPCC, Geneva, Switzerland, 104 pp.

IPCC, 2014: *Climate Change 2014: Synthesis Report. Contribution of Working Groups I, II and III to the Fifth Assessment Report of the Intergovernmental Panel on Climate Change* [Core Writing Team, R.K. Pachauri and L.A. Meyer (Eds.)]. IPCC, Geneva, Switzerland, 151 pp.

Jacob, D., Petersen, J., Eggert, B., Alias, A., Christensen, O. B., Bouwer, L. M. et al. 2014: EURO-CORDEX: new high-resolution climate change projections for European impact research. *Regional Environmental Change* 14:563–578.

Jacobs, C. M. J., 1994: *Direct impact of atmospheric CO₂ enrichment on regional transpiration*, PhD thesis, Agricultural University, Wageningen, The Netherlands, 192 p.

Jansson P.-E., 1991: *Simulation model for soil water and heat conditions. Description of the SOIL model (vol. 165)*. Swedish University of Agricultural Sciences, Department of Soil Sciences, Division of Agricultural Hydrotechnics, Uppsala, Sweden, 72 p.

Joetzjer, E., Delire, C., Douville, H., Ciais, P., Decharme, B., Carrer, D., Verbeeck, H., De Weirtdt, M., Bonal, D., 2015: Improving the ISBA_{cc} land surface model simulation of water and carbon fluxes and stocks over the Amazon forest. *Geoscientific Model Development*, 8:1709-1727.

Jorritsma, I. T. M., Van Hees, A. F. M., Mohren G. M. J., 1999: Forest development in relation to ungulate grazing: A Modeling Approach. *Forest Ecology and Management*, 120:23–34.

Kartschall, T., Döring, P., Suckow, F., 1989: Simulation of nitrogen, water and temperature dynamics in soil. *Systems Analysis Modelling Simulation Journal*, 6:117-123.

Keane, R. E., Morgan, P. Running, S. W., 1996: *FIRE-BGC - a mechanistic ecological process model for simulating fire succession on coniferous forest landscapes of the northern Rocky Mountains*. Research Paper INT-RP-484, United States Department of Agriculture, Forest Service, Intermountain Research Station, Missoula, MT, USA, 122 p.

Keenan, T. F., Baker, I., Barr, A., Ciais, P., Davis, K., Dietze, M., Dragoni, D., Gough, C.M., Grant, R., Hollinger, D., Hufkens, K., Poulter, B., Mccaughey, H., Raczka, B., Ryu, Y., Schaefer, K., Tian, H., Verbeeck, H., Zhao, M., Richardson, A. D., 2012: Terrestrial biosphere model performance for inter-annual variability of land-atmosphere CO₂ exchange. *Global Change Biology*, 18:1971-1987.

Kirtman, B., Power, S., Adedoyin, J., Boer, G., Bojariu, R., Camilloni, I., Doblas-Reyes, F., Fiore, A., Kimoto, M., Meehl, G., Prather, M., Sarr, A., Schär, C., Sutton, R., van Oldenborgh, G., Vecchi, G., Wang, H., 2013: Near-term climate change: projections and predictability. *Climate Change 2013: The physical science basis. Contribution of Working Group I to the Fifth Assessment Report of the Intergovernmental Panel on Climate Change*, T. Stocker, D. Qin, G.-K. Plattner, M. Tignor, S. Allen, J. Boschung, A. Nauels, Y. Xia, V. Bex, and P. Midgley, Eds., Cambridge University Press, Cambridge, United Kingdom and New York, NY, USA, 953–1028.

Koitzsch R., 1977: Schätzung der Bodenfeuchte aus meteorologischen Daten, Boden- und Pflanzenparametern mit einem Mehrschichtmodell. *Zeitschrift für Meteorologie*, 27:302-306.

Krause, P., Boyle, D. P., Base, F., 2005: Comparison of different efficiency criteria for hydrological model assessment. *Advances in Geosciences*, 5:89-97.

Laanaia, N., Carrer, D., Calvet, J.-C., Pagé, C., 2016. How will climate change affect the vegetation cycle over France? A generic modeling approach. *Climate Risk Management*, 13:31-42.

Landsberg, J. J., Waring, R. H., 1997: A generalised model of forest productivity using simplified concepts of radiation-use efficiency, carbon balance and partitioning. *Forest Ecology and Management*, 95:209-228.

Lasch, P., Badeck, F.-W., Suckow, F., Lindner, M., Mohr, P., 2005: Model-based analysis of management alternatives at stand and regional level in Brandenburg (Germany). *Forest Ecology and Management*, 207:59-74.

Lau, K. M., Wang, H.-Y., 1995: Climate signal detection using wavelet transform: How to make a time series sing? *Bulletin of the American Meteorological Society*, 76:2391-2402.

Laurent, J.-M., François, L., Bar-Hen, A., Bel, L., Cheddadi, R., 2008: European bioclimatic affinity groups: data-model comparisons. *Global and Planetary Change*, 61:28-40.

Lenoir, J., Gégout, J. C., Marquet, P. A., de Ruffray, P., Brisse, H., 2008: A significant upward shift in plant species optimum elevation during the 20th century. *Science*, 320:1768-1771.

Li, X. R., Zhao, Z., 2006: Evaluation of estimation algorithms, part I: Incomprehensive measures of performances. *IEEE Transactions on Aerospace and Electronic Systems*, 42:1340-1358.

Lloyd, J., Taylor, J. A., 1994: On the temperature dependence of soil respiration. *Functional Ecology*, 8:315-323

Loehle, C., LeBlanc, D., 1996: Model-based assessments of climate change effects on forests: a critical review. *Ecological Modelling*, 90:1-31.

Loubet, B., Laville, P., Lehuger, S., Larmanou, E., Fléchar, C., Mascher, N., Genermont, S., Roche, R.,

Ferrara, R. M., Stella, P., Personne, E., Durand, B., Decuq, C., Flura, D., Masson, S., Fanucci, O., Rampon, J.-N., Siemens, J., Kindler, R., Gabrielle, B., Schruppf, M., Cellier, P., 2011: Carbon, nitrogen and greenhouse gases budgets over a four years crop rotation in northern France. *Plant and Soil*, 343:109-137.

Lurgi, M., López, B. C., Montoya, J. M., 2012: Novel communities from climate change. *Philosophical Transactions of the Royal Society B-Biological Sciences*, 367:2913–2922.

Mahecha, M. D., Reichstein, M., Lange, H., Carvalhais, N., Bernhofer, C., Grünwald, T., Papale, D., Seufert, G., 2007: Characterizing ecosystem-atmosphere interactions from short to interannual time scales. *Biogeosciences*, 4:743-758.

Mahecha, M. D., Reichstein, M., Jung, M., Seneviratne, S. I., Zaehle, S., Beer, C., Braakhekke, M. C., Carvalhais, N., Lange, H., Le Maire, G., Moors, E., 2010: Comparing observations and process-based simulations of biosphere-atmosphere exchange on multiple time scales. *Journal of Geophysical Research*, 115: G02003.

Mäkelä, A., 1990: Modeling structural-functional relationships in whole-tree growth: resource allocation. In: Dixon, R. K., Meldahl, R. S., Ruark, G. A., Warren, W. G (eds.). *Process Modeling of Forest Growth Responses to Environmental Stress*. Timber Press, Portland, Oregon, 81-95.

Masson, V., 2000: A physically-based scheme for the urban energy budget in atmospheric models. *Boundary Layer Meteorology*, 94:357–397.

Masson, V., Champeaux, J.-L., Chauvin, F., Meriguet, C., Lacaze, R., 2003: A global database of land surface parameters at 1 km resolution in meteorological and climate models. *Journal of Climate*, 16:1261–1282.

Masson, V., Seity, Y., 2009: Including atmospheric layers in vegetation and urban offline surface schemes. *Journal of Applied Meteorology and Climatology*, 48:1377–1397.

Masson, V., Le Moigne, P., Martin, E., Faroux, S., Alias, A., Alkama, R., Belamari, S., Barbu, A., Boone, A., Bouyssel, F., Brousseau, P., Brun, E., Calvet, J.-C., Carrer, D., Decharme, B., Delire, C., Doniet, S., Essaouini, K., Gibelin, A.-L., Giordani, H., Habets, F., Jidane, M., Kerdraon, G., Kourzeneva, E., Lafaysse, M., Lafont, S., Lebeaupin Brossier, C., Lemonsu, A., Mahfouf, J.-F., Marguinaud, P., Mokhtari, M., Morin, S., Pigeon, G., Salgado, R., Seity, Y., Taillefer, F., Tanguy, G., Tulet, P., Vincendon, B., Vionner, V., Voldoire, A., 2013: The SURFEXv7.2 land and ocean surface platform for coupled or offline simulation of Earth surface variables and fluxes. *Geoscientific Model Development*, 6:929-960.

Medlyn, B. E., Robinson, A. P., Clement, R., McMurtrie, E., 2005: On the validation of models of forest CO₂ exchange using eddy covariance data: some perils and pitfalls. *Tree Physiology*, 25:839-857.

Meehl, G. A., Stocker, T.F., Collins, W.D., Friedlingstein, P., Gaye, A.T., Gregory, J.M., Kitoh, A., Knutti, R., Murphy, J.M., Noda, A., Raper, S.C.B., Watterson, I.G., Weaver, A.J., Zhao, Z.-C., 2007: Global Climate Projections. In: *Climate Change 2007: The Physical Science Basis. Contribution of Working Group I to the Fourth Assessment Report of the Intergovernmental Panel on Climate Change*

[Solomon, S., D. Qin, M. Manning, Z. Chen, M. Marquis, K.B. Averyt, M. Tignor and H.L. Miller (Eds.)]. Cambridge University Press, Cambridge, United Kingdom and New York, NY, USA.

Mintz, Y., Walker, G., 1993: Global fields of soil moisture and land surface evapotranspiration derived from observed precipitation and surface air temperature. *Journal of Applied Meteorology*, 32:1305-1334.

Moss, R. H., Edmonds, J. A., Hibbard, K. A., Manning, M. R., Rose, S. K., van Vuuren, D. P., Carter, T. R., Emori, S., Kainuma, M., Kram, T., Meehl, G. A., Mitchell, J. F., Nakicenovic, N., Riahi, K., Smith, S. J., Stouffer, R. J., Thomson, A. M., Weyant, J. P., Wilbanks, T. J., 2010: The next generation of scenarios for climate change research and assessment. *Nature*, 463:747-756.

Nakicenovic, N., Swart, R., (Eds.), 2000 : IPCC Special Report on Emissions Scenarios. Cambridge University Press, Cambridge, UK, 570 p.

Nash, J. E., Sutcliffe, J. V., 1970: River flow forecasting through conceptual models part I - A discussion of principles. *Journal of Hydrology*, 10:282-290.

Nemry, B., François, L. M., Warnant, P., Robinet, F., Gérard, J. C., 1996: The seasonality of the CO₂ exchange between the atmosphere and the land biosphere: a study with a global mechanistic vegetation model. *Journal Geophysical Research*, 01 (D3).

Noilhan, J., Planton, S., 1989: A simple parameterization of land surface processes for meteorological models. *Monthly Weather Review*, 117:536-549.

Noilhan, J., Mahfouf, J.F., 1996: The ISBA land surface parameterization scheme. *Global and Planetary Change*, 13:145-159.

Otto, D., Rasse, D., Kaplan, J., Warnant, P., François, L., 2002: Biospheric carbon stocks reconstructed and the Last Glacial Maximum: comparison between general circulation models using prescribed and computed sea surface temperature. *Global Planetary Change*, 33:117–138.

Paulson, C., 1970: The mathematical representation of wind speed and temperature profiles in the unstable atmospheric surface layer. *Journal of Applied Meteorology*, 9:857–861.

Parmesan, C., Yohe, G., 2003: A globally coherent fingerprint of climate change impacts across natural systems. *Nature*, 421:37-42.

Parton, W. J., Schimel, D. S., Cole, C. V., Ojima, D. S., 1987: Analysis of factors controlling soil organic matter levels in Great Plains grasslands. *Soil Science Society of America Journal*, 51:1173–1179.

Peltonen-Sainio, P., Jauhiainen, L., Hakala, K., 2009: Are there indications of climate change induced increases in yield variability of major field crops in the northernmost European conditions ? *Agricultural and Food Science*, 18:206-222.

Penuelas, J., Staudt, M. 2010: BVOCs and global change. *Trends in Plant Science*, 15:133-144.

Poudevigne, I., Alard, D., 1997: Landscape and agricultural patterns in rural areas: A case study in the Brionne Basin, Normandy, France. *Journal of Environmental Management*, 50:335–349.

Prein, A., Langhans, W., Fosser, G., Ferrone, A., Ban, N., Goergen, K., Keller, M., Tölle, M., Gutzjahr, O., Feser, F., Brisson, E., Kollet, S., Schmidli, J., van Lipzig, N., Leung, R., 2015: A review on regional convection-permitting climate modeling: Demonstrations, prospects, and challenges. *Reviews of Geophysics*, 53:323–361.

Raddatz, R. L., 2007: Evidence for the influence of agriculture on weather and climate through the transformation and management of vegetation: Illustrated by examples from the Canadian Prairies. *Agricultural and Forest Meteorology*, 142:186-202.

Reichstein, M., Falge, E., Baldocchi, D., Papale, D., Valentini, R., Aubinet, M., Berbigier, P., Bernhofer, C., Buchmann, N., Gilmanov, T., Granier, A., Grünwald, T., Havrnkov, K., Janous, D., Knohl, A., Laurila, T., Lohila, A., Loustau, D., Matteucci, G., Meyers, T., Miglietta, F., Ourcival, J.-M., Rambal, S., Rotenberg, E., Sanz, M. J., Seufert, G., Vaccari, F., Vesala, T., Yakir, D., 2005: On the separation of net ecosystem exchange into assimilation and ecosystem respiration: review and improved algorithm. *Global Change Biology*, 11:1–16.

Reyer C., Leuzinger, S., Rammig, A., Wolf, A., Bartholomeus, R. P., Bonfante, A., De Lorenzi, F., Dury, M., Gloning, P., Jaoudé, R. A., Klein, T., Kuster, T. M., Martins, M., Niedrist, G., Riccardi, M., Wohlfahrt, G., de Angelis, P., de Dato, G., François, L., Menzel, A., Pereira, M., 2013: A plant's perspective of extremes: Terrestrial plant and ecosystem responses to changing climatic variability. *Global Change Biology*, 19:75-89.

Richardson, A. D., Mahecha, M. D., Falge, E., Kattge, J., Moffat, A. M., Papale, D., Reichstein, M., Stauch, V. J., Braswell, B. H., Churkina, G., Kruijt, B., Hollinger, D. Y., 2008: Statistical properties of random CO₂ flux measurement uncertainty inferred from model residuals. *Agricultural and Forest Meteorology*, 148:38-50.

Richardson, A. D., Anderson, R. S., Arian, M. A., Barr, A. G., Bohrer, G., Chen, G., Bohrer, G., Chen, G., Chen, J. M., Ciais, P., Davis, K. J., Desia, A. R., Dietze, M. C., Dragoni, D., Garrity, S. R., Gough, C. M., Grant, R., Hollinger, D. Y., Margolis, H. A., McCaughey, H., Migliavacca, M., Monson, R. K., Munger, J. W., Poulter, B., Racka, B. M., Ricciuto, D. M., Sahoo, A. K., Schaefer, K., Tian, H. Q., Vargas, R., Verbeeck, H., Xiao, J. F., Xue, Y. K., 2012: Terrestrial biosphere models need better representation of vegetation phenology: results from the North American Carbon Program Site synthesis. *Global Change Biology*, 18:566-584.

Root, T. L., Price, J. T., Hall, K. R., Schneider, S. H., Rosenzweig, C., Pounds, J. A., 2003: Fingerprints of global warming on wild animals and plants. *Nature*, 421:57-60.

Rummukainen, M., 2010: State-of-the-art with regional climate models. *WIREs Climate Change*, 1:82–96.

Running, S. W., Gower, S. T., 1991: FOREST-BGC, A general model of forest ecosystem processes for regional applications II. Dynamic carbon allocation and nitrogen budgets. *Tree Physiology*, 9:147-160.

Saxton, K., Rawls, W. J., Romberger, J., Papendick, R., 1986: Estimating generalized soil-water characteristics from texture. *Soil Science Society of America Journal*, 50:1031-1036.

Schaber, J., Badeck, F.-W., 2003: Physiology based phenology models for forest tree species in Germany. *International Journal of Biometeorology*, 47:193-201.

Schultz, M., Mudelsee, M., 2002: REDFIT: estimating red-noise spectra directly from unevenly spaced paleoclimatic time series. *Computers & Geosciences*, 28:421-426.

Shinozaki, K., Yoda, K., Hozumi, K., Kira, T., 1964: A quantitative analysis of plant form - the pipe model theory. I. Basic analysis. *Japanese Journal of Ecology*, 14:97-105.

Siqueira, M.B., Katul, G.G., Sampson, D.A., Stoy, P.C., Juang, J.-Y., McCarthy, H.R., Oren, R., 2006: Multiscale model intercomparisons of CO₂ and H₂O exchange rates in a maturing southeastern US pine forest. *Global Change Biology*, 12:1189-1207.

Sivakumar, M. V. K., 2007: Interactions between climate and desertification. *Agricultural and Forest Meteorology*, 142:143-155.

Spangenberg, J. H., 2007: Integrated scenarios for assessing biodiversity risks. *Sustainable Development*, 16:343-356.

Statistics Belgium, 2015. *Agricultural surveys from 1980-2015*. Statbel.

Stoy, P. C., Katul, G. G., Siqueira, M. B., Juang, J.-Y., McCarthy, H. R., Kim, H.-S., Oishi, A. C., Oren, R., 2005: Variability in net ecosystem exchange from hourly to inter-annual time scales at adjacent pine and hardwood forests: a wavelet analysis. *Tree Physiology*, 25:887-902.

Suckow, F., Badeck, F.-W., Lasch, P., Schaber, J., 2001: Nutzung von Level-II-Beobachtungen für Test und Anwendungen des Sukzessionsmodells FORESEE. *Beiträge für Forstwirtschaft und Landschaftsökologie*, 35:84-87.

Sykes, M. T., Prentice, I. C., 1996: Carbon storage and climate change in Swedish forests: A comparison of static and dynamic modelling approaches. In: Apps, M.J., Price, D.T. (eds.). *Forest Ecosystems, Forest Management and the Global Carbon Cycle*. Springer-Verlag, Berlin, Germany, NATO ASI Series, 40:69-78.

Taylor, K. E., Stouffer, R. J., Meehl, G. A., 2012: An overview of CMIP5 and the experiment design. *Bull. Amer. Meteor. Soc.*, 93:485-498.

Thomas, C. D., 2010: Climate, climate change and range boundaries. *Diversity and Distributions*, 16:488-495.

Thuiller, W., Albert, C., Araújo, M. B., Berry, P. M., Cabeza, M., Guisan, A., Hickler, T., Midgley, G. F., Paterson, J., Schurr, F. M., Sykes, M. T., Zimmermann, N. E., 2008: Predicting global change impacts on plant species' distributions: Future challenges. *Perspectives in Plant Ecology, Evolution and Systematics*, 9:137-152.

Torrence, C., Compo, G.P., 1998: A practical guide to wavelet analysis. *Bulletin of the American Meteorological Society*, 79:61-78.

Uppala, S. M., Kallberg, P. W., Simmons, A. J., Andrea, U., Da Costa Bechtold, V., Fiorino, M., Gibson, J. K., Haseler, J., Hernandez, A., Kelly, G. A., Li, X., Onogi, K., Saarinen, S., Sokka, N., Allan, R. P.,

Andersson, E., Arpe, K., Balmaseda, M. A., Beljaars, A. C. M., Van De Berg, L., Bidlot, J., Bormann, N., Caires, S., Chevallier, F., Dethof, A., Dragosavac, M., Fisher, M., Fuentes, M., Hagemann, S., Holm, E., Hoskins, B. J., Isaksen, I., Janssen, P. A. E. M., Jenne, R., McNally, A. P., Mahfouf, J.-F., Morcrette, J.-J., Rayner, N. A., Saunders, R. W., Simon, P., Sterl, A., Trenberth, K. E., Untch, A., Vasiljevic, D., Viterbo, P., Woollen, J., 2005: The ERA-40 re-analysis. *Quarterly Journal of the Royal Meteorological Society*, 131:2961-3012.

Vinnichenko, N., 1970: The kinetic energy spectrum in the free atmosphere - 1 second to 5 years. *Tellus*, 22:158-166.

Voldoire, A., Sanchez-Gomez, E., Salas y Méliá, D., Decharme, B., Cassou, C., Sénési, S., Valcke, S., Beau, I., Alias, A., Chevalier, M., Déqué, M., Deshayes, J., Douville, H., Fernandez, E., Madec, G., Maisonnave, E., Moine, M.-P., Planton, S., Saint-Martin, D., Szopa, S., Tyteca, S., Alkama, R., Belamari, S., Braun, A., Coquart, L., Chauvin, F., 2013: The CNRM-CM5.1 global climate model: description and basic evaluation. *Climate Dynamics*, 40:2091–2121.

Wang, T., Brender, P., Ciais, P., Piao, S., Mahecha, M., Chevalier, F., Reichstien, M., Ottlé, C., Maignan, F., Arain, A., Bohrer, G., Cescatti, A., Kiely, G., Law, B. E., Lutz, M., Montagnani, L., Moors, E., Osborne, B., Panferov, O., Papale, D., Vaccari, F. P., 2012: State-dependent errors in a land surface model across biomes inferred from eddy covariance observations on multiple timescales. *Ecological Modelling*, 246:11-25.

Warnant, P., 1999: Modélisation du cycle du carbone dans la biosphère continentale à l'échelle globale. PhD thesis, University of Liège, Liège, Belgium, 276 pp.

Warnant, P., François, L. M., Strivay, D., Gérard, J.-C., 1994: CARAIB: a global model of terrestrial biological productivity. *Global Biogeochemical Cycles*, 8:255–270.

Wright, S. J., Muller-Landau, H. C., Schipper, J., 2009: The future of tropical species on a warmer planet. *Conservation Biology*, 23:1418-1426.

Wythers, K. R., Reich, P. B., Tjoelker, M. G., Bolstad, P. B., 2005 : Foliar respiration acclimation to temperature variable Q_{10} alter ecosystem carbon balance. *Global Change Biology*, 11:435-449.